



Universidade do Minho
Escola de Engenharia

Sara Carvalheira Neves

**Chitosan/Poly(ϵ -caprolactone) Blend
Scaffolds for Cartilage Repair**



Universidade do Minho
Escola de Engenharia

Sara Carvalheira Neves

**Chitosan/Poly(ϵ -caprolactone) Blend
Scaffolds for Cartilage Repair**

Tese de Mestrado em Engenharia Biomédica
Ramo de Biomateriais, Reabilitação e Biomecânica

Trabalho efectuado sob a orientação de

Professora Doutora Natália Maria de Araújo Alves
Professor Doutor João Filipe Colardelle da Luz Mano

É AUTORIZADA A REPRODUÇÃO PARCIAL DESTA TESE APENAS PARA EFEITOS DE INVESTIGAÇÃO, MEDIANTE DECLARAÇÃO ESCRITA DO INTERESSADO, QUE A TAL SE COMPROMETE

ACKNOWLEDGEMENTS

Esta tese representa o culminar da minha formação académica. Porém, os seus alicerces são muito mais do que anos lectivos. Estes últimos cinco anos formam uma etapa simplesmente fantástica da minha vida. A palavra que melhor a classifica será “crescer”. E muito. E muito mais do que aquilo que eu penso.

A todas as pessoas que fazem parte da minha vida e que não menciono nestes agradecimentos. À sua maneira, interferiram e interferem na minha formação, no tal “crescer”.

Em primeiro lugar, gostaria de agradecer à Professora Natália Alves, que desde o primeiro ano me ensina. Obrigada pela constante disponibilidade, pelo “saber ensinar” e pela ajuda em todos os aspectos desta tese – da análise de dados à escrita. Agradeço também ao Professor João Mano, pelo constante incentivo a fazer mais, melhor e diferente. Acima de tudo, pelo desafio constante a novas ideias.

A todo o staff dos 3B's, com especial apreço à Sofia e à Gisela, por toda a ajuda e principalmente paciência desde o meu 3º ano. Agradeço ainda o especial apoio à elaboração desta tese à Vera, à Ana Rita Duarte, ao Emanuel Fernandes, ao Vítor Correlo e ao Praveen Sher.

Ao Eng.º Maurício (DEP), por toda a ajuda disponibilizada na realização dos ensaios de FTIR.

Half the experiments that allowed me to write this thesis were performed during my ERASMUS experience. I wish to thank Prof. Marcel Karperien for welcoming me so well in the Tissue Regeneration group at University of Twente. Thank you for all the knowledge and teaching.

I am very grateful for the way that the TR group welcomed me. They made feel at home. Thank you all. However, without the “daily patience” of my daily supervisors, this work would be far from what it is now. I wish to thank Liliana for my “first steps” on cell culture. And I am sure that learning it in Portuguese turned things much easier. Thank you for all the advices and “tricks”. Lorenzo, my knowledge about cell-biomaterial relationship was greatly improved. Thank you for teaching me and for all the scientific English writing advices, I mean, the “straight to the point” writing.

Apart from the academic ERASMUS life, the “gypsy crew” made Calslaan 24 not a house but a home during those months. Your friendship and company were just marvelous. From the daily company of the Calslaan 24 residents – Clara, Bojan, Davide, Edgar, Julieta, Sam and Fred – to the “daily visitors” - Ilija, Marko, Ieva, Hector, María, Irina, Alina, Hajo and Dimitris. The crew was a genuine crew!

Agradeço também a todos os meus Professores.

Muito antes de ter chegado ao quinto ano, o primeiro “impacto” universitário foi partilhado com os meus colegas de Engenharia Biomédica. Principalmente aquele bando de “biomecos”. Todas as peripécias da minha vida académica começaram e foram passadas com vocês. É a vocês que agradeço todos aqueles pequenos grandes momentos que preencheram e deram cor a todo este percurso. Obrigada!

Clarinha, para além de fazeres parte daquele “bando”, este ano foste a minha companhia. Por todas as horas de laboratório e trabalho partilhadas, por todas as horas do “nosso” ERASMUS, e por quase saberes a minha tese de cor, obrigada.

Paulinha e Panhol, vocês são a família da minha segunda casa. Obrigada por todos aqueles momentos e pela indescritível e essencial companhia.

À Bé, por estar sempre lá e pela nossa inabalável amizade.

A todos os amigos que não refiro aqui.

Ao Gonçalo, pela companhia, paciência, optimismo, compreensão e dedicação. Esta tese é também muito tua.

A toda a minha família e à alegria de poder dizer que tenho uma segunda mãe. Nucha, obrigada.

Ao meu avô, porque sei e sinto o orgulho que teria por me ver chegar até aqui.

Ao meu irmão Hugo, porque somos e seremos sempre eu e tu.

Pais... obrigada. Por tudo. Pelo apoio incondicional. Por tudo o que aprendo com vocês. Pela vossa personalidade, experiência de vida, princípios, inteligência, humanismo e equilíbrio. Acima de tudo, convosco aprendo a ser forte. Pai, por me ensinares a ser determinada e perseverante. Mãe, por me equilibrares e seres o modelo que és. É com orgulho que vos dedico esta tese.

ABSTRACT

Tissue engineering (TE) is an evolving field with a great potential on providing permanent solutions for tissue damage or tissue loss problems. Its principles rely on the combination of cells, scaffolds and “helping factors” (like biomolecules), in order to reconstitute the damaged or lost tissue. Cartilage tissue is no exception to this approach and, additionally, it is one of the ideal candidates for TE, as it differs from other tissues on its limited capacity of self-repair. Regenerating defects that result from traumatic injury or degenerative joint diseases, i.e. articular cartilage (AC) (hyaline) problems, have a major impact on patients. The scaffold biomaterial is determinant for its TE application success. Blending naturally derived and synthetic polymers has been applied in TE in order to combine specific properties of each one of these polymer categories. The scaffold architecture is also another important parameter and a three-dimensional (3D) well interconnected porous structure plays an important role on the chondrogenic activity maintenance. In this context, fiber-based scaffolds are particularly interesting as they can provide large surface areas, highly interconnected structures and a variety of geometries.

The work presented at this thesis aimed to study the potential of chitosan (CHT)/poly(ϵ -caprolactone) (PCL) blend 3D fiber-mesh scaffolds as support structures for AC tissue repair. A new common solvent solution of 100 vol.% of formic acid was used to prepare three different polymeric solutions – 100, 75 and 50CHT (numbers represent CHT weight percentage) – that were wet-spun in order to obtain micro-fibers. Scanning electron microscopy (SEM) analysis showed a homogenous surface distribution of PCL. A good dispersion of PCL within the CHT phase was achieved as analyzed by differential scanning calorimetry (DSC) and Fourier transform infrared spectroscopy (FTIR). The fibers were folded into cylindrical moulds and underwent a thermal treatment to obtain the scaffolds. The μ CT analysis revealed an adequate porosity, pore size and interconnectivity of the scaffolds for TE applications. The PCL content increase in the blends diminished their swelling ratio and increased fiber surface roughness. Biological assays were performed after culturing bovine articular chondrocytes up to 21 days. SEM analysis, live-dead and metabolic activity assays showed that cells attached, proliferated, and were metabolically active over all scaffolds formulations. Differentiation studies showed cartilaginous ECM formation in all fiber-mesh formulations. The 75CHT scaffolds supported the most cartilage regeneration, as between the 14th and 21st days of culture DNA amount was similar but GAG production increased, being also the highest amount among all formulations. ECM overall distribution over the 75CHT and 50CHT 3D structures was homogeneous. CHT acellular scaffolds compressive mechanical properties were enhanced with the addition of PCL. The better mechanical performance was presented by the 50CHT formulation, whereas the 75CHT scaffolds presented the best biological response. As ECM formation is expected to increase structures mechanical properties, the 75CHT scaffold is potentially very promising for AC TE applications.

RESUMO

A engenharia de tecidos (ET) é uma área em constante evolução e que se baseia na combinação de células, estruturas de suporte (*scaffolds*) e factores co-adjuvantes, como biomoléculas, no intuito de regenerar/reconstituir tecidos nativos danificados ou perdidos. A cartilagem não é excepção a esta abordagem e, adicionalmente, é considerada como uma “candidata ideal” pois difere dos outros tecidos devido à sua limitada capacidade de auto-reparação. Para além disso, regenerar defeitos resultantes de traumas ou doenças degenerativas das articulações, isto é, da cartilagem articular (CA), é, hoje em dia, de elevada importância. O material do qual o *scaffold* é feito é um dos factores determinantes para o seu sucesso e a mistura de polímeros de origem natural com polímeros sintéticos tem sido uma estratégia muito utilizada em ET, combinando propriedades vantajosas específicas de cada uma das classes de materiais. A arquitectura do *scaffold* é também um parâmetro importante dado que uma estrutura tridimensional (3D) bem inter-conectada e porosa é determinante para a manutenção da actividade condrogénica. *Scaffolds* constituídos por fibras propiciam elevadas áreas de superfície, estruturas bem interconectadas e a possibilidade de se poderem obter variadas geometrias.

O trabalho apresentado nesta tese teve como objectivo o estudo do potencial de *scaffolds* de fibras obtidas a partir da mistura de quitosano (CHT) e poli(ϵ -caprolactona) (PCL), como estruturas de suporte para a regeneração de CA. Foi utilizada uma solução de 100 %vol. de ácido fórmico como solvente comum para preparar três soluções poliméricas diferentes – 100CHT, 75CHT e 50CHT (os números representam a percentagem de CHT na mistura). Estas foram processadas por *wet-spinning* de modo a obter micro-fibras. A análise efectuada por microscopia electrónica de varrimento (SEM) revelou homogeneidade na distribuição superficial de PCL. Foi possível verificar uma boa distribuição dos domínios de PCL pela fase de CHT, através de calorimetria diferencial de varrimento (DSC) e espectroscopia de infravermelhos por transformada de Fourier (FTIR). Para se obterem os *scaffolds*, as fibras foram colocadas em moldes cilíndricos e sujeitas a tratamento térmico. A análise através de micro-tomografia computadorizada e SEM revelou valores de porosidade, tamanho de poros e inter-conectividade dos *scaffolds* apropriados para aplicações de ET. O aumento de PCL nas misturas diminuiu a capacidade de retenção de água dos *scaffolds* e aumentou a rugosidade da superfície das fibras. Foram realizados ensaios biológicos com condrócitos articulares de origem bovina durante 21 dias. Através de SEM e ensaios de viabilidade celular e actividade metabólica, verificou-se que as células aderiram, proliferaram e estiveram metabolicamente activas durante o período de cultura. Estudos de diferenciação revelaram a produção de matriz extra-celular cartilágnea (ECM) em todas as três formulações. Os *scaffolds* de 75CHT revelaram suportar a melhor produção de ECM e a sua distribuição sobre as estruturas de 75CHT e 50CHT foi homogénea. As propriedades mecânicas do CHT foram melhoradas pela sua mistura com PCL, tendo os *scaffolds* de 50CHT revelado a melhor *performance* mecânica. Porém, como é espectável que a produção de ECM melhore as propriedades mecânicas de toda a estrutura e dado que a formulação de 75CHT suportou a melhor actividade condrogénica, esta revela-se bastante promissora para aplicações de ET para CA.

TABLE OF CONTENTS

ACKNOWLEDGEMENTS	iii
ABSTRACT	v
RESUMO	vi
TABLE OF CONTENTS	vii
LIST OF ABBREVIATIONS	ix
LIST OF FIGURES	x
LIST OF TABLES	xii

CHAPTER I

GENERAL INTRODUCTION

1. GENERAL INTRODUCTION	3
1.1. MOTIVATION AND CONTENT	3
1.2. ENGINEERING CARTILAGE TISSUE	4
1.3. THE ROLE OF THE SCAFFOLD IN CARTILAGE TISSUE ENGINEERING	5
1.4. BIODEGRADABLE POLYMERS IN CARTILAGE TISSUE ENGINEERING	7
1.4.1. Polymers from Natural Origin	7
1.4.2. Synthetic Polymers	7
1.4.3. Blending Natural and Synthetic Polymers	8
1.4.4. Chitosan and Poly(ϵ -caprolactone)	10
1.4.5. Blending Chitosan and Poly(ϵ -caprolactone)	11
1.5. SCAFFOLD STRUCTURE FOR CARTILAGE TISSUE ENGINEERING	15
1.5.1. Fiber-Based Scaffolds	15
1.5.2. Chitosan or PCL Based Scaffolds in Cartilage Tissue Engineering	21
1.6. CONCLUSION AND FUTURE ASPECTS	23
2. REFERENCES	24

CHAPTER II

MATERIALS AND METHODS

1. MATERIALS AND METHODS	35
1.1. MATERIALS	35
1.2. METHODS	36
1.2.1. Scaffolds Processing and Chondrocytes Isolation and Seeding	36
1.2.2. Characterization	38

CHAPTER III

CHITOSAN/POLY(ϵ -CAPROLACTONE) BLEND SCAFFOLDS FOR CARTILAGE REPAIR

ABSTRACT	50
1. INTRODUCTION	51
2. MATERIALS AND METHODS	53
2.1. MATERIALS	53
2.2. METHODS	53
2.2.1. Scaffolds Preparation	53
2.2.2. Characterization	54
3. RESULTS AND DISCUSSION	59
3.1. FIBERS PHYSICAL-CHEMICAL CHARACTERIZATION	59
3.2. 3D FIBER-MESH SCAFFOLDS CHARACTERIZATION	63
3.3. CHONDROCYTES RESPONSE OVER THE FIBER-MESHES	65
3.4. CHONDROGENIC ACTIVITY EVALUATION OVER THE SCAFFOLDS	68
4. CONCLUSIONS	74
5. REFERENCES	75

CHAPTER IV

GENERAL CONCLUSION AND FUTURE RESEARCH

GENERAL CONCLUSION AND FUTURE RESEARCH	79
--	----

LIST OF ABBREVIATIONS

A

AC articular cartilage
AcA acetic acid

B

bACs bovine articular chondrocytes

C

CHT chitosan
COL1 type I collagen
COL2 type II collagen

D

DSC differential scanning calorimetry

E

ECM extra-cellular matrix

F

Fb fibrin
fbACs fetal bovine articular chondrocytes
FDM fused deposition modeling
FTIR fourier transformed infrared

G

GAG glycosaminoglycan

H

HA hyaluronic acid
hAC human articular chondrocyte
hAS human adipose derived stem cell
hATMSC human adipose tissue derived mesenchymal stem cell
hBMMSC human bone marrow derived mesenchymal stem cell
HFIP 1,1,1,3,3,3-hexa-fluoro-2-propanol
hGF human gingival fibroblasts
hMSC human mesenchymal stem cell

M

MSC mesenchymal stem cell
MW molecular weight

P

pAC porcine articular chondrocyte
PBS phosphate buffered saline
PCL poly(ϵ -caprolactone)
PE poly(α -hydroxyl esters)
PEO poly(ethylene glycol/oxide)
PGA poly(glycolic-acid)
PLDLA poly(*L-D*lactide)
PLCL poly(lactide- ϵ -caprolactone)
PLGA poly(lactic-co-glycolic acid)
PLLA Poly(L-lactic acid)
PNiiPAM poly(*N*isopropylacrylamide)
PPF poly(propylene fumarate)
PU poly(urethane)
PVA poly(vinyl alcohol)
 γ -PGA-g-CS poly(γ -glutamic acid)-graft-chondroitin sulphate

R

rAC rabbit articular chondrocyte
RP rapid prototyping
RT-PCR real-time polymerase chain reaction

S

SEM scanning electron microscopy
semi-IPN semi-interpenetrating polymer network
SFF solid free-form fabrication
sNS sheep nasal septa
SPCL starch and poly(ϵ -caprolactone) blend

T

TE tissue engineering
TPP sodium triphosphate

CHAPTER I

GENERAL INTRODUCTION

-
- Figure 1.1. Articular cartilage structural and functional zones (adapted from [8]) 4
- Figure 1.2. General schematic of methodologies used in cartilage TE: from injectable systems to *in vitro* culture before implantation (adapted from [3]). 5
- Figure 1.3. Chitosan and poly(ϵ -caprolactone) (derived from ϵ -caprolactone molecule) structures (adapted from [166] and <http://en.wikipedia.org/wiki/File:PolycaprolactoneSynthesis.svg>, respectively). 11

CHAPTER II

MATERIALS AND METHODS

-
- Figure 2.1. Schematic representation of the fibers processing and scaffolds obtention procedure. 37

CHAPTER III

CHITOSAN/POLY(ϵ -CAPROLACTONE) BLEND SCAFFOLDS FOR CARTILAGE REPAIR

-
- Figure 3.1. SEM microphotographs of the fiber's surfaces, before (a, b, c) and after (d, e, f) the solvent etching procedure. 59
- Figure 3.2. DSC (a) first and (b) second heating scans for PCL, CHT and their blend fibers; PCL and blend fibers (c) melting temperature (T_m) and (d) crystallinity degree (χ_c) variations. 60
- Figure 3.3. Conventional FTIR spectra (only the 2000 to 800 cm^{-1} range is shown) of (a) 100CHT (solid line), PCL (dashed line) and epoxy resin (dotted line) and (b) of the blend fibers (solid line for 75CHT and dashed line for 50CHT). The shadow bands identify the regions that have been selected for the integration procedure used to obtain the images on Figure 3.4. 61
- Figure 3.4. Chemical maps of four discrete compositions of the fiber's cross-sections. The different color intensities that can appear in the images may result from the cross-sections different thicknesses. Green indicates the presence of CHT, red the presence of PCL and black corresponds to the epoxy resin. The smaller images present on the right side of the blends chemical maps individualize the presence of the CHT and the PCL in the blends. 62
- Figure 3.5. SEM microphotographs of the (a, d) 100CHT, (b, e) 75CHT and (c, f) 50CHT fiber-meshes after the thermal treatment at $T_a = 60^\circ\text{C}$ and $t_a = 3\text{h}$. The (d – f) images correspond to the magnification of the area delimited by the rectangular box on the (a - c) images; (g) 100CHT, (h) 75CHT and (i) 50CHT fiber-meshes representative 3D μCT images. 63
- Figure 3.6. (a) Fiber-meshes swelling behavior during 24h immersion in PBS at 37°C and (b) exemplificative stress deformation curves of the three formulations of fiber-meshes. 64
- Figure 3.7. Live-dead assay showing chondrocytes at the scaffold fibers at day 1, 7, 14 and 21 of culture, in proliferation medium. Cells were stained with calcein-AM/ethidium homodimer (dead cells stain red and living cells green) and visualized using fluorescence microscopy. Cell density: 5×10^5 cells/ $20\mu\text{L}$. 65

Figure 3.8. SEM images showing chondrocytes distribution and morphology over the scaffolds fibers after 1, 7, 14 and 21 days in culture, with proliferation medium. Cell density: 5×10^5 cells/20 μ L. 66

Figure 3.9. MTT assay showing chondrocytes over the scaffolds fibers after 1, 7, 14 and 21 days in culture with proliferation medium. Metabolically active cells stain purple. Constructs were visualized using light microscopy. Cell density: 5×10^5 cells/20 μ L. ((a – l) images: 7.5x magnification; inset images: 50x magnification). 66

Figure 3.10. SEM micrographs showing chondrocytes distribution and morphology over the scaffolds fibers surface after 1, 14 and 21 days in culture, with differentiation medium. Cell density: 5×10^5 cells/20 μ L. 68

Figure 3.11. Histological cross-sections show GAG production (stained red) on the (a - d) 100CHT, (e - h) 75CHT and (i - l) 50CHT scaffolds, on day 14 (a, b, e, f, i, j) and day 21 (c, d, g, h, k, l) of culture in differentiation medium, by safranin-O staining. Cells are represented by the dark spots and bluish regions correspond to the scaffold material. 69

Figure 3.12. Histological cross-sections show GAG production (stained blue) on the (a - d) 100CHT, (e - h) 75CHT and (i - l) 50CHT scaffolds, on day 14 (a, b, e, f, i, j) and day 21 (c, d, g, h, k, l) of culture in differentiation medium, by alcian blue staining. Fast red stained cell nuclei red and pale blue regions correspond to the scaffold material. 69

Figure 3.13. DNA, (b) GAG and (c) GAG/DNA ratio quantification assays of the constructs, after 1, 14 and 21 days of culture in differentiation medium. (*) stands for significant differences between different scaffold formulations on the same culture day ($p < 0.05$); (#) represents significant differences between the same scaffold formulation on different culture days ($p < 0.05$). 70

Figure 3.14. SEM micrographs showing the overall ECM distribution over the scaffolds after 1, 14 and 21 days in culture with differentiation medium. Arrows point out ECM aggregates. 72

CHAPTER I

GENERAL INTRODUCTION

Table 1.1. Structural scaffold design criteria and their corresponding function for engineered tissues (adapted from [14]).	6
Table 1.2. Types of biomaterials used in cartilage TE and some example references.	7
Table 1.3. Types of polymer blend [122].	8
Table 1.4. Examples of CHT/PCL blend 3D scaffolds developed.	14
Table 1.5. Spinning techniques.	16
Table 1.6. Example of fiber-based scaffolds studied for applications in the cartilage TE field.	20
Table 1.7. Some examples of CHT and PCL 3D scaffold studies for cartilage TE applications, with the respective construction methodology and cell source used.	21

CHAPTER II

MATERIALS AND METHODS

Table 2.1. Total polymer concentration of each formulation [14].	36
Table 2.2. Method used for the safranin-O and alcian blue stainings performed.	43

CHAPTER III

CHITOSAN/POLY(ϵ -CAPROLACTONE) BLEND SCAFFOLDS FOR CARTILAGE REPAIR

Table 3.1. Total polymer concentration of each formulation [17].	53
Table 3.2. Mechanical properties of the scaffolds (standard deviation error also presented and (*) stands for statistical significant difference between formulations with $p < 0.05$) and their estimated and exemplificative porosity and pore size, obtained from the μ CT analysis to the representative selected volumes presented on Figure 3.5 (g – i).	64

CHAPTER I

GENERAL INTRODUCTION

1. GENERAL INTRODUCTION

1.1. MOTIVATION AND CONTENT

Every year, millions of people suffer from tissue damage or even tissue loss. Thus, TE is an evolving field with a great potential on providing permanent solutions for these problems ^[1]. The principles of TE rely on the use of (a) builders of neo-tissue - cells -, (b) a structure for them to work - scaffolds -, (c) and all supporting factors that help cells to work – biomolecules -, alone or in combination. Engineering cartilage tissue is no exception to this approach and, additionally, it is one of the ideal candidates for TE, as it differs from other tissues on its limited capacity of self-repair ^[2]. Tissue regeneration is important for all cartilage types but young population is becoming more active, obesity problems are growing and population is aging. Therefore, regenerating defects that result from traumatic injury or degenerative joint diseases, i.e. AC (hyaline) problems, have a major impact on patients ^[3].

The scaffold interaction with cartilage cells and/or tissue is a complex equation and a lot of research has been done in order to process the ideal AC TE support structure. There is a wide range of parameters to have in consideration and every kind of scaffold has its own drawbacks. Therefore, one of the goals of TE relies also on processing simple but functional structures that can match some specific needs for the different problems that emerge from AC problems.

The work presented on this thesis aims to process CHT/PCL blend fiber-based scaffolds and to assess their potential in AC TE. The reason for blending these two polymers relies on their individual but potentially complementary characteristics, as a result from their already studied individual AC TE applications potential. The choice of a fiber-based 3D system is justified by the capability that the structure proposed presents, due to structural resemblance of fibers with the native AC ECM architecture. The process presented to obtain the scaffolds is very simple, when compared to other systems.

The present chapter provides an overview about the research work that has been done about supporting structures for cartilage TE, along with the potential of biodegradable polymers and fiber-based structures.

1.2. ENGINEERING CARTILAGE TISSUE

AC is a predominantly avascular, aneural and alymphatic tissue. It is biochemically comprised of water, sparsely distributed chondrocytes (1 - 10%), embedded within a dense ECM, and composed of primary COL2 and aggrecan, a highly glycosylated molecule with net negative charge [4-6]. Each AC zone is particularly defined by a certain cell and ECM molecules composition and organization (Figure 1.1) [7]:

- Superficial zone – chondrocytes are flattened, collagen fibrils are parallel to surface and there is a high cell density;
- Transitional zone – chondrocytes are round, collagen fibrils are thick and less parallel;
- Radial zone – chondrocytes are ordered in vertical columns, collagen fibrils are thick and perpendicular to surface and it has the greatest aggrecan content;
- Calcified zone – it is a zone of mineralized tissue, hypertrophic, with circular chondrocytes.

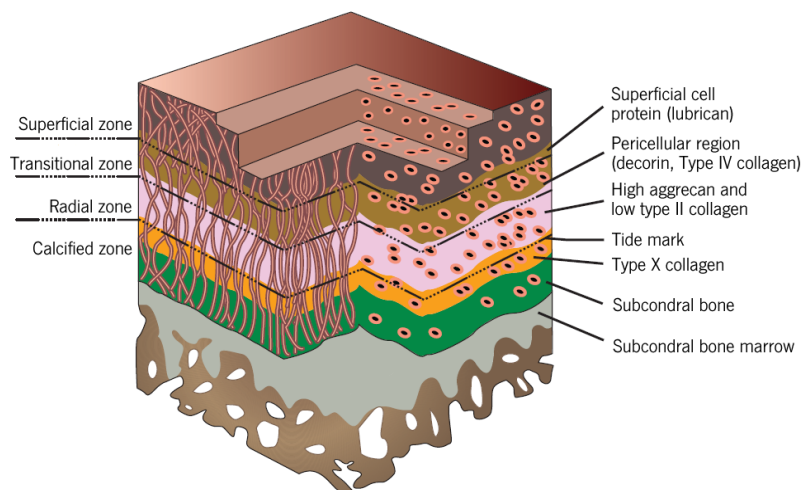


Figure 1.1. Articular cartilage structural and functional zones (adapted from [8]).

In all regions of the tissue, a highly interconnected matrix of collagen fibrils, on which aggrecans, bound in large numbers to HA chains, form proteoglycan aggregates. These aggregates raise the osmolarity of the tissue, which triggers a water influx. The consequent swelling is balanced by the resistance of the collagen matrix, generating large internal pressure, and giving AC its particular mechanical properties *in vivo* [4].

The origin of cartilage difficulty on self-repair seems to derive mainly due to the lack of a vasculature network, resulting in (a) insufficient turn-over of healthy chondrocytes to the defective sites and (b) low productivity of characteristic proteins of the surrounding ECM [3]. Even when some regeneration exists in adult AC, a different tissue is formed in the defect – fibrocartilaginous-like tissue [9-11] – which possesses lower mechanical properties compared to native AC. This compromises its physiological functional role,

i.e., shock absorbance, load bearing and reduction of surface friction, on the terminal parts of the bones, where it creates smooth gliding areas [12]. Therefore, the approach to overcome these problems can rely on the TE basis referred above: the use of *ex vivo* culture techniques, associated to supportive structures [13], focused on the regeneration of original cartilaginous tissue to restore the normal functional role of cartilage.

Although is not possible to cover (in this thesis) all AC TE studies performed, as a wide range of approaches was investigated to date, Figure 1.2 summarizes and illustrates the main steps that are being taken towards the production of engineered cartilaginous tissue [3].

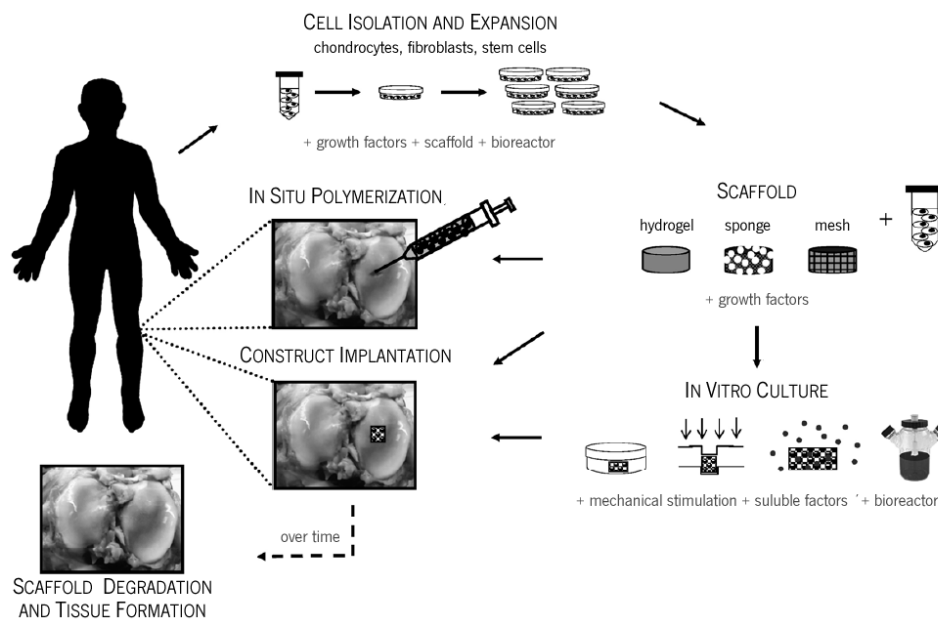


Figure 1.2. General schematic of methodologies used in cartilage TE: from injectable systems to *in vitro* culture before implantation (adapted from [3]).

1.3. THE ROLE OF THE SCAFFOLD IN CARTILAGE TISSUE ENGINEERING

The use of processed or preserved allograft and homograft tissues was one of the earliest used approaches for tissue replacement. These are usually obtained from cadaveric sources and cryo-preserved without chemical cross-linking, in order to control biological function for transplantation into another individual. However, even if tissues present in the body are the ideal scaffolds in their *in vivo* form and function, using these as ECM-based scaffolds has several drawbacks. Namely, the implant function can be hindered by an acute or chronic immunogenic host response, which results from host recognition of antigens. Additionally, processing methods for these materials may lead to inconsistencies between specimens, resulting in different degradation behaviors and mechanical responses. Therefore, using biodegradable synthetic support structures can circumvent pathogen transmission and immune system concerns associated, for instance, to collagen-based tissues from

animal or cadaver sources. The scaffold design in TE represents an approach “from the beginning to the end”, i.e., the supports are designed with the desired mechanical and physical-chemical characteristics, in a reproducible and controlled way, trying to mimic the native ECM structure and function [14].

To overcome 2D culture limitations, which can alter cell metabolism and reduce cell functionality [15-18], 3D cell culture matrices – the scaffolds - were introduced. These porous substrates can support cell growth and tissue formation on or within their structure. As many different kinds of tissues exist, different and more diversified cellular supports are needed. The scaffolds meet this needed higher material and structural diversity, when compared to 2D substrates. Some common 3D characteristics (Table 1.1) of interest comprise surface topography, to promote cell attachment, a highly porous microstructure, to allow tissue ingrowth, and a well interconnected porous network, allowing adequate nutrient transport, all while keeping a desired mechanical behavior.

Table 1.1. Structural scaffold design criteria and their corresponding function for engineered tissues (adapted from [14]).

SCAFFOLD DESIGN CRITERIA	RESULTING FUNCTION IN ENGINEERED TISSUE
biological compatibility	
non-thrombogenic	non-toxic and minimal inflammatory response
non-immunogenic	
low or zero toxicity (degradation products)	
3D matrix architecture	physiologically relevant environment for cell function; known multi-scale architectural features mediating macro-micro transmission of force
void space	highly porous and interconnected pores allow cell infiltration, transport factors, humoral factors and waste products
surface chemistry and topography	cell attachment and cell-matrix interactions
degradation rate	scaffold gives away to functional matrix formation
structural anisotropy	anisotropic mechanical behavior; influence orientation of cells and ECM deposition
appropriate mechanical behavior	seamless integration with surrounding tissue(s), able to withstand <i>in vivo</i> forces and avoid stress shielding

Scaffolds are particularly important for cartilage tissue regeneration approaches as the chondrogenic phenotype is maintained when chondrocytes are placed in a proper 3D environment. During cartilage development and growth, chondrocytes produce abundant matrices and encase themselves within cavities (named vacuoles) [19]. In contrast, chondrocytes isolated from the physiological 3D cartilaginous environment and expanded in 2D surfaces rapidly de-differentiate, losing the typical phenotype and protein synthesis [20]. Therefore, in cartilage TE, chondrocytes isolated from their original tissues would be ideally conditioned in a 3D environment mimicking the physiological cartilaginous milieu with a favorable scaffold, to maintain their functions and enhance protein synthesis [13].

1.4. BIODEGRADABLE POLYMERS IN CARTILAGE TISSUE ENGINEERING

The scaffold design characteristics referred before are intrinsically related to the material that the scaffold is made of. A wide range of naturally derived and synthetic materials have been investigated as scaffolding materials to be used in cartilage TE (Table 1.2).

Table 1.2. Types of biomaterials used in cartilage TE and some example references.

NATURAL-BASED POLYMERS		SYNTHETIC POLYMERS		SELF-ASSEMBLING PEPTIDES	
agarose	[21-25]	fibrin glue	[53-56]	PE	[71-96] [115-118]
alginate	[26-30]	gelatine	[57-59]	PEO	[97-102]
cellulose	[31,32]	hyaluronic acid	[60-65]	PNiPAAm	[103-105]
collagen	[10,33-36]	silk fibroin	[66-70]	PPF	[55,106-108]
chitosan	[37-49]			PU	[109-111]
chondroitin sulphate	[50-52]			PVA	[112-114]

1.4.1. POLYMERS FROM NATURAL ORIGIN

The growing interest in natural based polymers to be used in TE relies on their economic and environmental aspects. These have their basis on the material biodegradability, low toxicity, low manufacture costs, low disposal costs and renewability [119,120]. In addition, they offer a wide range of advantages in TE applications such as biological signaling, cell adhesion, cell responsive degradation and re-modeling. However, the inadequate physical properties of natural polymers that are soluble or rapidly degrade due to variable enzymatic host activity, along with the possible loss of biological properties during formulation, often compromise their use as unique scaffold material. Furthermore, proper screening and purification becomes necessary due to the risk of immune-rejection and disease transmission [120].

1.4.2. SYNTHETIC POLYMERS

Synthetic polymers are more controllable and predictable than naturally derived polymers, whereas chemical and physical properties of the polymer can be tailored to match specific mechanical and degradation characteristics. The wide range of different copolymers, polymer blends and composites with other materials, such as with bioceramics, broadens the group of properties of this class of materials. Moreover, risks like toxicity, immunogenicity and infections are much lower for pure synthetic polymers. However, they do not benefit from direct cell-scaffold interactions (unless specifically incorporated binding sites) that could promote the desired cell response, which are proven to play a role on cell adhesion, cell signaling, among others. In addition, some degradation products may be toxic or elicit an inflammatory response [3].

1.4.3. BLENDING NATURAL AND SYNTHETIC POLYMERS

A polymer blend is, by definition, a physical mixture of two or more different polymers or copolymers that are not linked by covalent bonds. Some desired material properties can be achieved just by mixing two or more existing polymers. The main objective of blending polymers is not to cause a drastic shift on their properties, but to overcome certain drawbacks that they present when acting alone, getting the most out of the individual components. Some of the techniques used to prepare polymeric blends are summarized in Table 1.3.

Table 1.3. Types of polymer blend [122].

BLEND TYPE	DESCRIPTION
MECHANICAL BLEND	Polymers are mixed at temperatures above T_g or T_m for amorphous or semi-crystalline polymers, respectively
Mechano-chemical blend	Polymers are mixed at shear rates, high enough to cause degradation. Resultant free radicals combine to form complex mixtures, including block and graft components
Solution-cast blend	Polymers are dissolved in common solvent and the solvent is removed
Latex* blend	Latexes are mixed and the mixed polymers are coagulated
CHEMICAL BLEND	
Interpenetrating polymer networks (IPN)	Crosslinked polymer is swollen with different monomer, then monomer is polymerized and crosslinked
Semi-interpenetrating polymer networks (semi-IPN)	Polyfunctional monomer is mixed with thermoplastic polymer, then monomer is polymerized to network polymer
Simultaneous interpenetrating polymer networks (SIN)	Different monomers are mixed, then homopolymerized and crosslinked simultaneously, but by non-interacting mechanisms
Interpenetrating elastomeric networks (IEN)	Latex polyblend is crosslinked after coagulation

(* Latex – fine dispersion of polymers in water)

Blending natural and synthetic polymers has been a more widely investigated field than the blends of fully natural or fully synthetic polymeric, as an effort to overcome certain drawbacks presented by both sources of materials. The main reasons rely on the fact that, typically, mechanical properties and durability can be enhanced by the synthetic component, and biological functionalities ensured by the natural one [123].

As an example, the biocompatibility improvement of the synthetic polymer PCL for cartilage TE applications was studied by Kuo-Yung Chang *et al.* [124], blending it with a biomacromolecule - γ -PGA-g-CS – and processing porous scaffolds by salt-leaching. The results showed that the water-binding capacity and degradation rate of the blend scaffolds substantially increased. Furthermore, a larger amount of secreted GAGs was present in the blend scaffolds, when compared to the pure PCL scaffolds. Therefore, not only the water-uptake capacity increased, but also the chondrogenic capacity of PCL was enhanced. Other examples of processed blends, with resulting synthetic polymer enhanced

biocompatibility, comprise PBS/CHT [125] surfaces (by injection molding) or PLGA/HA [126] porous scaffolds (by freeze-drying and particle-leaching).

In fiber processing methodologies, blending natural and synthetic polymers is not only performed to enhance the natural polymer spinnability, but also to improve the synthetic polymers biocompatibility. The enhancement of *in vitro* osteoblastic responses of PCL were studied by Lee *et al.* [127], processing PCL/COL1 electrospun blend nano-fibers. Different compositional non-woven fibrous matrices were obtained and, due to spinnability performance, the 50:50 wt.% of PCL/collagen blend was chosen for the studies. The PCL nano-fibers showed hydrophobic character but the incorporation of collagen significantly improved the water affinity, such as the water contact angle and water uptake capacity. Tensile mechanical tests showed that the blend nano-fiber had a significantly higher extension rate (approximately 2.8-fold) than the PCL, while maintaining the maximum tensile load in a similar range. The osteoblastic cells cultured on the PCL/COL1 nano-fibrous substrate showed better initial adhesion and a higher level of growth than those cultured on the PCL nano-fiber. Furthermore, RT-PCR revealed the expression of a series of bone-associated genes. The expression of these genes was significantly higher on the PCL/COL1 nano-fiber than on the PCL nano-fiber. When subcutaneously implanted in mouse, the blend membrane facilitated tissue cells to penetrate into the nano-fibrous structure at day 7, whilst no such cell penetration was noticed in the pure PCL nano-fiber.

A wide range of other studies were carried out, using electrospun blend nano-fibers of natural and synthetic polymers, with a resulting synthetic polymer improved bioactivity, like PGA/chitin [128,129], PEO/CHT [130], PCL/gelatine [131], PLCL/COL1 [132], PLCL/gelatine [133] and PLLA/gelatine [134] blends.

1.4.4. CHITOSAN AND POLY(ϵ -CAPROLACTONE)

CHITOSAN

Among naturally derived polymers, CHT has been found as an excellent candidate in a broad spectrum of TE applications. Besides its low cost and easy availability (it is derived from partial deacetylation of chitin, the second most abundant natural polymer - after cellulose -, found, for example, in arthropod exoskeletons) [135-138], it possesses unique biological properties like biocompatibility, biodegradability to harmless products, non-toxicity, physiological inertness, remarkable affinity to proteins, along with antibacterial, haemostatic, fungistatic, anti-tumoral and anti-cholesteremic properties [139-145].

CHT is a linear polysaccharide of β (1-4)-linked *D*-glucosamine and *N*-acetyl-*D*-glucosamine residues (Figure 1.3). The ratio between glucosamine and *N*-acetyl-glucosamine indicates the degree of deacetylation of CHT. Its MW may vary from 300 to over 1000kDa and the deacetylation degree from 30 to 95%, depending on the source and preparation procedure.

Much of CHT potential as a biomaterial derives from its cationic nature and high charge density in solution, as the first is primarily responsible for electrostatic interactions with anionic GAGs, proteoglycans and negatively charged molecules [146]. The ideal cell-carrier substance for AC TE applications should mimic the natural environment in the AC matrix, as cartilage-specific ECM components, such as the already referred COL2 and GAGs. These had been shown to play an important role on regulating expression of the chondrogenic phenotype and supporting chondrogenesis, both *in vitro* and *in vivo* [147,148]. Therefore, CHT structural resemblance with HA and various GAGs found in AC makes it an elite natural scaffolding material in AC TE [149]. Moreover, *in vitro* studies showed that CHT-based matrices efficiently supported chondrogenic activity [149] and that they also allowed the expression of cartilage ECM proteins by chondrocytes [37]. Chondrocytes may also maintain their inherent round morphology when cultured in CHT scaffolds [40]. CHT can also be enzymatically degraded *in vivo* by lysozyme [150,151], which is a polycationic protein present in the ECM of AC [152,153]. This polysaccharide is also a polymer with a hydrophilic character [123,136]. The main drawback of CHT, and in particular for AC TE applications where the mechanical properties are of great importance, is its brittleness in the wet state (with a strain break of 40-50%) [154]. It would be also of relevance to reduce CHT relatively fast degradation rate to allow enough neo-tissue formation before it is completely resorpted by the organism [155].

POLY(ϵ -CAPROLACTONE)

Among the above mentioned synthetic biomaterials, the semi-crystalline linear aliphatic polyester PCL (Figure 1.3) is of interest, due to its soft- and hard-tissue applications compatibility (skin [156] and bone [157], for example), its physical-chemical characteristics (specially its mechanical properties), and a relatively low melting point (ca. 60°C) [154], which allows easy processing. Its degradation products, which result from the susceptibility of its aliphatic ester linkage to hydrolysis, are non-toxic and can be either metabolized via the tri-carboxylic acid cycle or eliminated by direct renal secretion. Extensive studies have been performed about its *in vitro* and *in vivo* biocompatibility and efficacy, resulting in the Food and Drug Administration (FDA) approval for a number of medical and drug delivery devices [108,123,158-162]. Chondrocytes have been proven to attach and proliferate over PCL films [163], and showed ECM production over PCL scaffolds [93,164]. Similarly, MSCs could be differentiated into the chondrogenic lineage on PCL scaffolds, with consequent ECM production [165]. Nevertheless, like other kinds of biodegradable polyesters, biomedical applications for PCL can be hindered by several drawbacks [166] inherent to its structure, like (a) the absence of cell recognition sites over PCL-based materials, (b) hydrophobicity, (c) neutral charge contribution and (d) possible acidic degradation products. Moreover, degradation and resorption kinetics of PCL are considerably slower than other aliphatic polyesters, due to its high crystallinity degree [167].

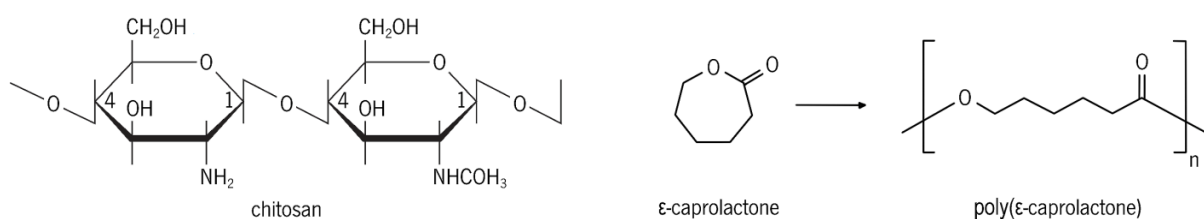


Figure 1.3. Chitosan and poly(ϵ -caprolactone) (derived from ϵ -caprolactone molecule) structures (adapted from [168] and <http://en.wikipedia.org/wiki/File:PolycaprolactoneSynthesis.svg>, respectively).

1.4.5. BLENDING CHITOSAN AND POLY(ϵ -CAPROLACTONE)

Besides the ability of both CHT and PCL to support normal chondrogenic activity under specific *in vitro* culture conditions [37,93,151], studies performed on PCL/natural polymer combination [169] also showed an enhancement on the referred bioactivity. Moreover, blending CHT with synthetic polymers has also proven to overcome the poor mechanical properties of the pure polysaccharide [154,170,171].

The above mentioned characteristics are a basis on the hypothesis that both polymers seem to have complementary potential for possible applications in cartilage TE field. Thus, there is a reasonable expectation that their individual deficiencies would be surpassed if PCL and CHT could be blended

together. Furthermore, CHT hydrophilic nature would provide a biomaterial with enhanced water and water soluble substances permeability, and consequently an acceleration of PCL hydrolytic degradation. On the other hand, PCL would lower the swelling ratio of the composite material and, at the same time, improve the mechanical properties of CHT in its wet state [172].

Over the time there have been used different methodologies to combine PCL with CHT. If we would like to add the functionality of CHT functional groups to PCL, grafting or graft-copolymerization would be a possible strategy. However, it is known that grafting of CHT occurs on the amine groups, thus hindering its cationic and biological properties [173]. Chung *et al.* [174] circumvented the referred loss of bioactivity and successfully grafted CHT over PCL films, cross-linking the CHT in order to preserve the referred bioactivity - FTIR analysis showed amine groups present on the films surface. Moreover, the grafting promoted the proliferation of hGFs over the films, when compared to non-grafted PCL surface. However, the use of cross-linking agents should be minimized, even if genipin crosslinked products have been demonstrated to be less toxic than those by glutaraldehyde [175,176].

Melt-processing, even if possible, is not the ideal processing method as well, due to the different thermal-chemical properties of the two polymers: CHT has a high glass transition temperature and decomposes before melting [177]; on the other hand, PCL has a relative low melting temperature.

In consequence, from the reasons referred before, solution mixing seems to be the best and simpler current choice for combining CHT and PCL, as it allows the co-existence of the two polymers with minimal chemical modification, and may increase the dispersion degree and homogeneity of both polymer phases [154]. However, common solvents for CHT and PCL are scarce. The use of HFIP as solvent for both polymers [178-180] has proven that it is possible to obtain CHT/PCL cast blend films. However, HFIP is a very toxic, carcinogenic, and expensive solvent, difficult to remove [181], and its use should be minimized. Blend films of CHT/PCL were also obtained, using glacial AcA to dissolve PCL and 0.5M aqueous AcA solution to dissolve CHT [154]. The authors stated that the blends were miscible for all compositions, but the mechanical properties were not improved due to the low polymeric concentrations used. A study where polymer concentration was increased was performed, but in this case phase separation was detected [182].

As in a blend the polymeric entities co-exist, phase separation would be expected after the processing of the blend solutions, i.e., when the desired structure is obtained. However, it is undesirable that this happens during the blend solution preparation and this occurs when mixing the glacial AcA/PCL and aqueous AcA/CHT solutions, as PCL precipitates due to the presence of water [183].

CHT/PCL blend 3D scaffolds for TE applications have been previously developed [154,183-185] (Table 1.4). Sarasam *et al.* [154] tried to obtain structures by freeze-drying, but they did not reproduce the mold

structure, neither achieved the desired structural stability. This was attributed to solvent used - 77% aqueous AcA solution. More recently, the same authors [184] reported the processing of 3D structures by freeze-gelation and extraction or by freeze-drying with a different solvent system – 25% aqueous AcA solution. The only scaffolds that showed some structural integrity were those obtained by freeze-drying. Even so, the stability and pore morphology of those was proven to be dependent on the relative mass ratio of CHT and PCL [184].

Particle leaching method was tried by Wan *et al.* with sodium chloride (NaCl) particles as porogen in two distinct works: using aqueous AcA solution [185] and HFIP [186] as common solvent solutions. On both works, stable structures were obtained with well interconnected pores. After exposing the structures obtained with HFIP to PBS or enzymatic degradation systems *in vitro* for various periods up to 10 weeks, it was observed that degradation of the PCL component could be accelerated at various rates, depending on the compositions of the scaffolds and the media. It was also shown that the CHT component could effectively buffer the acidic degradation products of the PCL component [185].

Houde *et al.*[187] reported the preparation of foam-like CHT/PCL blend structures, using AcA as common solvent. The scaffolds showed a honeycomb-like structure, as a result of viscoelastic phase separation. A high porosity (from 80% to 90%) was achieved and it increased with a corresponding increase of CHT content in the blend, as the super-abundant volumes in the blend solution were mainly determined by CHT.

García Cruz *et al.* [183] prepared semi-interpenetrating polymer networks of CHT and PCL, using AcA as solvent solution, followed by a physical crosslinking of CHT with TPP, in order to entrap the PCL chains. The porous 3D structures were obtained by melt-processing and leaching techniques, using PEO as porogen.

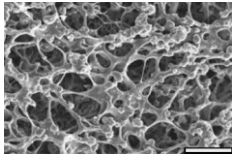
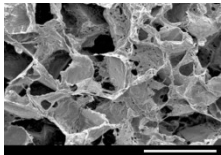
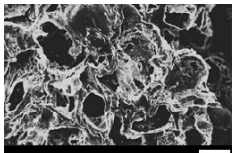
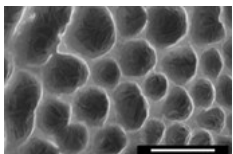
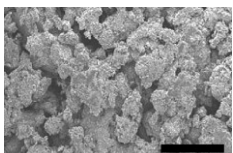
As far as it is known, processing CHT/PCL blend in the form of fibers was only reported for the first time by Prabhakaran *et al.* [188], using and electrospinning as processing technique, for neural TE applications. Schwann cell proliferation increased over CHT/PCL blend fibers when compared to pure PCL. However, distinct solvents were used for each polymer, which can compromise the miscibility of the components of the blends and blends of just one composition were studied. Yang *et al.* [189] also reported the processing of CHT/PCL fibers by electrospinning. Although using HFIP, they showed that the incorporation of CHT in PCL fibers improved osteogenic activity by osteoblasts when compared to pure PCL fibers.

Malheiro *et al.* [177] reported the processing of CHT/PCL non-woven fibers by wet-spinning - CHT, PCL and 25:75, 50:50 and 75:25 wt.% CHT/PCL. They used a new common solvent solution - 70:30 vol.% formic acid/acetone – and showed that a certain degree of interaction between the polymers exists,

although it did not seem to be a result of chemical interaction [177]. Fibers showed roughness and porosity (at the micron-level scale) at their surface that could be potentially advantageous for cell attachment. Preliminary studies on folding the blend fibers in order to obtain 3D fiber-mesh structures for potential TE applications were also performed [177]. This new solvent solution was later used by Shalumon *et al.* [190] to obtain electrospun CHT/PCL blend fibers. None of these two studies assessed the biological potential of the blend fibers processed with the common solvent solution system referred.

As far as it is known, the potential of CHT/PCL blend 3D fiber-meshes was still not evaluated for cartilage TE applications.

Table 1.4. Examples of CHT/PCL blend 3D scaffolds developed.

REFERENCE	PROCESSING TECHNIQUES STUDIED	BLENDS STUDIED AND COMMON SOLVENT SOLUTIONS USED	
Sarasam <i>et al.</i> [154]	freeze-drying	25, 50 and 75 wt.% CHT 77% aqueous AcA	(no consistent structures were achieved)
Sarasam <i>et al.</i> [184]	freeze extraction, freeze gelation and freeze drying	25, 50 and 75 wt.% CHT 25% aqueous AcA	 (freeze-dried; 50 wt.% PCL) (scale bar - 50µm)
Wan <i>et al.</i> [185]	particle-leaching	25, 50 and 75 wt.% CHT 80% aqueous AcA	 (50 wt.% PCL) (scale bar - 200µm)
Wan <i>et al.</i> [186]	particle-leaching	10, 30 and 50 wt.% CHT HFIP solution	 (50 wt.% PCL) (scale bar - 200µm)
Houde <i>et al.</i> [187]	foam-like porous scaffold formed gradually as phase separation occurred during the process	5, 10, 15 and 20 wt.% CHT aqueous AcA	 (80 wt.% PCL) (scale bar - 10µm)
García Cruz <i>et al.</i> [183]	melt-processing and particle leaching	semi-IPN with 10, 20 and 30 wt.% CHT; 0, 30, 45, and 55 wt.% of PEO, as porogen. aqueous AcA; TPP as CHT crosslinking agent	 (10 wt.% CHT) (scale bar - 1mm)

1.5. SCAFFOLD STRUCTURE FOR CARTILAGE TISSUE ENGINEERING

A variety of biomatrices can be achieved with a wide range of fabrication processes and biomaterials, adapted or newly developed, to fabricate support structures meeting a range of different characteristics [18]. The structure of scaffolds can vary between hydrogel, sponge and fibrous mesh-like [3]. Within recent years, fiber-mesh scaffolds started to be used in TE applications [191,192] mainly due to their (a) remarkably increased surface area for cell attachment, (b) improved pore architecture, which provides good pathways for the transportation of cells, metabolites, nutrients, signaling molecules, gases and, of course, waste products of cell activity, both between the scaffold and the local environment, as well as within the scaffold [14,191-194], and (c) good mechanical stability [3].

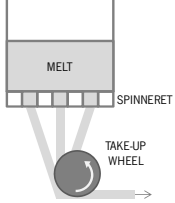
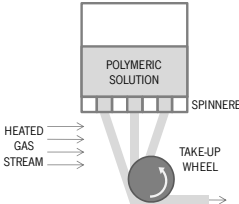
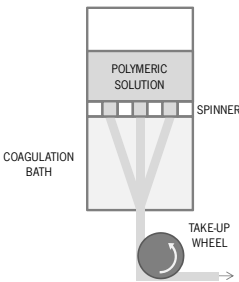
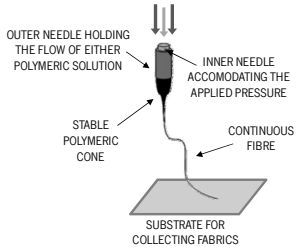
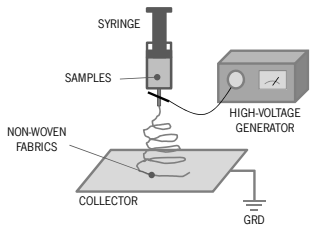
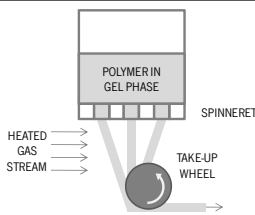
In the cartilage TE field, processing tissue-like tensile mechanical behaviors can be a hard task with non-fibrous scaffolds. This results from the fact that these kinds of scaffolds hardly match the high anisotropic and highly non-linear characteristic response of soft collagenous tissues. On the other hand, fibrous scaffolds have the ability to bear significant tensile loads, while maintaining relatively low bending rigidities. Moreover, they can be manufactured to exhibit varying mechanical behaviors. Long fiber composites also better mimic the native ECM architectures, with the potential to direct 3D tissue formation and organization [195].

1.5.1. FIBER-BASED SCAFFOLDS

The group of methodologies developed for the textile industry can be adapted to be applied in TE applications in order to process cell-invasive fibrous scaffolds. The traditional non-woven textiles fabrication is based in the principle that continuous, micron-diameter fibers can be obtained extruding a polymer melt or polymeric solution through a spinneret and then mechanically drawn onto a winder, or a series of winders, and collected on a spool. The speed(s) of the winder(s) – with a constant drawing rate -, along with the extrusion rate, dictate a continuous and uniform diameter fiber. The extrusion conditions affect polymer properties, namely polymer crystallinity, consequently influencing the degradation behavior and its mechanical strength [196].

The process in which the polymeric solutions are extruded into filaments and hardened is described as “spinning”, a synthetic analogy to the way that spiders and silkworms process their filaments [197]. The processing methods used to process fibers differ from each other in the way that fibers are hardened, from the most traditional processes, like melt-[198,199], dry-[200] and wet-spinning[177,201-208], to the most recent aerodynamically assisted threading [209]: pressure-assisted-[210], electro-[128,211] and gel-spinning [212] (Table 1.5).

Table 1.5. Spinning techniques.

SPINNING TECHNIQUE	SPINNING DOPE	PROCESS SUMMARY	SCHEMATIC REPRESENTATION
Melt-spinning	melt	solidification through cooling of the produced fibers	 <p>(adapted from [213])</p>
Dry-spinning	solution	solvent evaporation by, for example, a stream of hot air	 <p>(adapted from [213])</p>
Wet-spinning	solution	polymer precipitation in a coagulation bath	 <p>(adapted from [213])</p>
Pressure-assisted spinning	solution	a media cone is formed from a pressure-assisted drawing of the flowing polymer medium in the outer needle; consequently, a uniaxial thread emerges from the media cone, by means of stretching the viscoelastic medium.	 <p>(adapted from [210])</p>
Electro-spinning	melt or solution	electric field driven process with fast solvent evaporation	 <p>(adapted from [213])</p>
Gel-spinning	solution	the extruded fibers are firstly air-dried and then cooled in a liquid bath	 <p>(schematic from textual description in [213])</p>

In addition to spinning techniques, SFF and RP can be used to obtain fiber-based scaffolds. These techniques have been applied to fabricate complex-shaped tissue engineered constructs. Conversely to conventional machining, that involves constant removal of materials, SFF is able to build scaffolds by selectively adding materials, layer-by-layer, as specified by a computer program. Each one of these layers represents the shape of the cross-section of the computer-aided design (CAD) model at a specific level. This is a fabrication technology has a great potential for the generation of scaffold technology platforms. Due its computed controlled fabrication, one of the main benefits offered by SFF technology is the ability to create parts with highly reproducible architecture and compositional variation across the entire structure [214].

A number of groups [215-218] have developed SFF machines that can perform extrusion of strands/filaments and/or plotting of dots in 3D with or without incorporation of cells. These systems are built to make use of a wide variety of polymer hot melts as well as pastes/slurries (i.e. solutions and dispersions of polymers and reactive oligomers). Techniques such as FDM, 3D plotting, multiphase jet solidification and precise extrusion manufacturing all employ extrusion of a material in a layered fashion to build a scaffold. Depending on the type of machine, a variety of biomaterials can be used for scaffold fabrication [214].

The biomedical uses of fibers range from the oldest and simplest use of fibers in the medical field – surgical sutures – to 3D fiber-meshes, capable of stimulating isolated cells to regenerate tissues [219,220]. Needed non-woven scaffolds can be manufactured quickly, at relatively low cost, and withstand sterilization processes necessary for *in vivo* use. Isolated cells of a desired lineage can then be seeded and cultured in static or dynamic conditions. As these fiber-meshes are highly porous and exhibit an open pore structure, the seeded cells can easily and quickly infiltrate the structure, leading to a construct populated throughout.

Non-woven textile of PGA/PLLA sheets have been employed to mimic the geometry of the native pulmonary valve and trunk by Sutherland *et al.* [220]. Ovine endothelial progenitor cells were seeded and cultured on the non-woven scaffolds and the obtained constructs were implanted into the pulmonary valve position of a juvenile ovine model. The engineered valve constructs were explanted after 16-20 weeks for histological evaluation. The histological preparations of the ECM architecture interestingly resembled that of native valves notably, with a tri-layered structure of organized tissue.

A modeling framework was developed by Engelmayer *et al.* [221,222] for the flexural properties of these needed non-woven scaffolds, with the main objective of investigate more fundamental mechanisms of tissue evolution in response to mechanical cues and their resulting effects on mechanical behavior. This model accounts for the exclusive fiber morphologies, which result from the manufacturing process and

the production of new ECM, to predict the scaffold effective stiffness during bending, which also corroborated the experimental values. Moreover, ECM deposition during culture led to an increase on scaffold stiffness. This can be attributed to an increased number of fiber-fiber bonds due to ECM production.

In cartilage TE field, different kinds of polymeric matrices (with or without cells) have been tested for their ability to promote cartilaginous tissue repair (Table 1.6). Poly- α -hydroxyl acid based fibrous matrices, for instance, have been widely investigated as AC grafts. PGA fiber-meshes properties and respective seeding and culture conditions were investigated in order to optimize cartilage constructs [78-81]. In order to improve cells distribution throughout the polymeric mesh, like, for example, keep them suspended, synthetic non-woven structures have been combined with some natural derived materials such as alginate, collagen, and Fb. Using this approach, Ameer *et al.* [82] have prepared a hybrid system, consisting on a PGA non-woven mesh coated by Fb gel. After 4 weeks of *in vitro* culture, GAG content in Fb coated PGA mesh scaffolds revealed that this system performed better than the uncoated PGA mesh scaffolds. PLGA meshes were used in a similar study, combined with chondrocytes suspended in alginate gel and tested *in vitro* and *in vivo*. They presented a uniform cell distribution and similar performance regarding expression of aggrecan, COL1 and COL2 [83]. Other researchers have used COL1 for chondrocyte encapsulation and tried to combine this gel with a non-woven PLLA scaffold [84]. This method allowed the encapsulation of a higher number of chondrocytes into the scaffolds quite homogeneously. COL1 has also been used to create web-like structures within PLGA knitted meshes in order to achieve a uniform cell distribution [85]. The bACs seeded on these scaffolds showed a homogenous distribution, maintained their phenotype and filled the void spaces in the scaffolds with ECM. To obtain thicker scaffolds, the cell/composite constructs have been laminated or rolled after one day of culture and implanted subcutaneously in the dorsum of athymic nude mice. *In vivo* results have demonstrated the formation of AC after 12 weeks of implantation.

Cell migration and homogenous ECM production throughout the scaffolds had been enhanced through the use of bioreactors during the *in vitro* experiments, as a result of an improved nutrient transfer. These systems have been successfully applied for creating a tissue engineered cartilage constructs using fiber-based scaffolds. Davisson *et al.* [86] reported the positive effect of perfusion on cell content and ECM production by bACs cultured over PGA scaffolds. The synthesis of sulphated GAGs has been found to be 40% higher when compared to static conditions. Griffon *et al.* [87] compared two different dynamic culturing techniques for culturing pACs over a scaffold composed of PGA mesh or CHT sponge. Using a vacuum-reactor system, cell attachment to these scaffolds has proven to be better and more uniform. Within the last years, biodegradable non-woven nano-fibers processed by

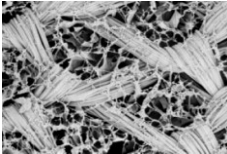
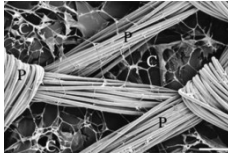
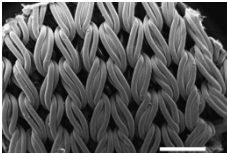
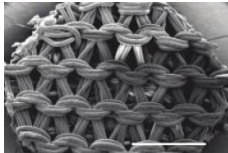
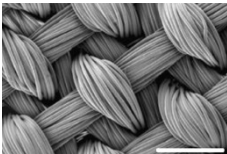
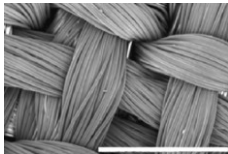
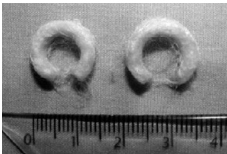
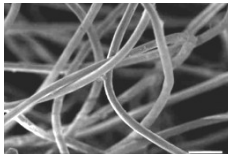
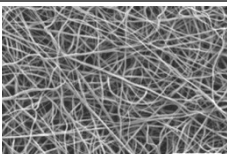
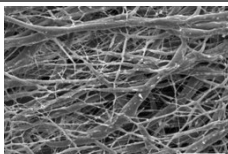
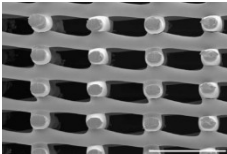
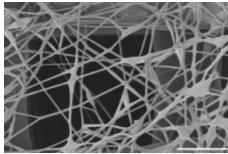
electrospinning have started to be studied as cartilaginous tissue regeneration support [71,72,88,91,96,97]. Li *et al.* [71] study reported that chondrocytes seeded onto nano-fibrous PCL-based scaffolds proliferated and efficiently maintained their differentiated phenotype, as indicated by the expression of cartilage-associated genes. Later [88] they also proved that these nano-fibrous meshes significantly enhanced the chondrogenic differentiation of hMSCs, compared to cell pellet culture system, which is a widely used culture protocol for studying chondrogenesis of MSCs. PLGA nano-fibrous mats chondrogenic potential was also assessed by Shin *et al.* [72], using freshly isolated pACs. The scaffolds were non-toxic, and cell proliferation and ECM formation in nano-fiber scaffolds were superior to those in membrane-type scaffolds. Moreover, intermittent hydrostatic pressure applied to the cell-seeded nano-fiber scaffolds increased chondrocyte proliferation and ECM formation. *In vivo* studies using PLG electrospun 3D constructs showed that these were capable to repair a 5mm osteochondral defect created in a rabbit model without exogenous cultured cells. In contrast, the non-treated defect (filled with hematoma as control) showed irregular and not so well organized tissue.

The application of RP techniques in AC TE can be exemplified by Huang *et al.* [223] and Moroni *et al.* [224,225] studies. Huang *et al.* [223] processed a biphasic implant made of PCL scaffold, obtained by FDM, in combination with TGF- β 1-loaded Fb glue. They wanted to determine whether the implant made of a PCL scaffold and TGF- β 1-loaded Fb glue could recruit MSCs and induce the process of cartilage formation when implanted in ectopic sites of 6 month-old Zealand White rabbits. All specimens revealed that the entire pore space of the scaffolds was filled with tissue. The entire volume of the scaffolds in the groups loaded with TGF- β 1 and implanted intra-muscularly and sub-cutaneously was populated with MSCs surrounded with an abundant ECM and blood vessels. The scaffold loaded with TGF- β 1 and implanted sub-periosteally was found to be richly populated with chondrocytes at 2 and 4 weeks and immature bone formation was identified at 6 weeks. Thus, the scaffolds loaded with TGF- β 1 could successfully recruit MSCs and that chondrogenesis occurred when this construct was implanted sub-periosteally.

Moroni *et al.* [224] processed 3D scaffolds fabricated by combining 3D fiber deposition (3DF) (a SFF technique) and electrospinning. Scaffolds consisted of integrated 3DF periodical macro-fiber and random electrospun micro-fiber networks (3DFESP). The 3DF scaffold provided structural integrity and mechanical properties, while the electrospun network worked as “sieving” and cell entrapment system offering, at the same time, cues at the ECM scale. Primary bACs were isolated, seeded, and cultured for four weeks on 3DF and 3DFESP scaffolds to evaluate the influence of the integrated electrospun network on cell entrapment and on cartilage tissue formation. 3DFESP scaffolds enhanced cell entrapment as compared to 3DF scaffolds. This was accompanied by a higher amount of ECM and a

significantly higher GAG/DNA ratio after 28 days. SEM analysis revealed rounded cell morphology on 3DFESP scaffolds. Spread morphology was observed on 3DF scaffolds, suggesting a direct influence of fiber dimensions on cell differentiation. Furthermore, the electrospun fibers surface topology also influenced cell morphology.

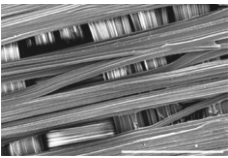
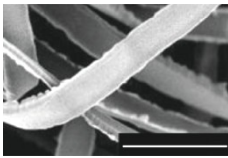
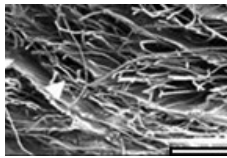
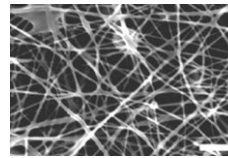
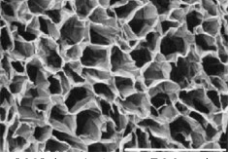
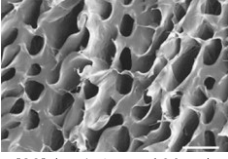
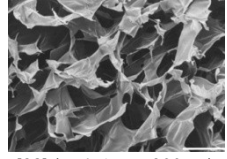
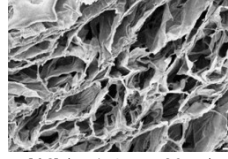
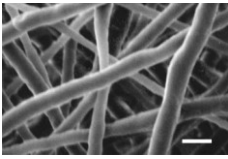
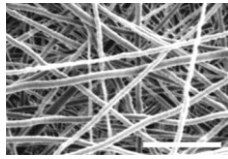
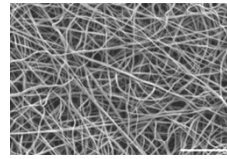
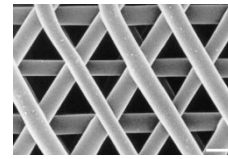
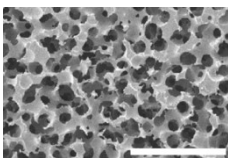
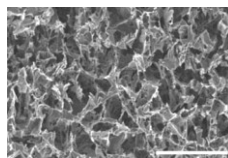
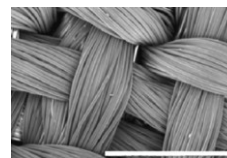
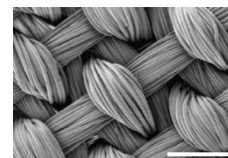
Table 1.6. Example of fiber-based scaffolds studied for applications in the cartilage TE field.

		BIOMATERIALS	SCAFFOLD STRUCTURE DESCRIPTION	SCAFFOLD REPRESENTATIVE IMAGE AND CELL SOURCE USED	
KNITTED		PLGA COL1	web-like COL1 micro-sponges formed in the openings of a mechanically strong knitted mesh of PLGA [85,226]	 bAC [85] (90x mag.)	 hMSC [226] (scale bar - 100µm)
		PLDLA	three knitted PLDLA layers [227,228]	 bAC [227] (scale bar - 1000µm)	 pAC [228] (scale bar - 2000µm)
		PCL	3D orthogonally woven multi-filament PCL yarns, by interlocking multiple layers [89,90]	 hASC [89] (scale bar - 500µm)	 hMSC [90] (scale bar - 1000µm)
NON-WOVEN		PLGA COL1	non-woven PLGA mesh in "C" shape (composed by disassembled polyglactin 910 (Vicryl) sutures) and enforced by COL1 [229]	 sNS and <i>in vivo</i> study [229] (scale bar - 50µm)	
		PCL SPCL	non-woven electrospun nano-fiber meshes [91]	 (PCL)	 (SPCL)
				bACs [91] (scale bars - 50µm)	
RAPID-PROTOTYPING		PEOT PBT	scaffolds processed by 3DF incorporated with electrospun nano-fibers [225]	 [224] (scale bar - 1mm)	 bACs [225] (scale bar - 200µm)

1.5.2. CHITOSAN OR PCL BASED SCAFFOLDS IN CARTILAGE TISSUE ENGINEERING

As previously referred, CHT and PCL have a high complementary potential for being used in cartilage TE. Table 1.7 summarizes some scaffold examples of both polymers studies in cartilage TE filed, along with the methods used for the 3D structures processing.

Table 1.7. Some examples of CHT and PCL 3D scaffold studies for cartilage TE applications, with the respective construction methodology and cell source used.

CHITOSAN			
3D fibrous structure			
3D structure composed by fiber-sheets; fibers obtained by wet-spinning	3D non-woven; replica molding	3D nano-micro fibrous matrix; electrospinning of nano-fibers over extruded micro-fibers sheets	nano-fibrous matrix; electrospinning
rACs	pACs	bACs	HTB-94 *
			
[42] (scale bar – 500µm)	[43] (scale bar – 50µm)	[44] (scale bar – 500µm)	[45] (scale bar – 1µm)
sponge-like 3D structure			
freeze-drying			
	pACs		ATDC5 **
			
[40] (scale bar – 500µm)	[39] (scale bar – 100µm)	[38] (scale bar – 200µm)	[46] (scale bar – 30µm)
PCL			
3D fibrous structure			
	electrospinning		rapid prototyping (FDM)
fbCs	hBMMSCs [218]	bACs	<i>in vivo</i> study
			
[71] (scale bar - 1µm)	[88] (scale bar - 10µm)	[91] (scale bar - 50µm)	[223] (scale bar - 500µm)
sponge-like 3D structure		3D woven	
(a) fabrication of a template of interconnected PEMA microspheres; (b) introduction PCL; (c) elimination of the template by a selective solvent		modified melt-molding particulate-leaching and consequent freeze-drying	
		multi-filament PCL yarns weaved by a custom built-in loom	
hACs	hATMSCs [95]; hBMMSCs [167]	hMSCs	hASCs
			
[93] (scale bar – 1000µm)	[95] (scale bar – 500µm)	[90] (scale bar – 1000µm)	[89] (scale bar - 500µm)

(* HTB-94 - human chondrocytes cell line; ** ATDC5 - murine chondrogenic cell line)

In cartilage TE field, there are few studies that correlate (a) CHT or PCL, (b) the scaffold structure and (c) chondrogenic activity. Therefore, Ragetly *et al.* [41] and Wise *et al.* [92] studies must be highlighted as they compare, respectively, CHT and PCL fiber-based scaffolds with other kinds of porous structures, in terms of their structural impact on the referred bioactivity.

Ragetly *et al.* [41] evaluated the influence of CHT-based scaffolds microstructure on MSC proliferation and chondrogenesis. They compared two kinds of scaffold structures: wet-spun CHT micro-fibers and CHT freeze-dried sponges. On both scaffolds, MSCs viability was maintained above 90% and cell number was similar for all time-points (up to 21 days of culture). However, matrix production was improved in fibrous CHT constructs, based on the GAGs quantification and COL2 mRNA expression.

The potential of PCL fibrous scaffolds was also evaluated by Wise *et al.* [92]. They compared oriented electrospun PCL nano-fibrous scaffolds with a simple non-electrospun randomly porous PCL film. Based on the assessment of chondrogenic markers, the use of the nano-fibrous scaffold (500 nm) appeared to enhance the chondrogenic differentiation. These findings indicated that hMSCs seeded over a structurally controllable PCL scaffold may lead to an alternate methodology to mimic the cell and ECM organization that is found, for example, in the superficial zone of AC (Figure 1.1).

As far as it is known, the combination of CHT and PCL and its evaluation for cartilage TE applications was only performed by Schagemann *et al.* [47,48] and Casper *et al.* [49]. The first [47] processed hybrid scaffolds constituted by PCL macroporous scaffolds and naturally derived polymer gels – HA, CHT, F and COL1. These hybrids were seeded with rACs and cultured statically from up to 50 days. The sulphated GAGs *per* DNA increased in all hybrids between days 25 and 50 and PCL/HA scaffolds consistently promoted highest yields. In contrast, total sulphated GAG and total COL2 decreased in all hybrids except PCL/CHT, which favored increasing values and a significantly higher total COL2 at day 50. These hybrids provided distinct short-term environments for implanted chondrocytes, with not all of them being explicitly beneficial (PCL/F, PCL/COL1). However, the PCL/HA and PCL/CHT hybrids promoted specific neo-cartilage formation and initial cell retention. Later, Schagemann *et al.* [48] studied the effect of these scaffolds composition on the early structural characteristics of chondrocytes and expression of adhesion molecules.

On its turn, Casper *et al.* [49] tried to determine the potential of periosteal cells to infiltrate PCL nano-fiber scaffolds – with or without CHT-coating *in vivo* - and subsequently produce cartilage *in vitro*. The scaffolds were implanted under periosteum in 6-month-old rabbits. After 1, 3, 5 or 7 days, scaffolds were removed, separated from the periosteum, and the scaffolds and periosteum were cultured separately for 6 weeks under chondrogenic conditions. Sulfated GAG, COL2 and DNA content, cartilage yield, and calcium deposition were then analyzed. Cell infiltration was observed in all the scaffolds and

cartilage formation in the uncoated scaffolds increased with duration of implantation (maximum at 7 days). Cells in the uncoated scaffolds implanted for 7 days produced significantly higher levels of both GAGs and cartilage yield compared to CHT-coated scaffolds. Having in consideration the well-known properties of CHT and its favorable studied characteristics in chondrogenic activity, these results are contradictory, as also the authors stated: while it is possible that the CHT-coating may have slowed cellular infiltration into the PCL nano-fiber scaffolds, resulting in decreased *in vitro* chondrogenesis, it is also possible that the CHT-coating inhibited cell proliferation and/or chondrogenic differentiation. The observed lack of chondrogenesis in the CHT-coated scaffolds is also in contrast with their previous results, which demonstrated CHT coating of macro-porous PCL scaffolds resulted in higher GAG production from seeded hACs (unpublished results), as well as published reports demonstrating that CHT supports chondrocyte differentiation [145,102]. However, these apparently conflicting results may be accounted for by the obvious differences in approach between this study and other studies such as cell type, scaffold design (pore size, fiber size, architecture, etc.), cell-seeding technique and culture conditions.

1.6. CONCLUSION AND FUTURE ASPECTS

From this chapter, it is clear that a wide range of materials and methodologies can be used in cartilage TE. However, the combination of some specific materials and methods will certainly lead to an optimal solution for cartilage regeneration. Many parameters have to be considered, having as major achievement an optimal cell-biomaterial interaction and resulting construct integration at the defective site. Biomaterials impact on further enhancement of human health will increase, as the success of regenerative medicine is getting even more dependent on biomaterials based TE. The major challenge for cartilage TE is the cell source. Studies on alternatives are increasing, as, for instance, the potential of stem cells. On the other hand, biomaterials development is also continuously evolving, and it is reaching to more controllable and known biomaterials chemistry and structure. Aiding methodologies, like mechanical loading, bioreactors, incorporated stimulatory factors and gene therapy are also being studied in order to improve cartilage production. Despite the number of patented and applying cartilage products for FDA approval, most of the studies were performed using mostly young adult or even fetal animal cells, and not with cells from elderly osteoarthritis patients. Therefore, extensive research will be needed to determine whether the results can be extended to the human situation. Therefore, professionals working in this multidisciplinary area have assumed huge responsibility that certainly will lead to solutions that will improve the quality of human lives.

2. REFERENCES

- [1] Langer RS and Vacanti JP. Tissue engineering: the challenges ahead. *Scientific American*, 1999. 280(4) pp. 86–89.
- [2] Huckle J, *et al.* Differentiated chondrocytes for cartilage tissue engineering. *Novartis Found Symposium*, 2003. 249 pp. 103–112.
- [3] Chung C and Burdick JA. Engineering cartilage tissue. *Advanced Drug Delivery Reviews*, 2008. 60(2) pp. 243–262.
- [4] Ulrich-Vinther M, *et al.* Articular cartilage biology. *Journal of the American Academy of Orthopaedic Surgeons*, 2003. 11(6) pp. 421-430.
- [5] Stockwell RA and Meachim GT. The chondrocytes. In: Freeman MAR (editor). *Adult Articular Cartilage*. Tunbridge Wells, England: Pitman Medical, 1979. pp. 69–144.
- [6] Poole AR, *et al.* Composition and structure of articular cartilage: a template for tissue repair. *Clinical Orthopaedics and Related Research*, 2001. 391(Supp) pp. S26-S33.
- [7] Schinagl RM, *et al.* Depth-dependent confined compression modulus of full thickness bovine articular cartilage. *Journal of Orthopaedic Research*, 1997. 15(4) pp. 499-506.
- [8] Brittberg M and Lindahlvan A. Chapter 18: Tissue Engineering of Cartilage. In: van Blitterswijk C (senior editor), Thomsen P, et al (editors). *Tissue Engineering*. Academic Press Series in Biomedical Engineering, 2008. p. 535.
- [9] Temenoff JS and Mikos AG. Review: tissue engineering for regeneration of articular cartilage. *Biomaterials*, 2000. 21(5) pp. 431–440.
- [10] Lee CR, *et al.* Articular cartilage chondrocytes in type I and type II collagen–GAG matrices exhibit contractile behavior *in vitro*. *Tissue Engineering*, 2000. 6(5) pp. 555–565.
- [11] Gugala Z and Gogolewski S. *In vitro* growth and activity of primary chondrocytes on a resorbable polylactide three-dimensional scaffold. *Journal of Biomedical Materials Research*, 2000. 49(2) pp. 183–191.
- [12] Yaylaoglu MB, *et al.* Novel osteochondral implant. *Biomaterials*, 1999. 20(16) pp. 1513–1520.
- [13] Yamaoka H, *et al.* Cartilage tissue engineering using human auricular chondrocytes embedded in different hydrogel materials. *Journal of Biomedical Materials Research Part A*, 2006. 78A pp. 1–11.
- [14] Stella JA, *et al.* On the biomechanical function of scaffolds for engineering load-bearing soft tissues. *Acta Biomaterialia*, 2010. 6(7) pp. 2365-2381.
- [15] Zhang S. Beyond the Petri dish. *Nature Biotechnology*, 2004. 22(2) pp. 151–152.
- [16] Abbott A. Cell culture: biology's new dimension. *Nature*, 2003. 424(6951) pp. 870-872.
- [17] Cukierman E, *et al.* Taking cell-matrix adhesions to the third dimension. *Science*, 2001. 294(5547) pp. 1708-1712.
- [18] Lee J, Cuddihy MJ and Kotov NA. Three-dimensional cell culture matrices: state of the art. *Tissue Engineering Part B: Reviews*, 2008. 14(1) pp. 61–86.
- [19] Kessel R. Connective Tissue: Cartilage. In: *Basic Medical Histology*. New York: Oxford University press, 1998. pp. 128–137.
- [20] von der Mark K, *et al.* Relationship between cell shape and type of collagen synthesised as chondrocytes lose their cartilage phenotype in culture. *Nature*, 1977. 267(5611) pp. 531–532.
- [21] Buschmann MD, *et al.* Chondrocytes in agarose culture synthesize a mechanically functional extracellular matrix. *Journal of Orthopaedic Research*, 1992. 10(6) pp.745–758.
- [22] Mauck RL, Yuan X and Tuan RS. Chondrogenic differentiation and functional maturation of bovine mesenchymal stem cells in long-term agarose culture. *Osteoarthritis and Cartilage*, 2006. 14(2) pp. 179–189.
- [23] Mauck RL, *et al.* Functional tissue engineering of articular cartilage through dynamic loading of chondrocyte-seeded agarose gels. *Journal of Biomechanical Engineering*, 2000. 122(3) pp. 252–260.
- [24] Mauck RL, *et al.* Synergistic action of growth factors and dynamic loading for articular cartilage tissue engineering. *Tissue Engineering*, 2003. 9(4) pp. 597–611.
- [25] Buschmann MD, *et al.* Mechanical compression modulates matrix biosynthesis in chondrocyte/agarose culture. *Journal of Cell Science*, 1995. 108(Pt 4) pp. 1497–1508.
- [26] Park Y, *et al.* BMP-2 induces the expression of chondrocyte-specific genes in bovine synovium-derived progenitor cells cultured in three-dimensional alginate hydrogel. *Osteoarthritis and Cartilage*, 2005. 13(6) pp. 527–536.
- [27] Park KS, *et al.* Chondrogenic differentiation of bone marrow stromal cells in transforming growth factor- β (1) loaded alginate bead. *Macromolecular Research*, 2005. 13(4) pp. 285–292.

- [28] Genes NG, *et al.* Effect of substrate mechanics on chondrocyte adhesion to modified alginate surfaces. *Archives of Biochemistry and Biophysics*, 2004. 422(2) pp. 161–167.
- [29] Miralles G, *et al.* Sodium alginate sponges with or without sodium hyaluronate: *in vitro* engineering of cartilage. *Journal of Biomedical Materials Research*, 2001. 57(2) pp. 268–278.
- [30] Hauselmann HJ, *et al.* Phenotypic stability of bovine articular chondrocytes after long-term culture in alginate beads. *Journal of Cell Science*, 1994. 107(Pt 1) pp. 17–27.
- [31] Vinatier C, *et al.* Engineering cartilage with human nasal chondrocytes and a silanized hydroxypropyl methylcellulose hydrogel. *Journal of Biomedical Materials Research Part A*, 2007. 80(1) pp. 66–74.
- [32] Muller FA, *et al.* Cellulose-based scaffold materials for cartilage tissue engineering. *Biomaterials*, 2006. 27(21) pp. 3955–3963.
- [33] De Franceschi L, *et al.* Transplantation of chondrocytes seeded on collagen based scaffold in cartilage defects in rabbits. *Journal of Biomedical Materials Research Part A*, 2005. 75(3) pp. 612–622.
- [34] Fujisato T, *et al.* Effect of basic fibroblast growth factor on cartilage regeneration in chondrocyte-seeded collagen sponge scaffold. *Biomaterials*, 1996. 17(2) pp. 155–162.
- [35] Buma P, *et al.* Cross-linked type I and type II collagenous matrices for the repair of full-thickness articular cartilage defects – a study in rabbits. *Biomaterials*, 2003. 24(19) pp. 3255–3263.
- [36] Lee CR, Grodzinsky AJ and Spector A. Biosynthetic response of passaged chondrocytes in a type II collagen scaffold to mechanical compression. *Journal of Biomedical Materials Research Part A*, 2003. 64(3) pp. 560–569.
- [37] Kuo YC and Lin CY. Effect of genipin-crosslinked chitin-chitosan scaffolds with hydroxyapatite modifications on the cultivation of bovine knee chondrocytes. *Biotechnology and Bioengineering*, 2006. 95(1) pp. 132–144.
- [38] Nettles DL, Elder SH and Gilbert JA. Potential use of chitosan as a cell scaffold material for cartilage tissue engineering. *Tissue Engineering*, 2002. 8(6) pp. 1009–1016.
- [39] Xia WY, *et al.* Tissue engineering of cartilage with the use of chitosan gelatin complex scaffolds. *Journal of Biomedical Materials Research Part B - Applied Biomaterials*, 2004. 71(2) pp. 373–380.
- [40] Kim SE, *et al.* Porous chitosan scaffold containing microspheres loaded with transforming growth factor- β 1: implications for cartilage tissue engineering. *Journal of Controlled Release*, 2003. 91(3) pp. 365–374.
- [41] Ragety GR, *et al.* Effect of chitosan scaffold microstructure on mesenchymal stem cell chondrogenesis. *Acta Biomaterialia*, 2010. 6(4) pp. 1430–1436.
- [42] Yamane S, *et al.* Feasibility of chitosan-based hyaluronic acid hybrid biomaterial for a novel scaffold in cartilage tissue engineering. *Biomaterials*, 2005. 26(6) pp. 611–619.
- [43] Ragety GR, *et al.* Cartilage tissue engineering on fibrous chitosan scaffolds produced by a replica molding technique. *Journal of Biomedical Materials Research Part A*, 2010. 93(1) pp. 46–55.
- [44] Shim IK, *et al.* Chitosan nano-/microfibrous double-layered membrane with rolled-up three-dimensional structures for chondrocyte cultivation. *Journal of Biomedical Materials Research: Part A*, 2009. 90(2) pp. 595–602.
- [45] Bhattarai N, *et al.* Electrospun chitosan-based nanofibers and their cellular compatibility. *Biomaterials*, 2005. 26(31) pp. 6176–6184.
- [46] Tiğlia RS and Gümüşdereliöğlü M. Evaluation of RGD- or EGF-immobilized chitosan scaffolds for chondrogenic activity. *International Journal of Biological Macromolecules*, 2008. 43(2) pp. 121–128.
- [47] Schagemann JC, *et al.* Poly-epsilon-caprolactone/gel hybrid scaffolds for cartilage tissue engineering. *Journal of Biomedical Materials Research Part A*, 2010. 93(2) pp. 454–463.
- [48] Schagemann JC, *et al.* The effect of scaffold composition on the early structural characteristics of chondrocytes and expression of adhesion molecules. *Biomaterials*, 2010. 31(10) pp. 2798–2805.
- [49] Casper ME, *et al.* Tissue engineering of cartilage using poly- ϵ -caprolactone nanofiber scaffolds seeded *in vivo* with periosteal cells. *Osteoarthritis and Cartilage*. In Press, Uncorrected Proof. Available online 29 April 2010. DOI: 10.1016/j.joca.2010.04.009.
- [50] Fan HB, *et al.* Porous gelatin-chondroitin-hyaluronate tri-copolymer scaffold containing microspheres loaded with TGF- β 1 induces differentiation of mesenchymal stem cells *in vivo* for enhancing cartilage repair. *Journal of Biomedical Materials Research Part A*, 2006. 77A pp. 785–794.
- [51] Li Q, *et al.* Photocrosslinkable polysaccharides based on chondroitin sulfate. *Journal of Biomedical Materials Research A*, 2004. 68(1) pp. 28–33.
- [52] Chang CH, *et al.* Gelatin-chondroitin-hyaluronan tri-copolymer scaffold for cartilage tissue engineering. *Biomaterials*, 2003. 24(26) pp. 4853–4858.

- [53] Eyrich D, *et al.* Long-term stable fibrin gels for cartilage engineering. *Biomaterials*, 2007. 28(1) pp. 55–65.
- [54] Silverman RP, *et al.* Injectable tissue-engineered cartilage using a fibrin glue polymer. *Plastic and Reconstructive Surgery*, 1999. 103(7) pp. 1809–1818.
- [55] Lee CR, *et al.* Fibrin-polyurethane composites for articular cartilage tissue engineering: a preliminary analysis. *Tissue Engineering*, 2005. 11(9-10) pp. 1562–1573.
- [56] Ting V, *et al.* *In vitro* prefabrication of human cartilage shapes using fibrin glue and human chondrocytes. *Annals of Plastic Surgery*, 1998. 40(4) pp. 413–420 discussion 420–421.
- [57] Hoshikawa A, *et al.* Encapsulation of chondrocytes in photopolymerizable styrenated gelatin for cartilage tissue engineering. *Tissue Engineering*, 2006. 12(8) pp. 2333–2341.
- [58] Goodstone NJ, Cartwright A and Ashton B. Effects of high molecular weight hyaluronan on chondrocytes cultured within a resorbable gelatin sponge. *Tissue Engineering*, 2004. 10(3-4) pp. 621–631.
- [59] Ibusuki S, *et al.* Tissue-engineered cartilage using an injectable and in situ gelable thermoresponsive gelatin: fabrication and *in vitro* performance. *Tissue Engineering*, 2003. 9(2) pp. 371–384.
- [60] Aigner J, *et al.* Cartilage tissue engineering with novel nonwoven structured biomaterial based on hyaluronic acid benzyl ester. *Journal of Biomedical Materials Research*, 1998. 42(2) pp. 172–181.
- [61] Smeds KA, *et al.* Photocrosslinkable polysaccharides for in situ hydrogel formation. *Journal of Biomedical Materials Research*, 2001. 54(1) pp. 115–121.
- [62] Burdick JA, *et al.* Controlled degradation and mechanical behavior of photopolymerized hyaluronic acid networks. *Biomacromolecules*, 2005. 6(1) pp. 386–391.
- [63] Chung C, *et al.* Influence of gel properties on neocartilage formation by auricular chondrocytes photoencapsulated in hyaluronic acid networks. *Journal of Biomedical Materials Research Part A*, 2006. 77(3) pp. 518–525.
- [64] Radice M, *et al.* Hyaluronan-based biopolymers as delivery vehicles for bone-marrow derived mesenchymal progenitors. *Journal of Biomedical Materials Research*, 2000. 50(2) pp. 101–109.
- [65] Marcacci M, *et al.* Articular cartilage engineering with Hyalograft® C – 3-year clinical results. *Clinical Orthopaedics and Related Research*, 2005. 435 pp. 96–105.
- [66] Meinel L, *et al.* Engineering cartilage-like tissue using human mesenchymal stem cells and silk protein scaffolds. *Biotechnology and Bioengineering*, 2004. 88(3) pp. 379–391.
- [67] Wang YZ, *et al.* *In vitro* cartilage tissue engineering with 3D porous aqueous-derived silk scaffolds and mesenchymal stem cells. *Biomaterials*, 2005. 26(34) pp. 7082–7094.
- [68] Hofmann S, *et al.* Cartilage-like tissue engineering using silk scaffolds and mesenchymal stem cells. *Tissue Engineering*, 2006. 12(10) pp. 2729–2738.
- [69] Wang YZ, *et al.* Stem cell-based tissue engineering with silk biomaterials. *Biomaterials*, 2006. 27(36) pp. 6064–6082.
- [70] Wang YZ, *et al.* Cartilage tissue engineering with silk scaffolds and human articular chondrocytes. *Biomaterials*, 2006. 27(25) pp. 4434–4442.
- [71] Li WJ, *et al.* Biological response of chondrocytes cultured in three-dimensional nanofibrous poly(epsilon-caprolactone) scaffolds. *Journal of Biomedical Materials Research Part A*, 2003. 67(4) pp. 1105–1114.
- [72] Shin HJ, *et al.* Electrospun PLGA nanofiber scaffolds for articular cartilage reconstruction: mechanical stability, degradation and cellular responses under mechanical stimulation *in vitro*. *Journal of Biomaterials Science - Polymer Edition*, 2006. 17(1-2) pp. 103–119.
- [73] Hsu SH, *et al.* Evaluation of biodegradable polyesters modified by type II collagen and Arg-Gly-Asp as tissue engineering scaffolding materials for cartilage regeneration. *Artificial Organs*, 2006. 30(1) pp. 42–55.
- [74] Uematsu K, *et al.* Cartilage regeneration using mesenchymal stem cells and a three-dimensional poly-lactic-glycolic acid (PLGA) scaffold. *Biomaterials*, 2005. 26(20) pp. 4273–4279.
- [75] Freed LE, *et al.* Neocartilage formation *in vitro* and *in vivo* using cells cultured on synthetic biodegradable polymers. *Journal of Biomedical Materials Research*, 2003. 27(1) pp. 11–23.
- [76] Li WJ, *et al.* Electrospun nanofibrous structure: a novel scaffold for tissue engineering. *Journal of Biomedical Materials Research*, 2002. 60(4) pp. 613–621.
- [77] Sittinger M, *et al.* Resorbable polyesters in cartilage engineering: affinity and biocompatibility of polymer fiber structures to chondrocytes. *Journal of Biomedical Materials Research*, 1996. 33(2) pp. 57–63.
- [78] Blunk T, *et al.* Differential effects of growth factors on tissue engineered cartilage. *Tissue Engineering*, 2002. 8(1) pp. 73–84.

- [79] Freed LE, *et al.* Tissue engineering of cartilage in space. Proceedings of the National Academy of Sciences of the United States of America USA, 1997. 94(25) pp. 13885-13890.
- [80] Vunjak-Novakovic G, *et al.* Bioreactor cultivation conditions modulate the composition and mechanical properties of tissue-engineered cartilage. Journal of orthopaedic research: official publication of the Orthopaedic Research Society, 1999. 17(1) pp. 130-138.
- [81] Ma PX, *et al.* Development of biomechanical properties and morphogenesis of *in vitro* tissue engineered cartilage. Journal of Biomedical Materials Research, 1995. 29(12) pp. 1587-1595.
- [82] Ameer GA, Mahmood TA and Langer RA. A biodegradable composite scaffold for cell transplantation. Journal of orthopaedic research: official publication of the Orthopaedic Research Society, 2002. 20(1) pp. 16-19.
- [83] Cohen SB, *et al.* The use of absorbable co-polymer pads with alginate and cells for articular cartilage repair in rabbits. Biomaterials, 2003. 24(15) pp. 2653-2660.
- [84] Ushida T, *et al.* Three-dimensional seeding of chondrocytes encapsulated in collagen gel into PLLA scaffolds. Cell Transplantation, 2002. 11(5) pp. 489-494.
- [85] Chen G, *et al.* The use of a novel PLGA fiber/collagen composite web as a scaffold for engineering of articular cartilage tissue with adjustable thickness. Journal of Biomedical Materials Research, 2003. 67(4) pp. 1170-1180.
- [86] Davisson T, Sah RL and Ratcliffe A. Perfusion increases cell content and matrix synthesis in chondrocyte three-dimensional cultures. Tissue Engineering, 2002. 8(5) pp. 807-816.
- [87] Griffon DJ, *et al.* Evaluation of vacuum and dynamic cell seeding of polyglycolic acid and chitosan scaffolds for cartilage engineering. American Journal of Veterinary Research, 2005. 66(4) pp. 599-605.
- [88] Li WJ, *et al.* A three-dimensional nanofibrous scaffold for cartilage tissue engineering using human mesenchymal stem cells. Biomaterials, 2005. 26(6) pp. 599-609.
- [89] Moutos FT and Guilak F. Functional properties of cell-seeded three-dimensionally woven poly(ϵ -caprolactone) scaffolds for cartilage tissue engineering. Tissue Engineering: Part A, 2010. 16(4) pp. 1291-1301.
- [90] Valonen PK, *et al.* *In vitro* generation of mechanically functional cartilage grafts based on adult human stem cells and 3D-woven poly(ϵ -caprolactone) scaffolds. Biomaterials, 2010. 31(8) pp. 2193-2200.
- [91] da Silva MA, *et al.* Evaluation of extracellular matrix formation in polycaprolactone and starch-compounded polycaprolactone nanofiber meshes when seeded with bovine articular chondrocytes. Tissue Engineering: Part A, 2009. 15(2) pp. 377-385.
- [92] Wise JK, *et al.* Chondrogenic differentiation of human mesenchymal stem cells on oriented nanofibrous scaffolds: engineering the superficial zone of articular cartilage. Tissue Engineering Part A, 2009. 15(4) pp. 913-921.
- [93] Garcia-Giralt N, *et al.* A porous PCL scaffold promotes the human chondrocytes redifferentiation and hyaline-specific extracellular matrix protein synthesis. Journal of Biomedical Materials Research - Part A, 2008. 85(4) pp. 1082-1089.
- [94] Izquierdo R, *et al.* Biodegradable PCL scaffolds with an interconnected spherical pore network for tissue engineering. Journal of Biomedical Materials Research: Part A, 2008. 85(1) pp. 25-35.
- [95] Lim SM, *et al.* Dual-growth-factor-releasing pcl scaffolds for chondrogenesis of adipose-tissue-derived mesenchymal stem cells. Advanced Engineering Materials, 2010. 12(1-2) pp. B62-B69.
- [96] Li WJ, *et al.* Multilineage differentiation of human mesenchymal stem cells in a three-dimensional nanofibrous scaffold. Biomaterials, 2005. 26(25) pp. 5158-5166.
- [97] Williams CG, *et al.* *In vitro* chondrogenesis of bone marrow-derived mesenchymal stem cells in a photopolymerizing hydrogel. Tissue Engineering, 2003. 9(4) pp. 679-688.
- [98] Hwang NS, *et al.* Chondrogenic differentiation of human embryonic stem cell-derived cells in arginineglycine-aspartate modified hydrogels. Tissue Engineering, 2006. 12(9) pp. 2695-2706.
- [99] Bryant SJ and Anseth KS. Controlling the spatial distribution of ECM components in degradable PEG hydrogels for tissue engineering cartilage. Journal of Biomedical Materials Research Part A, 2003. 64(1) pp. 70-79.
- [100] Lee HJ, *et al.* Collagen mimetic peptide-conjugated photopolymerizable PEG hydrogel. Biomaterials, 2006. 27(30) pp. 5268-5276.
- [101] Bryant SJ, *et al.* Encapsulating chondrocytes in degrading PEG hydrogels with high modulus: engineering gel structural changes to facilitate cartilaginous tissue production. Biotechnology and Bioengineering, 2004. 86(7) pp. 747-755.
- [102] Elisseff J, *et al.* Photoencapsulation of chondrocytes in poly(ethylene oxide)-based semi-interpenetrating networks. Journal of Biomedical Materials Research, 2000. 51(2) pp. 164-171.
- [103] An YH, *et al.* Regaining chondrocyte phenotype in thermosensitive gel culture. Anatomical Record, 2001. 263(4) pp. 336-341.

- [104] Au A, *et al.* Thermally reversible polymer gel for chondrocyte culture. *Journal of Biomedical Materials Research Part A*, 2003. 67(4) pp. 1310–1319.
- [105] Na K, *et al.* Synergistic effect of TGF β 3 on chondrogenic differentiation of rabbit chondrocytes in thermo-reversible hydrogel constructs blended with hyaluronic acid by *in vivo* test. *Journal of Biotechnology*, 2007. 128(2) pp. 412–422.
- [106] Kim TK, *et al.* Experimental model for cartilage tissue engineering to regenerate the zonal organization of articular cartilage. *Osteoarthritis and Cartilage*, 2003. 11(9) pp. 653–664.
- [107] Holland TA, Tabata Y and Mikos AG. Dual growth factor delivery from degradable oligo(poly(ethylene glycol) fumarate) hydrogel scaffolds for cartilage tissue engineering. *Journal of Controlled Release*, 2005. 101(1-3) pp. 111–125.
- [108] Liao E, *et al.* Tissue-engineered cartilage constructs using composite hyaluronic acid/collagen I hydrogels and designed poly(propylene fumarate) scaffolds. *Tissue Engineering*, 2007. 13(3) pp. 537–550.
- [109] Chia SL, *et al.* Biodegradable elastomeric polyurethane membranes as chondrocyte carriers for cartilage repair. *Tissue Engineering*, 2006. 12(7) pp. 1945–1953.
- [110] Grad S, *et al.* The use of biodegradable polyurethane scaffolds for cartilage tissue engineering: potential and limitations. *Biomaterials*, 2003. 24(28) pp. 5163–5171.
- [111] Liu Y, *et al.* Composite articular cartilage engineered on a chondrocyte seeded aliphatic polyurethane sponge. *Tissue Engineering*, 2004. 10(7-8) pp. 1084–1092.
- [112] Bray JC and Merrill EW. Poly(vinyl alcohol) hydrogels for synthetic articular cartilage material. *Journal of Biomedical Materials Research*, 1973. 7(5) pp. 431–443.
- [113] Bryant SJ, *et al.* Synthesis and characterization of photopolymerized multifunctional hydrogels: water-soluble poly(vinyl alcohol) and chondroitin sulfate macromers for chondrocyte encapsulation. *Macromolecules*, 2004. 37(18) pp. 6726–6733.
- [114] Martens PJ, Bryant SJ and Anseth KS. Tailoring the degradation of hydrogels formed from multivinyl poly(ethylene glycol) and poly(vinyl alcohol) macromers for cartilage tissue engineering. *Biomacromolecules*, 2003. 4(2) pp. 283–292.
- [115] Holmes TC. Novel peptide-based biomaterial scaffolds for tissue engineering. *Trends in Biotechnology*, 2002. 20(1) pp. 16–21.
- [116] Zhang S, *et al.* Spontaneous assembly of a selfcomplementary oligopeptide to form a stable macroscopic membrane. *Proceedings of the National Academy of Sciences of the USA*, 2003. 90(8) pp. 3334–3338.
- [117] Kisiday J, *et al.* Self-assembling peptide hydrogel fosters chondrocyte extracellular matrix production and cell division: implications for cartilage tissue repair. *Proceedings of the National Academy of Sciences of the USA*, 2002. 99(15) pp. 9996–10001.
- [118] Kisiday JD, *et al.* Effects of dynamic compressive loading on chondrocyte biosynthesis in selfassembling peptide scaffolds. *Journal of Biomechanics*, 2004. 37(5) pp. 595–604.
- [119] Kaplan DL. Introduction to polymers from renewable resources. In: Kaplan DL (editor). *Biopolymers from Renewable Resources*. Berlin: Springer Verlag, 1998. pp. 1–29.
- [120] Shogren RL and Bagley EB. Natural polymers as advanced materials: some research needs and directions. In: Iman SH, Greene RV and Zaidi BR (editors). *Biopolymers. Utilizing nature's advanced materials*, ACS symposium series 723. Cary, USA: Oxford University Press, 1999. pp. 2–11.
- [121] Varghese S and Elisseeff J. Hydrogels for musculoskeletal tissue engineering. In: Werner C (editor). *Polymers for regenerative medicine*. Springer, 2006. p. 95–144.
- [122] Stevens M. *Polymer Chemistry: An Introduction*. New York; Oxford University Press, 1999.
- [123] Gunn J and Zhang M. Polyblend nanofibers for biomedical applications: perspectives and challenges. *Trends in Biotechnology*, 2010. 28(4) pp. 189–187.
- [124] Chang KY, *et al.* Fabrication and characterization of poly(γ -glutamic acid)-graft-chondroitin sulfate/polycaprolactone porous scaffolds for cartilage tissue engineering. *Acta Biomaterialia*, 2009. 5(6) pp. 1937–1947.
- [125] Coutinho DF, *et al.* The effect of chitosan on the *in vitro* biological performance of chitosan-poly(butylene succinate) blends. *Biomacromolecules*, 2008. 9(4) pp. 1139–1145.
- [126] Lee CT and Lee YD. Preparation of porous biodegradable poly(lactide-co-glycolide)/hyaluronic acid blend scaffolds: characterization, *in vitro* cells culture and degradation behaviors. *Journal of Materials Science: Materials in Medicine*, 2006. 17(12) pp. 1411–20.
- [127] Lee JJ, *et al.* Nanofibrous membrane of collagen-polycaprolactone for cell growth and tissue regeneration. *Journal of Material Science: Materials in Medicine*, 2009. 20(9) pp. 1927–1935.

- [128] Park KE, *et al.* Biomimetic nanofibrous scaffolds: preparation and characterization of PGA/chitin blend nanofibers. *Biomacromolecules*, 2006. 7(2) pp. 635-643.
- [129] Jeong SI, *et al.* Electrospun gelatin/poly(L-lactide-co-epsilon-caprolactone) nanofibers for mechanically functional tissue-engineering scaffolds. *Journal of Biomaterials Science - Polymer Edition*, 2008. 19(3) pp. 339-357.
- [130] Duan B, *et al.* Electrospinning of chitosan solutions in acetic acid with poly(ethylene oxide). *Journal of Biomaterials Science - Polymer Edition*, 2004. 15(6) pp. 797-811.
- [131] Ghasemi-Mobarakeh L, *et al.* Electrospun poly(epsilon-caprolactone)/gelatin nanofibrous scaffolds for nerve tissue engineering. *Biomaterials*, 2008. 29(34) pp. 4532-4539.
- [132] Prabhakaran MP, Venugopal JR and Ramakrishna S. Mesenchymal stem cell differentiation to neuronal cells on electrospun nanofibrous substrates for nerve tissue engineering. *Biomaterials*, 2009. 30(28) pp. 4996-5003.
- [133] Huang L, *et al.* Engineered collagen-PEO nanofibers and fabrics. *Journal of Biomaterials Science - Polymer Edition*, 2001. 12(9) pp. 979-993.
- [134] Gu SY, *et al.* Electrospinning of gelatin and gelatin/poly(L-lactide) blend and its characteristics for wound dressing. *Materials Science and Engineering: C*, 2009. 29(6) pp. 1822-1828.
- [135] Rinaudo M. Chitin and chitosan: properties and applications. *Progress in Polymer Science*, 2006. 31(7) pp. 603-632.
- [136] Ravi Kumar MNV. A review of chitin and chitosan applications. *Reactive Polymers*, 2000. 46(1) pp. 1-27.
- [137] Ravi Kumar MNV. Chitin and chitosan fibres: a review. *Bulletin of Materials Science*, 1999. 22(5) pp. 905-915.
- [138] Nishimura K, *et al.* Immunological activity of chitin and its derivatives. *Vaccine*, 1984. 2(1) pp. 93-99.
- [139] Tanigawa T, *et al.* Various biological effects of chitin derivatives. In: Brine CJ, Sandford PA and Zikakis JP (editors). *Advances in chitin and chitosan*. Elsevier, 1992. pp. 206-215.
- [140] Okamoto Y, *et al.* Polymeric N-acetyl-D-glucosamine (chitin) induces histionic activation in dogs. *The Journal of Veterinary Medical Science*, 1999. 55(5) pp. 739-742.
- [141] Khnor E and Lim L. Implantable applications of chitin and chitosan. *Biomaterials*, 2003. 24(13) pp. 2339-2349.
- [142] Mori T, *et al.* Effects of chitin and its derivatives on the proliferation and cytokine production of fibroblasts *in vitro*. *Biomaterials*, 1997. 18(13) pp. 947-951.
- [143] Tokura S, *et al.* Molecular weight dependent antimicrobial activity by chitosan. *Macromolecular Symposia*, 1997. 120 pp. 1-9.
- [144] Singla AK and Chawla M. Chitosan: some pharmaceutical and biological aspects — an update. *The Journal of Pharmacy and Pharmacology*, 2001. 53(8) pp. 1047-1067.
- [145] Di Martino A, Sittinger M and Risbud MV. Chitosan: A versatile biopolymer for orthopaedic tissue-engineering. *Biomaterials*, 2005. 26(30) pp. 5983-5990.
- [146] Kosher RA, Lash JW and Minor RR. Environmental enhancement of *in vitro* chondrogenesis: IV. Stimulation of somite chondrogenesis by exogenous chondromucoprotein. *Developmental Biology*, 1973. 35(2) pp. 210-220.
- [147] Kosher RA and Church RL. Stimulation of *in vitro* somite chondrogenesis by procollagen and collagen. *Nature*, 1975. 258(5533) pp. 327-330.
- [148] Suh JK and Matthew HW. Application of chitosan-based polysaccharide biomaterials in cartilage tissue engineering: a review. *Biomaterials*, 2000. 21(24) pp. 2589-2598.
- [149] Lahiji A, *et al.* Chitosan supports the expression of extracellular matrix proteins in human osteoblasts and chondrocytes. *Journal of Biomedical Materials Research Part A*, 2000. 51(4) pp. 586-595.
- [150] Vårum KM, *et al.* *In vitro* degradation rates of partially N-acetylated chitosans in human serum. *Carbohydrate Research*, 1997. 299(1-2) pp. 99-101.
- [151] Pangburn S, Trescony P and Heller J. Lysozyme degradation of partially deacetylated chitin, its films and hydrogels. *Biomaterials*, 1982. 3(2) pp. 105-108.
- [152] Moss JM, *et al.* Purification, characterization, and biosynthesis of bovine cartilage lysozyme isoforms. *Archives of Biochemistry and Biophysics*, 1997. 339(1) pp. 172-182.
- [153] Greenwald RA, *et al.* Human cartilage lysozyme. *The Journal of Clinical Investigation*, 1972. 51(9) pp. 2264-2270.
- [154] Sarasam A and Madihally SV. Characterization of chitosan-polycaprolactone blends for tissue engineering applications. *Biomaterials*, 2005. 26(27) pp. 5500-5508.
- [155] Wang A, *et al.* Fiber-based chitosan tubular scaffolds for soft tissue engineering: fabrication and *in vitro* evaluation. *Tsinghua Science and Technology*, 2005. 10(4) pp. 449-453.

- [156] Dai N-T, *et al.* Human single-donor composite skin substitutes based on collagen and polycaprolactone copolymer. *Biochemical and Biophysical Research Communications*, 2009. 386(1) pp. 21–5.
- [157] Abbah SA, *et al.* Biological performance of a polycaprolactone-based scaffold used as fusion cage device in a large animal model of spinal reconstructive surgery. *Biomaterials*, 2009. 30(28) pp. 5086–5093.
- [158] Bezwada RS, *et al.* Monocryl® suture, a new ultra-pliable absorbable monofilament suture. *Biomaterials*, 1995. 16(15) pp. 1141–1148.
- [159] Darney PD, *et al.* Clinical evaluation of the Capronor contraceptive implant: preliminary report. *American Journal of Obstetrics and Gynecology*, 1989. 160(5 pt 2) pp. 1292–1295.
- [160] Woodward SC, Brewer PS and Moatamed F. The intracellular degradation of poly(ϵ -caprolactone). *Journal of Biomedical Materials Research*, 1985. 19(4) pp. 437–444.
- [161] Pitt CG, *et al.* Aliphatic polyesters: II. The degradation of poly(DL-lactide), poly(ϵ -caprolactone), and their copolymers *in vivo*. *Biomaterials*, 1981. 2(4) pp. 215–220.
- [162] Averous L, *et al.* Properties of thermoplastic blends: starch-polycaprolactone. *Polymer*, 2000. 41(11) pp. 4157–4167.
- [163] Ishaug-Riley SL, *et al.* Human articular chondrocyte adhesion and proliferation on synthetic biodegradable polymer films. *Biomaterials*, 1999. 20(23-24) pp. 2245-2256.
- [164] Hoque ME, *et al.* Processing of polycaprolactone and polycaprolactone-based copolymers into 3D scaffolds, and their cellular responses. *Tissue Engineering Part A*, 2009. 15(10) pp. 3013-3024.
- [165] Kim H-J, Lee J-H and Im G-I. Chondrogenesis using mesenchymal stem cells and PCL scaffolds. *Journal of Biomedical Materials Research Part A*, 2010. 92(2) pp. 659-666.
- [166] Ratner BR, *et al.* *Biomaterials Science*. Academic Press, New York, 1996.
- [167] Zhu Y, *et al.* Surface modification of polycaprolactone membrane via aminolysis and biomacromolecule immobilization for promoting cytocompatibility of human endothelial cells. *Biomacromolecules*, 2002. 3(6) pp. 1312–1319.
- [168] Gomes M, *et al.* Chapter 6: Natural Polymers in Tissue Engineering Applications. In: van Blitterswijk C (senior editor), Thomsen P, et al (editors). *Tissue Engineering*. Academic Press Series in Biomedical Engineering. Academic Press, 2008. p. 156.
- [169] Eyrich D, *et al.* *In vitro* and *in vivo* cartilage engineering using a combination of chondrocyte-seeded long-term stable fibrin gels and polycaprolactone-based polyurethane scaffolds. *Tissue Engineering*, 2007. 13(9) pp. 2207–2218.
- [170] Zhou Z, *et al.* Simultaneous enhancement of the strength and elongation of polycaprolactone: The role of Chitosan-graft-Polycaprolactone. *Journal of Applied Polymer Science*, 2009. 112(2) pp. 692-699.
- [171] Zeng M and Fang Z. Preparation of sub-micrometer porous membrane from chitosan/polyethylene glycol semi-IPN. *Journal of Membrane Science*, 2004. 245(1-2) pp. 95-102.
- [172] Cruz DMG, *et al.* Blending polysaccharides with biodegradable polymers. II. Structure and biological response of chitosan/polycaprolactone blends. *Journal of Biomedical Materials Research. Part B, Applied Biomaterials*, 2008. 87(2) pp. 544-554.
- [173] Muzzarelli RAA and Peter MG (editors). *Chitin handbook*. Grottammare, Italy, European Chitin Society, 1997.
- [174] Chung TW, *et al.* Enhancing growth and proliferation of human gingival fibroblasts on chitosan grafted poly(ϵ -caprolactone) films is influenced by nano-roughness chitosan surfaces. *Journal of Materials Science: Materials in Medicine*, 2009. 20(1) pp. 397-404.
- [175] Sung HW, *et al.* Feasibility study of a natural crosslinking reagent for biological tissue fixation. *Journal of Biomedical Materials Research*, 1998. 42(4) pp. 560-567.
- [176] Sung HW, *et al.* Evaluation of gelatin hydrogel crosslinked with various crosslinking agents as bioadhesives: *in vitro* study. *Journal of Biomedical Materials Research*, 1999. 46(4) pp. 520-530.
- [177] Malheiro VN, *et al.* New poly(ϵ -caprolactone)/chitosan blend fibers for tissue engineering applications. *Acta Biomaterialia*, 2010. 6(2) pp. 418-428.
- [178] Honma T, Senda T and Inoue Y. Thermal properties and crystallization behaviour of blends of poly(ϵ -caprolactone) with chitin and chitosan. *Polymer International*, 2003. 52(12) pp. 1839-1846.
- [179] Senda T, He Y and Inoue Y. Biodegradable blends of poly(ϵ -caprolactone) with α -chitin and chitosan: specific interactions, thermal properties and crystallization behavior. *Polymer International*, 2002. 51(1) pp. 33-39.
- [180] Honma T, Zhao L, Asakawa N, Inoue Y. Poly(ϵ -caprolactone)/chitin and poly(ϵ -caprolactone)/chitosan blend films with compositional gradients: fabrication and their biodegradability. *Macromolecular Bioscience*, 2006. 6(3) pp. 241-249.
- [181] Nielsen GD, *et al.* Sensory irritation mechanisms investigated from model compounds: Trifluoroethanol, hexafluoroisopropanol and methyl hexafluoroisopropyl ether. *Archives of Toxicology*, 1996. 70(6) pp. 319-328.

- [182] Cruz DMG, Ribelles JLG and Sanchez MS. Blending polysaccharides with biodegradable polymers. I. Properties of chitosan/polycaprolactone blends. *Journal of Biomedical Materials Research. Part B, Applied Biomaterials*, 2008. 85(2) pp. 303-313.
- [183] Cruz DMG, *et al.* Physical interactions in macroporous scaffolds based on poly(ϵ -caprolactone)/chitosan semi-interpenetrating polymer networks. *Polymer*, 2009. 50(9) pp. 2058–2064.
- [184] Sarasam AR, *et al.* Blending chitosan with polycaprolactone: porous scaffolds and toxicity. *Macromolecular Bioscience*, 2007. 7(9-10) pp. 1160-1167.
- [185] Wan Y, *et al.* Compressive mechanical properties and biodegradability of porous poly(caprolactone)/chitosan scaffolds. *Polymer Degradation and Stability*, 2008. 93(10) pp. 1736-1741.
- [186] Wan Y, *et al.* Development of polycaprolactone/chitosan blend porous scaffolds. *Journal of Materials Science: Materials in Medicine*, 2009. 20(3) pp. 719-724.
- [187] Houde S, Xiufeng X and Rongfang L. Preparation and characterization of polycaprolactone-chitosan composites for tissue engineering applications. *Journal of Materials Science*, 2007. 42(19) pp. 8113-8119.
- [188] Prabhakaran MP, *et al.* Electrospun biocomposite nanofibrous scaffolds for neural tissue engineering. *Tissue Engineering Part A*, 2008. 14(11) pp. 1787-1797.
- [189] Yang X, Chen X and Wang H. Acceleration of osteogenic differentiation of preosteoblastic cells by chitosan containing nanofibrous scaffolds. *Biomacromolecules*, 2009. 10(10) pp. 2772-2778.
- [190] Shalumon KT, *et al.* Single step electrospinning of chitosan/poly(caprolactone) nanofibers using formic acid/acetone solvent mixture. *Carbohydrate Polymers*, 2010. 80(2) pp. 413-419.
- [191] Wan Y, *et al.* Fibrous poly(chitosan-g-DL-lactic acid) scaffolds prepared via electro-wet-spinning. *Acta Biomaterialia*, 2008. 4(4) pp. 876-886.
- [192] Shim IK, *et al.* Homogeneous chitosan–PLGA composite fibrous scaffolds for tissue regeneration. *Journal of Biomedical Materials Research Part A*, 2008. 84(1) pp. 247-255.
- [193] Santos MI, *et al.* Endothelial cell colonization and angiogenic potential of combined nano- and micro-fibrous scaffolds for bone tissue engineering. *Biomaterials*, 2008. 29(32) pp. 4306-4313.
- [194] Kim IY, *et al.* Chitosan and its derivatives for tissue engineering applications. *Biotechnology Advances*, 2008. 26(1) pp. 1–21.
- [195] Baker BM and Mauck RL. The effect of nanofiber alignment on the maturation of engineered meniscus constructs. *Biomaterials*, 2007. 28(11) pp. 1967–1977.
- [196] Hutmacher D, *et al.* Chapter 14: Scaffold Design and Fabrication. In van Blitterswijk C (senior editor), Thomsen P, et al (editors). *Tissue Engineering. Academic Press Series in Biomedical Engineering*, 2008. pp. 426-427.
- [197] Cook JG. *Handbook of Textile Fibres: Merrow*, 1993.
- [198] Gomes ME, *et al.* Starch-poly(epsilon-caprolactone) and starch-poly(lactic acid) fibre-mesh scaffolds for bone tissue engineering applications: structure, mechanical properties and degradation behaviour. *Journal of Tissue Engineering and Regenerative Medicine*, 2008. 2(5) pp. 243-252.
- [199] Fambri L, Bragagna S and Migliaresi C. Biodegradable fibers of poly-L,DL-lactide 70/30 produced by melt spinning. *Macromolecular Symposia*, 2006. 234(1) pp. 20-25.
- [200] Leenslag JW and Pennings AJ. High-strength poly(L-lactide) fibers by a dry-spinning hot-drawing process. *Polymer*, 1987. 28(10) pp. 1695-1702.
- [201] Zhang X, *et al.* *In vitro* degradation and biocompatibility of poly(L-lactic acid)/chitosan fiber composites. *Polymer*, 2007. 48(4) pp. 1005-1011.
- [202] Liu C and Bai R. Preparation of chitosan/cellulose acetate blend hollow fibers for adsorptive performance. *Journal of Membrane Science*, 2005. 267(1-2) pp. 68-77.
- [203] Chung YS, *et al.* Preparation of hydroxyapatite/poly(vinyl alcohol) composite fibers by wet spinning and their characterization. *Journal of Applied Polymer Science*, 2007. 106(5) pp. 3423-3429.
- [204] Zhu ZH, *et al.* Preparation and characterization of regenerated Bombyx mori silk fibroin fiber containing recombinant cell-adhesive proteins; nonwoven fiber and monofilament. *Journal of Applied Polymer Science*, 2008. 109(5) pp. 2956-2963.
- [205] Lee SH, Kim Y and Kim Y. Effect of the concentration of sodium acetate (SA) on crosslinking of chitosan fiber by epichlorohydrin (ECH) in a wet spinning system. *Carbohydrate Polymers*, 2007. 70(1) pp. 53-60.
- [206] Zuo BQ, Liu L and Wu Z. Effect on properties of regenerated silk fibroin fiber coagulated with aqueous methanol/ethanol. *Journal of Applied Polymer Science*, 2007. 106(1) pp. 53-59.

- [207] Ki CS, *et al.* Dissolution and wet spinning of silk fibroin using phosphoric acid/formic acid mixture solvent system. *Journal of Applied Polymer Science*, 2007. 105(3) pp. 1605-1610.
- [208] Gupta B, *et al.* Preparation of poly(lactic acid) fiber by dry-jet-wet spinning. I. Influence of draw ratio on fiber properties. *Journal of Applied Polymer Science*, 2006. 100(2) pp. 1239-1246.
- [209] Arumuganathar S, *et al.* A novel direct aerodynamically assisted threading methodology for generating biologically viable microthreads encapsulating living primary cells. *Journal of Applied Polymer Science*, 2008. 107(2) pp. 1215-1225.
- [210] Arumuganathar S and Jayasinghe SN. Pressure-assisted spinning: a versatile and economical, direct fibre to scaffold spinning methodology. *Macromolecular Rapid Communications*, 2007. 28(14) pp. 1491-1496.
- [211] Barnes CP, *et al.* Nanofiber technology: designing the next generation of tissue engineering scaffolds. *Advanced Drug Delivery Reviews*, 2007. 59(14) pp. 1413-1433.
- [212] Kim SH, *et al.* Fabrication of a new tubular fibrous PLCL scaffold for vascular tissue engineering. *Journal of Biomaterials Science-Polymer Edition*, 2006. 17(74) pp. 1359-1374.
- [213] Tuzlakoglu K and Reis RL. Chapter 11: Processing and Biomedical Applications of Degradable Polymeric Fibers. In: Reis RL and San Román J (editors). *Biodegradable Systems in Tissue Engineering and Regenerative Medicine*. Boca Raton, Florida: CRC Press, 2004. pp. 165,168.
- [214] Hutmacher D, *et al.* Chapter 14: Scaffold Design and Fabrication. In van Blitterswijk C, *et al.* (editors). *Tissue Engineering*. Academic Press Series in Biomedical Engineering, 2008. pp. 433,434,440.
- [215] Ciardelli G, *et al.* Innovative tissue engineering structures through advanced manufacturing technologies. *Journal of Materials Science: Materials in Medicine*, 2004. 15(4) pp. 305–310.
- [216] Hutmacher DW, Sittinger M and Risbud MV. Scaffold-based tissue engineering: rationale for computer-aided design and solid free-form fabrication systems. *Trends in Biotechnology*, 2004. 22(7) pp. 354-362.
- [217] Landers R, *et al.* Rapid prototyping of scaffolds derived from thermoreversible hydrogels and tailored for applications in tissue engineering. *Biomaterials*, 2002. 23(23) pp. 4437-4447.
- [218] Landers R, *et al.* Fabrication of soft tissue engineering scaffolds by means of rapid prototyping techniques. *Journal of Materials Science*, 2002. 37(15) pp. 3107-3116.
- [219] Freed LE, *et al.* Biodegradable polymer scaffolds for tissue engineering. *Nature Biotechnology*, 1994. 12(7) pp. 689–693.
- [220] Sutherland FW, *et al.* From stem cells to viable autologous semilunar heart valve. *Circulation*, 2005. 111(21) pp. 2783–2791.
- [221] Engelmayer GC Jr and Sacks MS. A structural model for the flexural mechanics of nonwoven tissue engineering scaffolds. *Journal of Biomechanical Engineering*, 2006. 128(4) pp. 610–622.
- [222] Engelmayer GC Jr and Sacks MS. Prediction of extracellular matrix stiffness in engineered heart valve tissues based on nonwoven scaffolds. *Biomechanics and Modeling in Mechanobiology*, 2008. 7(4) pp. 309-321.
- [223] Huang Q, *et al.* *In vivo* mesenchymal cell recruitment by a scaffold loaded with transforming growth factor β 1 and the potential for in situ chondrogenesis. *Tissue engineering*, 2002. 8(3) pp. 469-482.
- [224] Moroni L, De Wijn JR and Van Blitterswijk CA. 3D fiber-deposited scaffolds for tissue engineering: Influence of pores geometry and architecture on dynamic mechanical properties. *Biomaterials*, 2006. 27(7) pp. 974–985.
- [225] Moroni L, *et al.* 3D fiber-deposited electrospun integrated scaffolds enhance cartilage tissue formation. *Advanced Functional Materials*, 2008. 18(1) pp. 53-60.
- [226] Chen G, *et al.* Chondrogenic differentiation of human mesenchymal stem cells cultured in a cobweb-like biodegradable scaffold. *Biochemical and Biophysical Research Communications*, 2004. 322(1) pp. 50-55.
- [227] Tiitu V, *et al.* Bioreactor improves the growth and viability of chondrocytes in the knitted poly-L,D-lactide scaffold. *Biorheology*, 2008. 45(3-4) pp. 539-546.
- [228] Pulliainen O, *et al.* Poly-L-D-lactic acid scaffold in the repair of porcine knee cartilage lesions. *Tissue Engineering*, 2007. 13(6) pp. 1347-1355.
- [229] Wu W, *et al.* Engineering of human tracheal tissue with collagen-enforced poly-lactic-glycolic acid non-woven mesh: A preliminary study in nude mice. *British Journal of Oral and Maxillofacial Surgery*, 2007. 45(4) pp. 272–278.

CHAPTER II

MATERIALS AND METHODS

1. MATERIALS AND METHODS

1.1. MATERIALS

CHITOSAN AND POLY(ϵ -CAPROLACTONE)

The CHT used in this work was a low MW CHT purchased from Sigma-Aldrich (ref. 448869) with a deacetylation degree between 75 and 85%. The low MW choice is related with the need of low viscosity solutions, in order to be possible to work with higher solution concentrations.

Before use, CHT was purified by recrystallization before being used, as described elsewhere [14]. It was dissolved in 1% (wt./vol.) AcA solution and then filtered through porous membranes (Whatman® ashes filter paper, 20-25 μ m, and nylon filter sheet) into a Buckner flask under vacuum. Adjusting the pH of the solution to about 8, through the addition of NaOH, caused flocculation due to deprotonation and insolubility of the polymer at neutral pH. The polymer was then neutralized until the pH equaled that of distilled water, frozen at -80°C and lyophilized.

The PCL (Sigma-Aldrich, ref. 440744) used in this work has a MW of 80 kDa. This choice is related to the attempt to balance the interaction between the two polymers, keeping, at the same time, good mechanical properties.

SOLVENT SYSTEM

The two most used solvent solution systems for blending CHT and PCL are HFIP [1,2] and AcA [3-7]. The more common methodology when using AcA is the dissolution of PCL in glacial AcA and an diluted AcA to dissolve CHT, with a consequent mixture of the two solutions. These two strategies present some drawbacks. With HFIP it was possible to create stable structures [1,2] but HFIP is a very toxic, carcinogenic, and expensive solvent difficult to remove [8], which is undesirable for the biological purposes of the scaffolds. Blend films of CHT/PCL were obtained, using glacial AcA to dissolve PCL and 0.5M aqueous AcA solution to dissolve CHT [3]. The blends were miscible for all compositions, but the mechanical properties were not improved due to the low concentrations of polymers used. A study on the polymer concentration increase was performed, but phase separation was detected [9]. This occurs because when mixing the glacial AcA/PCL and aqueous AcA/CHT solutions, PCL precipitates due to the presence of water in the CHT solution [10].

Even if the dissolution of CHT in an aqueous solution AcA is the starting point for most applications of CHT, formic acid has also been explored for this purpose, like blending CHT with other polymers such as silk fibroin, gelatin and polyamide [11-13]. The use of formic acid for blending CHT and PCL was used

for the first time by Malheiro *et al.* [14], with a solvent system composed by 70:30 vol.% formic acid/acetone.

The approach presented to prepare the CHT/PCL blends in this work consisted of using a common solvent solution of 100 vol.% of formic acid, in order to simplify the solvent system used by Malheiro *et al.* [14] and, at the same time, trying to improve the blends homogeneity.

COAGULATION BATH

The use of methanol as coagulation bath is justified by the studies performed by Malheiro *et al.* [14]. Methanol was chosen among other experimentally tested precipitation agents like NaOH, KOH, ethanol, H₂O, etc.

POLYMERIC SOLUTIONS

One of the main purposes of this work was to study the biological influence that blending PCL to CHT has on chondrocytes behavior. The formulations studied in this work were 100:0, 75:25 and 50:50 wt.% CHT/PCL (100CHT, 75CHT and 50CHT, respectively). As the solvent solution used is similar to that used by Malheiro *et al.* [14] and no structural differences on the fibers are expected, it was decided to use the polymeric solutions concentrations that they reported (Table 2.1).

Table 2.1. Total polymer concentration of each formulation [14].

FORMULATION	CHT/PCL WEIGHT RATIO	TOTAL POLYMER CONCENTRATION (wt./vol. %)
100CHT	100 : 0	13
75CHT	75 : 25	17
50CHT	50 : 50	21

1.2. METHODS

1.2.1. SCAFFOLDS PROCESSING AND CHONDROCYTE ISOLATION AND SEEDING

3D FIBER-MESHES PROCESSING

The fiber processing method used in this work was the wet-spinning technique. It is a non-solvent-induced phase inversion technique that allows the production of polymer micrometric fibers through immersion precipitation. In detail, a continuous polymer fiber is produced by precipitation of a polymer solution filament in a coagulation bath composed by a poor solvent (non-solvent) or a non-solvent-solvent mixture with respect to the processed polymer. A homogeneous solution filament, composed of polymer, solvent and possible additives, solidifies because of polymer desolvation, caused by solvent-non-solvent exchange [15].

Figure 2.1 illustrates the process used to obtain the fibers. The polymeric solutions prepared were placed into a 5mL syringe with a capillary tip having an inner diameter of 0.8mm. A syringe pump was used to feed the solutions into the needle tip. The filament extruded was then precipitated into the coagulation bath of methanol. No air gap is left between the needle tip and the coagulation bath. In order to process standardized fiber-mesh scaffolds, it was established that each scaffold was composed by an extruded polymer filament volume of 0.1mL, at an extrusion rate of 0.01 μ L/min. The collected fibers were then left in methanol overnight to complete the solidification process. Afterwards, the obtained fibers were neutralized with (1M) NaOH solution to fully regenerate the free amine form of the polymer chains and to avoid any re-dissolution of CHT. Subsequently, the fibers were washed with distilled water until the fibers pH equilibrated with that of the distilled water.

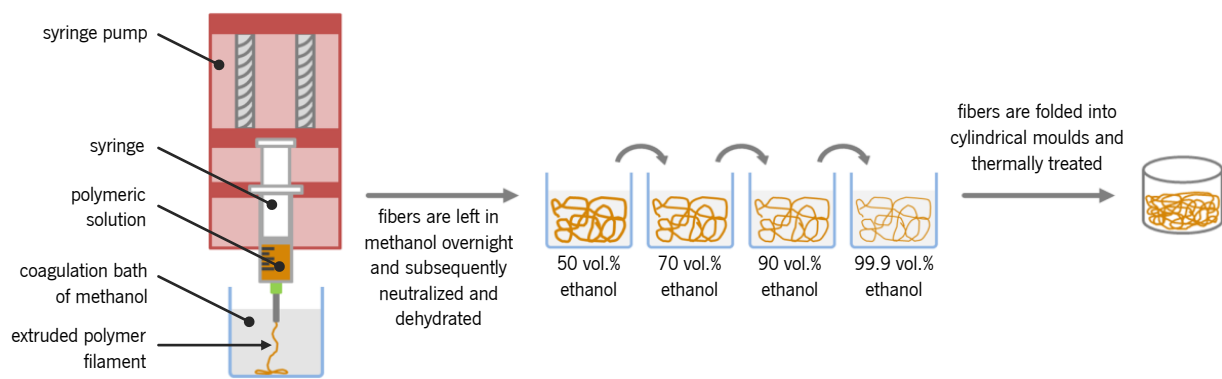


Figure 2.1. Schematic representation of the fibers processing and scaffolds obtention procedure.

In order to process the fiber-mesh scaffolds, the washed fibers were dehydrated with a series of aqueous ethanol solutions – 50, 70, 90 and 99.9 vol.% of ethanol -, folded into plastic cylindrical moulds and thermally treated in a oven at different temperatures ($T_a = 45, 50, 55, 60, 65$ and 70°C), either for $t_a = 1.5$ or 3h.

CHONDROCYTES ISOLATION AND SEEDING

Bovine cartilage was harvested from the patellar–femoral groove of calf legs. Cartilage tissue was cut into small pieces and chondrocytes were isolated by incubation in Dulbecco’s modified Eagle’s medium (Gibco) (DMEM) containing 0.2% type II collagenase at 37°C for 8h. The isolated chondrocytes were washed, centrifuged and re-suspended in DMEM with 10% heat inactivated fetal bovine serum (FBS, Sigma-Aldrich), Penicillin/Streptomycin 100U/100 μ g/mL (Invitrogen), 0.1mM MEMnonessential amino acids (Gibco), 0.2mM ascorbic acid 2-phosphate (Invitrogen) and 0.4mM proline (Sigma-Aldrich) and culture expanded. At confluence, the cells were detached using 0.25 wt.% trypsin in sterile PBS, washed with PBS, re-suspended in culture medium, and seeded (passage 2) on the scaffolds. The seeded constructs were incubated with the medium referred above.

For chondrogenic activity assessment studies, freshly isolated chondrocytes (passage 0) from the cartilage tissue were immediately seeded on the scaffolds and the constructs were cultured in chondrocyte differentiation medium composed of high glucose DMEM with 0.1 μ M dexamethasone (Sigma), 2mM L-glutamine (Glutamax, Gibco), 100 μ g/mL sodium pyruvate (Sigma), 0.2mM ascorbic acid 2-phosphate (Invitrogen), 0.4mM proline (Sigma-Aldrich), 50mg/mL insulin–transferrin–selenite (ITS + Premix, BD biosciences), 100 μ g/mL penicillin, 100 μ g/mL streptomycin and 10ng/mL transforming growth factor- β 3 (TGF- β 3, R&D Systems).

Prior cell seeding in both studies, the scaffolds were sterilized by immersion in a solution of 70 vol.% of ethanol for 4h, washed in PBS for 1h (three times) and, left immersed in PBS overnight. Then the scaffolds were incubated in the following culture media for 2 days: proliferation medium for cell viability studies and differentiation medium (serum-free) for chondrogenic activity studies. Cells in culture flasks and on scaffolds were incubated in a humidified atmosphere of 5% CO₂ at 37°C. The medium was replaced every 2 or 3 days. For both proliferation and differentiation studies, each scaffold was seeded with 5x10⁵ cells (in 20 μ L of cell suspension).

1.2.2. CHARACTERIZATION

SCANNING ELECTRON MICROSCOPY (SEM)

The SEM allows the observation and characterization of heterogeneous organic and inorganic materials on a nanometer (nm) to a micrometer (μ m) scale. Its popularity relies on its capability of obtaining 3D-like images of the surfaces of a very wide range of materials [16].

In SEM, the area or micro-volume to be analyzed is irradiated with a finely focused electron beam, which may be swept in a raster across the surface of the specimen to form images, or may be static to obtain an analysis at one position. The types of signals produced from the interaction of the electron beam with the sample include secondary electrons, backscattered electrons, characteristic X-rays, and other photons of various energies. These signals are obtained from specific emission volumes within the sample and are used to analyze many characteristics of the sample, like surface topography, composition, etc. [16]

The secondary and backscattered electrons imaging signals are the ones of highest interest. These vary primarily as a result of differences in surface topography. The secondary electron emission, confined to a very small volume near the beam impact area for certain choices of the beam energy, permits images to be obtained at a resolution approximating the size of the focused electron beam. The 3D appearance of the images is due to the large depth of field of the SEM as well as to the shadow relief effect of the secondary and backscattered electron contrast [16].

In SEM, characteristic X-rays are also emitted as a result of electron bombardment. The analysis of the characteristic X-radiation emitted from samples can yield both qualitative identification and quantitative elemental information from regions of a specimen, nominally $1\mu\text{m}$ in diameter and $1\mu\text{m}$ in depth under normal operating conditions [16].

A XL 30 ESEM-FEG Philips microscope was used to analyze the phase structures of the fibers, before and after solvent etching, to evaluate the overall 3D structure of the constructs and for chondrocyte proliferation and differentiation studies.

Prior SEM analysis, the constructs were fixed with formalin (only for the biological assays), dehydrated using graded ethanol solutions and critical point dried (Balzers CPD 030). All samples were coated with gold (Cressington Sputter Coater). The analysis was performed at an accelerating voltage of 10kV and magnifications from 200x to 2000x.

DIFFERENTIAL SCANNING CALORIMETRY (DSC)

The most popular thermal analysis technique is DSC that is used to measure endothermic and exothermic processes in materials as a function of temperature. DSC is used widely to characterize a broad range of materials including polymers, pharmaceuticals, food and biologicals, organic chemicals and inorganic materials. Typical transitions measured include the glass transition temperature, melting, crystallisation processes, curing and cure kinetics, onset of oxidation, and heat capacity. The two major types of DSCs include the heat flux device and the power compensation device [17].

The most common design for a DSC heat flux device consists in the sample, encapsulated in an aluminum pan, and an empty reference. Both sit on a thermoelectric disk surrounded by a furnace and as the furnace temperature is changed, usually in a linear fashion, heat is transferred to the sample and reference through the thermoelectric disk. The differential heat flow to the sample and reference is measured by area thermocouples using the thermal equivalent of Ohm's Law. However, this simplified one-term equation does not account for the heat flows into and out of the sensor and sample pan. The results achieved, though good, are not optimized with regards to baseline flatness, sensitivity, and resolution. The TA Instruments Q100 calorimeter with a refrigerated system used in this work, applies the Tzero™ technology, specifically designed to account for these extraneous heat flows. A much more accurate representation of the heat flow into and out of the sample is achieved. Rather than assume cell symmetry, which is required when using the conventional one-term heat flow equation, the Tzero™ technology accounts for the difference in the heating rate between the sample and reference, which has its largest impact during enthalpic events such as melting, also providing a way to model each individual DSC cell without assumptions [17].

Prior the scans, the temperature and energy calibrations were performed with an indium standard. All the samples were (a) left at 0°C for 2 minutes, (b) heated from 0 to 100°C, (c) left at 100°C for 2 minutes to erase the thermal history, (d) cooled down to 0°C, (e) left again at 0°C for 2 minutes, and (f) re-heated to 100°C. The heating and cooling rate was of 10°C/min. The melting temperature (T_m) and melting enthalpy (ΔH_m) of PCL were determined from the first and second heating scans. The peak temperature (T_m) and peak area (ΔH_m) values were calculated using the TA Instruments Universal Analysis software. The crystallinity degree (χ_c) can be calculated applying equation (1).

$$\chi_c = \frac{\Delta H_m}{\Delta H_u^0 w} \quad (1)$$

where ΔH_u^0 is the melting enthalpy of 100% crystalline PCL (i.e. 166 J/g [14]) and w is the weight fraction of PCL in the blend.

FOURIER TRANSFORM INFRARED (FTIR) SPECTROSCOPIC IMAGING MEASUREMENTS

A conventional way to infer about the miscibility of polymers is to investigate the structural information of the blend, via a detailed structural analysis provided by active vibrational transitions by FTIR [18-20]. This is performed analyzing the characteristic band shifts of the individual components in the blend. FTIR imaging systems also allow the combination of spectral and spatial information, enabling a spatial chemical visualization of the samples, which is highly interesting for the analysis of blends. FTIR can operate separately in three different modes: (a) transmission, in which the samples must be in thin sections ($\approx 20\mu\text{m}$), (b) reflection, which may lead to distorted spectra, depending on whether the reflection regime is specular or diffuse or, as is often the case, a mixture of both, or (c) attenuated total reflection (ATR) mode, which can overcome these problems, but in this case the surface has to be flat.

A Perkin-Elmer Spectrum Spotlight 200 FTIR Microscope System was used to perform the imaging measurements. The sample fibers were embedded in a resin (Epofix Kit, Struers, composition as given by the company: bisphenol-A-(epichlorhydrin), epoxy resin, oxirane and mono[(C12-14-alkyloxy)methyl] resin) for further cross-sections observation and consequent analysis in order to study the distribution of the polymers in the fibers. The preparation of the raw PCL sample consisted in a transversal cut of a PCL bead. The resin was left to solidify overnight at room temperature and the samples were subsequently cut into $\approx 10\mu\text{m}$ thick slices. The sectioning of the resin embedded samples was performed with a Leitz 1401 microtome using a glass knife at room temperature. Spectra were collected in continuous scan mode in order to construct FTIR maps, with an area of $240 \times 240\mu\text{m}^2$ and a spectral resolution of 16cm^{-1} , by averaging 15 scans for each spectrum. The samples were analyzed

in transmittance. Both spectra were collected in the spectral range of $4000 - 720\text{cm}^{-1}$ and integrated by taking the areas under the curve between the limits of the peaks of interest. The chosen region for CHT identification corresponds to C=O stretching of amide I, centered at approximately 1650cm^{-1} [20], and for the PCL the carbonyl stretching absorption at about 1730cm^{-1} [20]. There is also a characteristic peak of CHT that corresponds to the amine deformation vibration, centered at 1590cm^{-1} , but it could not be used due to overlap with an epoxy resin characteristic peak. To represent PCL and CHT in the chemical maps, the carbonyl stretching band was integrated between 1760 and 1710 cm^{-1} , while for CHT the integrated intensity of the band from 1670 to 1630 cm^{-1} was evaluated.

MICRO-COMPUTED TOMOGRAPHY (μCT)

μCT popularity can be attributed to its ability to provide precise quantitative and qualitative information on the 3D morphology of a specimen, which interior can be studied in great detail without comprising its structural integrity, as it remains intact after analysis, neither using toxic chemicals. As researchers began to recognize the potential of this radiographic technique, various biomedical applications are being explored, like the assessment of scaffolds, regenerated tissue [22] and vasculature networks [23-25]. Scaffolds with complex internal structures can be examined as any spatial location can be digitally isolated out. There is a wide range of information that can be obtained by μCT like the scaffolds material volume and surface area. These can be subsequently used to calculate the porosity and surface area to volume ratio. The 3D imaging allows a close up view of any specific location. Thus, informations like pore shape and the measurement of pore size can be obtained. By measuring the total and the interconnected pore volumes, interconnectivity can be derived [26]. Moreover, as μCT employs penetrative X-rays, closed pores can also be imaged.

The fiber-mesh scaffolds were analyzed using a high-resolution μCT Skyscan 1072 scanner (Skyscan, Kontich, Belgium). The scaffolds were scanned in a high-resolution mode using a pixel size of $8.70\mu\text{m}$ and integration time of 1.7ms . The X-ray source was set at 50keV of energy and $201\mu\text{A}$ of current. Representative data sets of 150 slices were transformed into a binary picture using a dynamic threshold of 60-255 (grey values) to distinguish polymer material from pore voids. This data was used for morphometric analysis (CT Analyser v1.5.1.5, SkyScan), which included quantifying the porosity and pore size. 3D virtual models of representative regions in the bulk of the scaffolds were also created, visualized, and registered using both image processing softwares (ANT 3-D creator v2.4, SkyScan).

SWELLING TESTS

For the swelling studies, dried scaffolds of each formulation were weighted (W_d) - prior immersion in PBS for 24h, at 37°C. After 2, 4, 6, 8 and 24 hours of immersion, the samples were weighted (wet, W_s) ($n = 2$). The superficial water was removed prior weighing with oil paper. The swelling ratio (Q) was obtained using equation (2).

$$Q = \frac{(W_s - W_d)}{W_d} \quad (2)$$

MECHANICAL PROPERTIES

The mechanical behavior of the three formulation scaffolds in wet state was assessed, under static compressive solicitation. A compression test determines the behavior of materials under crushing loads. The specimen is compressed and the deformation at various loads is recorded. Compressive stress and strain are calculated and plotted as a stress-strain diagram, which is used to determine its elastic limit, proportional limit, yield point, yield strength and, for some materials, compressive strength. From this test, the Young modulus can be obtained, which gives an insight about the stiffness of the material.

The scaffolds were immersed in PBS at physiological pH (≈ 7.4) and temperature ($\approx 37^\circ\text{C}$) for 3 days for complete hydration. The unconfined static compressive mechanical properties of the scaffolds were measured using an INSTRON 5543 (Instron Int. Ltd., U.S.A.), with a load cell of 1kN, for 60% of strain, at a loading rate of 2mm/min. The initial linear modulus on the stress/strain curves ($n = 3$), obtained by the secant method, defines the compressive modulus (or Young modulus).

CELL VIABILITY STUDIES

Cell viability and metabolic activity was studied using a live–dead assay and MTT [3-(4,5-dimethyl-2-thiazolyl)-2,5-diphenyl-2HO tetrazolium bromide] assay. At days 1, 3, 7, 14 and 21, the 3D constructs were rinsed with sterile PBS and stained with calcein/ethidium homodimer using the live–dead assay Kit (Invitrogen). Specifically, constructs were incubated in a PBS solution containing 6mM ethidium homodimer-1 and 2mM calcein-AM for 30 min at 37°C. Sections were immediately examined with an inverted fluorescence microscope (Nikon Eclipse E400) using a FITC/Texas Red filter. MTT staining was performed using 1% (total medium volume) of MTT solution (5mg/mL, Gibco) and an incubation time of 2h. Samples were then visualized using a light microscope.

Calcein AM is capable of permeating the plasma membrane of viable cells, where it is cleaved by intracellular esterases - and produces green fluorescence [27]. Ethidium-bromide homodimer-1 is able to enter cells with damaged membranes and bind to fragmented nucleic acids, thereby producing red

fluorescence in dead cells [27]. The MTT assay measures the metabolic activity of viable cells. MTT is a water-soluble tetrazolium salt [3-(4,5-dimethyl-2-thiazolyl)-2,5-diphenyl-2HO tetrazolium bromide] that yields a yellowish solution when dissolved in cell culture media lacking phenol red. Dissolved MTT can be converted to an insoluble purple formazan by dehydrogenase enzymes that catalyze the cleavage of the tetrazolium ring in MTT [28].

CHONDROGENIC ACTIVITY AND EXTRACELLULAR MATRIX PRODUCTION ASSESSMENT STUDIES

For histological analysis, samples were fixed in 10% formalin for 1h, embedded in paraffin, and processed using standard histological procedures. Sections (5µm thick) were obtained with a microtome and used for all stainings. The samples were stained with safranin-O/fast green (GAGs red and cytoplasm green) [29] and alcian blue/nuclear fast red (stains GAGs blue and cell nuclei red [30]), according to the procedure described on Table 2.2.

Table 2.2. Method used for the safranin-O and alcian blue stainings performed.

HYDRATION STEP	STAINING	DEHYDRATION STEP
	<u>SAFRANIN-O</u>	
	- stain with haematoxylin for 7 min. (optional);	
	- wash in the running tap water for a minimum of 10 min;	
2 min. in xylene (2x)	- stain with fast green solution for 3 min.;	
1 min. in 100% ethanol (2x)	- rinse quickly with 1% AcA solution for 10 to 15 seconds;	
1 min. in 96% ethanol	- stain in 0.1% safranin-O solution for 5 min.	2 min. 96% ethanol (2x)
1 min. in 90% ethanol		2 min. 100% ethanol (2x)
1 min. in 80% ethanol		2 min. xylene (2x)
1 min. in 70% ethanol	<u>ALCIAN BLUE</u>	
10 min. in distilled water	- clear with 3% AcA for 3 min;	
	- stain with Alcian blue (1% in AcA) solution for 30 min;	
	- wash in running water for 2 minutes and rinse in distilled water;	
	- counterstain with nuclear fast red for 5 minutes and rinse in tap water.	

Slides were assembled with resinous medium for visualization using a light microscope (Nikon Eclipse E400) and representative images captured using a digital camera (Sony Corporation, Japan) and Matrix Vision Software (Matrix Vision GmbH, Germany). Safranin-O is a cationic stain that binds to cartilage proteoglycans and GAGs such as chondroitin and keratan sulfate [31]. Alcian blue is one of the most widely used cationic dye for the demonstration of GAGs. It is thought to work by forming reversible electrostatic bonds between the cationic dye and the negative (anionic) sites on the polysaccharide [31].

DNA and GAG quantification assays were performed after 1, 14, and 21 days of culture in differentiation medium. The constructs were taken from the chondrocyte differentiation medium, washed in PBS and frozen at -80°C until further processing. Afterwards, they were digested overnight at

56°C (> 16h) in a Tris-EDTA buffered solution containing 1mg/mL proteinase-K, 18.5µg/mL pepstatin A, and 1µg/mL iodoacetamide (Sigma–Aldrich).

Quantification of total DNA was performed with Cyquant dye kit according to the manufacturers description (Molecular Probes, Eugene, Oregon, U.S.A.), using a spectrofluorometer (Victor³, Perkin-Elmer, U.S.A.), at an excitation wavelength of 480nm and an emission wavelength of 520nm (n = 3, in triplicate). GAG amount was determined spectrophotometrically (Monochromator Microplate Reader TECAN Safire2, Austria) after reaction with dimethylmethylene blue dye (DMMB, Sigma-Aldrich) by measuring absorbance at 520nm. The final amount was calculated using a standard of chondroitin sulphate B (Sigma–Aldrich) (n = 3, in triplicate).

STATISTICAL ANALYSIS

Values on this study are reported as mean and standard deviation. Statistical analysis was performed using the one-way ANOVA test, with $p < 0.05$ considered as being statistically significant.

2. REFERENCES

- [1] Wan Y, *et al.* Development of polycaprolactone/chitosan blend porous scaffolds. *Journal of Materials Science: Materials in Medicine*, 2009. 20(3) pp. 719-724.
- [2] Yang X, Chen X and Wang H. Acceleration of osteogenic differentiation of preosteoblastic cells by chitosan containing nanofibrous scaffolds. *Biomacromolecules*, 2009. 10(10) pp. 2772-2778.
- [3] Sarasam A and Madihally SV. Characterization of chitosan–polycaprolactone blends for tissue engineering applications. *Biomaterials*, 2005. 26(27) pp. 5500-5508.
- [4] Sarasam AR, *et al.* Blending chitosan with polycaprolactone: porous scaffolds and toxicity. *Macromolecular Bioscience*, 2007. 7(9-10) pp. 1160-1167.
- [5] Wan Y, *et al.* Compressive mechanical properties and biodegradability of porous poly(caprolactone)/chitosan scaffolds. *Polymer Degradation and Stability*, 2008. 93(10) pp. 1736-1741.
- [6] Houde S, Xiufeng X and Rongfang L. Preparation and characterization of polycaprolactone-chitosan composites for tissue engineering applications. *Journal of Materials Science*, 2007. 42(19) pp. 8113-8119.
- [7] Prabhakaran MP, *et al.* Electrospun biocomposite nanofibrous scaffolds for neural tissue engineering. *Tissue Engineering Part A*, 2008. 14(11) pp. 1787-1797.
- [8] Nielsen GD, *et al.* Sensory irritation mechanisms investigated from model compounds: Trifluoroethanol, hexafluoroisopropanol and methyl hexafluoroisopropyl ether. *Archives of Toxicology*, 1996. 70(6) 319-328.
- [9] Cruz DMG, Ribelles JLG and Sanchez MS. Blending polysaccharides with biodegradable polymers. I. Properties of chitosan/polycaprolactone blends. *Journal of Biomedical Materials Research. Part B, Applied Biomaterials*, 2008. 85(2) pp. 303-313.
- [10] Cruz DMG, *et al.* Physical interactions in macroporous scaffolds based on poly(ϵ -caprolactone)/ chitosan semi-interpenetrating polymer networks. *Polymer*, 2009. 50(9) pp. 2058–2064.
- [11] Leffler CC and Müller BW. Influence of the acid type on the physical and drug liberation properties of chitosan-gelatin sponges. *International Journal of Pharmaceutics*, 2000. 194(2) pp. 229-237.
- [12] Dufresne A, *et al.* Morphology, phase continuity and mechanical behaviour of polyamide 6/chitosan blends. *Polymer*, 1999. 40(7) pp. 1657-1666.
- [13] Park WH, *et al.* Effect of chitosan on morphology and conformation of electrospun silk fibroin nanofibers. *Polymer*, 2004. 45(21) pp. 7151-7157.
- [14] Malheiro VN, *et al.* New poly(ϵ -caprolactone)/chitosan blend fibers for tissue engineering applications. *Acta Biomaterialia*, 2010. 6(2) pp. 418-428.
- [15] Puppi D, *et al.* Polymeric materials for bone and cartilage repair. *Progress in Polymer Science*, 2010. 35(4) pp. 403-440.
- [16] Goldstein J, *et al.* *Scanning Electron Microscopy and X-ray Microanalysis*. Springer US, 2003. pp. 1,2.
- [17] Danley R, Kelly T and Groh J. Improved DSC Performance Using Tzero Technology. *International Laboratory*, 2001. pp. 30–31.
- [18] Zhou X, *et al.* Influence of maleic anhydride grafted polypropylene on the miscibility of polypropylene/polyamide-6 blends using ATR-FTIR mapping. *Vibrational Spectroscopy*, 2009. 49(1) pp. 17-21.
- [19] De Giacomo O, Cesàro A and Quaroni L. Synchrotron Based FTIR Spectromicroscopy of Biopolymer Blends Undergoing Phase Separation. *Food Biophysics*, 2008. 3(1) pp. 77-86.
- [20] Vogel C, Wessel E and Siesler HW. FT-IR imaging spectroscopy of phase separation in blends of poly(3-hydroxybutyrate) with poly(L-lactic acid) and poly(ϵ -caprolactone). *Biomacromolecules*, 2008. 9(2) pp. 523–527.
- [21] Chiono V, *et al.* Characterisation of blends between poly(ϵ -caprolactone) and polysaccharides for tissue engineering applications. *Materials Science and Engineering C*, 2009. 29(7) pp. 2174-2187.
- [22] Verna C, *et al.* Healing patterns in calvarial bone defects following guided bone regeneration in rats. *Journal of Clinical Periodontology*, 2002. 29(9) pp. 865–870.
- [23] Bentley MD, *et al.* The use of microcomputed tomography to study microvasculature in small rodents, *American Journal of Physiology - Regulatory, Integrative and Comparative Physiology*, 2002. 282(5) pp. 1267–1279.
- [24] Jorgensen SM, Demirkaya O and Ritman EL. Three-dimensional imaging of vasculature and parenchyma in intact rodent organs with X-ray micro-CT, *American Journal of Physiology - Heart Circulatory Physiology*, 1998. 275(3 pt 2) pp. H1103–H1114.

- [25] Ortiz MC, *et al.* Microcomputed tomography of kidneys following chronic bile duct ligation. *Kidney International*, 2000. 58(4) pp. 1632–1640.
- [26] Wang F, *et al.* Precision extruding deposition and characterization of cellular poly- ϵ -caprolactone tissue scaffolds. *Rapid Prototyping Journal*, 2004. 10(1) pp. 42-49.
- [27] Haugland RP. Handbook of fluorescent probes and research chemicals. *Molecular Probes* (7th edition), Eugene, OR, 1999.
- [28] Liu H, *et al.* An *in vitro* evaluation of the Ca/P ratio for the cytocompatibility of nano-to-micron particulate calcium phosphates for bone regeneration. *Acta Biomaterialia*, 2008. 4(5) pp. 1472-1479.
- [29] Lien SM, Ko LY and Huang TJ. Effect of pore size on ECM secretion and cell growth in gelatin scaffold for articular cartilage tissue engineering. *Acta Biomaterialia*, 2009. 5(2) pp. 670-679.
- [30] Alves da Silva ML, *et al.* Chitosan/polyester-based scaffolds for cartilage tissue engineering: Assessment of extracellular matrix formation. *Acta Biomaterialia*, 2010. 6(3) pp. 1149-1157.
- [31] Delorme B and Charbord P. Culture and Characterization of Human Bone Marrow Mesenchymal Stem Cells. In: Hauser H and Fussenegger M (editors). *Methods in Molecular Medicine, 2nd edition Tissue Engineering*. Humana Press Inc, Totowa, NJ, 2007. p. 77.

CHAPTER III

CHITOSAN/POLY(ϵ -CAPROLACTONE) BLEND SCAFFOLDS FOR CARTILAGE REPAIR

CHITOSAN/POLY(ϵ -CAPROLACTONE) BLEND SCAFFOLDS FOR CARTILAGE REPAIR

Sara C. Neves^{1,2}, Liliana S. Moreira Teixeira³, Lorenzo Moroni³, Rui L. Reis^{1,2}, Clemens A. Van Blitterswijk³, Natália M. Alves^{1,2}, Marcel Karperien³, João F. Mano^{1,2*}

¹ 3B's Research Group – Biomaterials, Biodegradables and Biomimetics, Headquarters of the European Institute of Excellence on Tissue Engineering and Regenerative Medicine. Department of Polymer Engineering, University of Minho. AvePark, 4806-909 Taipas, Guimarães, Portugal.

² IBB – Institute for Biotechnology and Bioengineering, PT Associated Laboratory, Guimarães, Portugal.

³ MIRA - Institute for BioMedical Technology and Technical Medicine, University of Twente. Department of Tissue Regeneration, P.O. Box 217, Enschede 7500 AE, The Netherlands.

* Corresponding author.

Address: 3B's Research Group - Biomaterials, Biodegradables and Biomimetics, AvePark, Zona Industrial da Gandra, S. Cláudio do Barco, 4806-909 Caldas das Taipas, Guimarães, Portugal.

TEL.:+351-253510904; fax: +351-253510909; e-mail address: jmano@dep.uminho.pt.

ABSTRACT

CHT/PCL blend 3D fiber-mesh scaffolds were studied as possible support structures for AC tissue repair. Micro-fibers were obtained by wet-spinning of three different polymeric solutions: 100:0 (100CHT), 75:25 (75CHT) and 50:50 (50CHT) wt.% CHT/PCL, using a common solvent solution of 100 vol.% of formic acid. SEM analysis showed a homogenous surface distribution of PCL. PCL was well dispersed throughout the CHT phase as analyzed by DSC and FTIR. The fibers were folded into cylindrical moulds and underwent a thermal treatment to obtain the scaffolds. μ CT analysis revealed an adequate porosity, pore size and interconnectivity for TE applications. The PCL component led to a higher fiber surface roughness, decreased the scaffolds swelling ratio and increased their compressive mechanical properties. Biological assays were performed after culturing bACs up to 21 days. SEM analysis, live-dead and metabolic activity assays showed that cells attached, proliferated, and were metabolically active over all scaffolds formulations. Cartilaginous ECM formation was observed in all formulations. The 75CHT scaffolds supported the most neo-cartilage formation, as demonstrated by an increase in GAG production. In contrast to 100CHT scaffolds, ECM was homogeneously deposited on the 75CHT and 50CHT scaffolds. Although mechanical properties of the 50CHT scaffold were better, the 75CHT scaffold facilitated better neo-cartilage formation. Taken together, and having in consideration that ECM formation is expected to improve the scaffold's mechanical properties, the 75CHT formulation is potentially very promising for ACT engineering applications.

Keywords: chitosan, polycaprolactone, scaffold, cartilage tissue engineering

1. INTRODUCTION

AC regeneration by TE approaches has tempting for a long time due to its limited capacity of self-repair [1,2]. This mainly derives from the lack of a vasculature network, resulting in insufficient turn-over of healthy chondrocytes to the defective sites and low productivity of characteristic proteins of the surrounding ECM [1,2]. 3D scaffolds are particularly important for AC TE approaches because the chondrogenic phenotype is maintained when chondrocytes are placed in a proper 3D environment [2].

Cartilage-specific ECM components play an important role in regulating expression of the chondrogenic phenotype and supporting chondrogenesis [3,4]. CHT, a naturally derived polysaccharide, is an excellent candidate as AC TE scaffolding biomaterial, due to its structural similarity with various GAGs found in cartilage [5]. It was shown to support chondrogenic activity [5] and to allow cartilage ECM proteins expression by chondrocytes [6,7]. However, the brittleness in the wet state (40-50% of strain at break) of CHT scaffolds [8] is a major drawback for application in AC TE.

Among synthetic biomaterials, PCL is highly appealing due to its (a) physical-chemical and mechanical characteristics [9], (b) easy processability related to a relatively low melting temperature (ca. 60°C) [8], (c) non-toxic degradation products and (d) Food and Drug Administration (FDA) approval for biomedical applications [9]. It has been previously reported that chondrocytes attach and proliferate on PCL films [10] and, additionally, start to produce a cartilaginous ECM in PCL scaffolds [11,12]. However, PCL main drawbacks as scaffolding material comprise the (a) absence of cell recognition sites, (b) its hydrophobicity and (c) its relatively slower degradation/resorption kinetics compared to other polyesters [13,14].

Taken together, both polymers seem to have complementary desirable properties. When combined, the hydrophilic nature of CHT will enhance the wettability and permeability, with a consequent acceleration of PCL hydrolytic degradation. The PCL component is expected to lower the swelling ratio and improve the wet state mechanical properties of CHT scaffolds [15]. Moreover, the bioactivity of PCL can be enhanced when combined with natural polymers [16], as sub-micron phase separation of hydrophilic and hydrophobic domains could be beneficial for cell adhesion.

Different methodologies have been used to combine CHT and PCL. Due to its simplicity and effectiveness, blending allows tailoring the materials properties by adjusting the blend composition [17]. Moreover, polymers can co-exist with minimal chemical modification [8]. However, common solvents for CHT and PCL are scarce. HFIP [18,19] or AcA [8,20] are, by far, the most used solvents. However, HFIP is very toxic, carcinogenic, expensive and difficult to remove [21]. Alternatively, diluted AcA solutions lead to phase separation [20].

3D scaffolds of blends of CHT and PCL for TE applications have been previously developed by freeze-drying [22] and particle-leaching [23,24]. 3D fiber-mesh scaffolds started to be used in TE applications [25,26] as they present (a) an increased surface area for cell attachment [2], (b) improved pore architecture [2], and (c) good mechanical stability [2]. Processing CHT/PCL blends fibers was reported for the first time by electrospinning, first for neural TE applications [27], and later in bone TE applications [28]. Recently, Malheiro *et al.* [17] processed non-woven fibers of blends of CHT and PCL, by wet-spinning. A common solvent solution of 70:30 vol.% formic acid/acetone was used and preliminary studies were performed on folding the fibers to obtain 3D fiber-meshes. Shalumon *et al.* [29] processed CHT/PCL blend electrospun fibers using this solvent solution.

The aim of the present work was to develop CHT/PCL blend scaffolds, based on a previous methodology to produce CHT/PCL fibers [17]. Furthermore, the suitability of these structures as cartilage TE supports was analyzed. Three different formulations – 100:0, 75:25 and 50:50 wt.% CHT/PCL – were used, in order to investigate the effect of polymer composition in the physical-chemical and biological properties of the fiber-meshes.

2. MATERIALS AND METHODS

2.1. MATERIALS

CHT (low MW, 75-85% deacetylation degree, Ref. 448869), PCL (80KDa, Ref. 440744), formic acid, and methanol were purchased from Sigma-Aldrich. The solvents were used without further purification. CHT was purified by recrystallization before being used, as described elsewhere [17]. Briefly, it was dissolved in 1% (wt./vol.) AcA solution and then filtered through porous membranes (Whatman® ashes filter paper, 20-25 μ m, and nylon filter sheet) into a Buckner flask under vacuum. Adjusting the pH of the solution to about 8, through the addition of NaOH, caused flocculation due to deprotonation and insolubility of the polymer at neutral pH. The polymer was then neutralized until the pH equaled that of distilled water, frozen at -80°C and lyophilized. Polymeric solutions with distinct concentrations were prepared according to the concentrations presented in Table 3.1.

Table 3.1. Total polymer concentration of each formulation [17].

FORMULATION	CHT/PCL WEIGHT RATIO	TOTAL POLYMER CONCENTRATION (wt./vol. %)
100CHT	100 : 0	13
75CHT	75 : 25	17
50CHT	50 : 50	21

2.2. METHODS

2.2.1. SCAFFOLDS PREPARATION

The polymeric solutions of CHT and CHT/PCL blends were prepared by dissolving CHT and PCL in 100 vol.% formic acid, in the proportions of 100, 75, and 50 wt.% in CHT content (Table 3.1), from now referred to as 100CHT, 75CHT, and 50CHT, respectively. The solutions were left at 30°C overnight for a complete dissolution of both polymers. After that, the solutions were placed into a 5mL syringe with a capillary tip having an inner diameter of 0.8mm. A syringe pump was used to feed the solutions into the needle tip. A coagulation bath of methanol was used to precipitate the solutions (0.1mL to obtain a continuous fiber, in order to process one scaffold), and no air gap was left between the tip and the referred bath during the extrusion. The fibers were left in the methanol bath overnight to complete the solidification process. They were neutralized with 1M NaOH solution to fully regenerate the free amine form of the polymer chains and to avoid any CHT re-dissolution. Afterwards, the fibers were washed (at least four times) with distilled water until the pH reached a physiological value. Subsequently, they were dehydrated in a series of ethanol aqueous solutions (50, 70, 90 and 99.9 vol.% ethanol), folded in

plastic cylindrical moulds and dried in an oven at different temperatures ($T_a = 45, 50, 55, 60, 65$ and 75°C) for either $t_a = 1.5\text{h}$ or 3h , in a similar way as described in [17].

2.2.2. CHARACTERIZATION

SCANNING ELECTRON MICROSCOPY (SEM)

An XL 30 ESEM-FEG Philips microscope was used to analyze the phase structures of the fibers, before and after solvent etching, to evaluate the overall 3D structure of the constructs and for chondrocyte proliferation and differentiation studies. Prior SEM analysis, the constructs were fixed with formalin (only for the biological assays), dehydrated using graded ethanol solutions and critical point dried (Balzers CPD 030). All samples were coated with gold (Cressington Sputter Coater). The analysis was performed at an accelerating voltage of 10kV and magnifications from 200x to 2000x.

DIFFERENTIAL SCANNING CALORIMETRY (DSC)

The DSC experiments were conducted in a Q100 calorimeter with refrigerated cooling system (TA Instruments). Prior the scans, the temperature and energy calibrations were performed with an indium standard. All the samples were (a) left at 0°C for 2 minutes, (b) heated from 0 to 100°C , (c) left at 100°C for 2 minutes to erase the thermal history, (d) cooled down to 0°C , (e) left again at 0°C for 2 minutes, and (f) re-heated to 100°C . The heating and cooling rate was of $10^\circ\text{C}/\text{min}$. The melting temperature (T_m) and melting enthalpy (ΔH_m) of PCL were determined from the first and second heating scans. The peak temperature (T_m) and peak area (ΔH_m) values were calculated using the TA Instruments Universal Analysis software. The crystallinity degree (χ_c) can be calculated applying equation (1).

$$\chi_c = \frac{\Delta H_m}{\Delta H_u^0 w} \quad (1)$$

where ΔH_u^0 is the melting enthalpy of 100% crystalline PCL (i.e. 166 J/g [17]) and w is the weight fraction of PCL in the blend.

FOURIER TRANSFORM INFRARED (FTIR) SPECTROSCOPIC IMAGING MEASUREMENTS

A Perkin-Elmer Spectrum Spotlight 200 FTIR Microscope System was used to perform the imaging measurements. The sample fibers were embedded in a resin (Epofix Kit, Struers, composition as given by the company: bisphenol-A-(epichlorhydrin), epoxy resin, oxirane and mono[(C12-14-alkyloxy)methyl] resin) for further cross-sections observation and consequent analysis in order to study the distribution of the polymers in the fibers. The preparation of the raw PCL sample consisted in a transversal cut of a

PCL bead. The resin was left to solidify overnight at room temperature and the samples were subsequently cut into $\approx 10\mu\text{m}$ thick slices. The sectioning of the resin embedded samples was performed with a Leitz 1401 microtome using a glass knife at room temperature. Spectra were collected in continuous scan mode in order to construct FTIR maps, with an area of $240 \times 240\mu\text{m}^2$ and a spectral resolution of 16cm^{-1} , by averaging 15 scans for each spectrum. The samples were analyzed in transmittance. Both spectra were collected in the spectral range of $4000 - 720\text{cm}^{-1}$ and integrated by taking the areas under the curve between the limits of the peaks of interest. The chosen region for CHT identification corresponds to C=O stretching of amide I, centered at approximately 1650cm^{-1} [30], and for the PCL the carbonyl stretching absorption at about 1730cm^{-1} [30]. There is also a characteristic peak of CHT that corresponds to the amine deformation vibration, centered at 1590cm^{-1} , but it could not be used due to overlap with an epoxy resin characteristic peak. To represent PCL and CHT in the chemical maps, the carbonyl stretching band was integrated between 1760 and 1710cm^{-1} , while for CHT the integrated intensity of the band from 1670 to 1630cm^{-1} was evaluated.

MICRO-COMPUTED TOMOGRAPHY (μCT)

The fiber-mesh scaffolds were analyzed using a high-resolution micro-computed tomography (μCT) Skyscan 1072 scanner (Skyscan, Kontich, Belgium). The scaffolds were scanned in a high-resolution mode using a pixel size of $8.70\mu\text{m}$ and integration time of 1.7ms . The X-ray source was set at 50keV of energy and $201\mu\text{A}$ of current. Representative data sets of 150 slices were transformed into a binary picture using a dynamic threshold of 60-255 (grey values) to distinguish polymer material from pore voids. This data was used for morphometric analysis (CT Analyser v1.5.1.5, SkyScan), which included quantifying the porosity and pore size. 3D virtual models of representative regions in the bulk of the scaffolds were also created, visualized, and registered using both image processing softwares (ANT 3-D creator v2.4, SkyScan).

SWELLING TESTS

For the swelling studies, dried scaffolds of each formulation were weighted (W_d) - prior immersion in PBS for 24h, at 37°C . After 2, 4, 6, 8 and 24 hours of immersion, the samples were weighted (wet, W_s) ($n = 2$). The superficial water was removed prior weighing with oil paper. The swelling ratio (Q) was obtained using equation (2).

$$Q = \frac{(W_s - W_d)}{W_d} \quad (2)$$

MECHANICAL PROPERTIES

The mechanical behavior of the three formulation scaffolds in wet state was tested, under static compression solicitation. The scaffolds were immersed in PBS at physiological pH (≈ 7.4) and temperature ($\approx 37^\circ\text{C}$) for 3 days for complete hydration. The unconfined static compressive mechanical properties of the scaffolds were measured using an INSTRON 5543 (Instron Int. Ltd., U.S.A.), with a load cell of 1kN, for 60% of strain, at a loading rate of 2mm/min. The initial linear modulus on the stress/strain curves ($n = 3$), obtained by the secant method, defines the compressive modulus (or Young modulus).

CHONDROCYTES ISOLATION AND SEEDING

Bovine cartilage was harvested from the patellar–femoral groove of calf legs. Cartilage tissue was cut into small pieces and chondrocytes were isolated by incubation in Dulbecco's modified Eagle's medium (Gibco) (DMEM) containing 0.2% type II collagenase at 37°C for 8h. The isolated chondrocytes were washed, centrifuged and re-suspended in DMEM with 10% heat inactivated fetal bovine serum (FBS, Sigma-Aldrich), Penicillin/Streptomycin 100U/100 $\mu\text{g}/\text{mL}$ (Invitrogen), 0.1mM MEMnonessential amino acids (Gibco), 0.2mM ascorbic acid 2-phosphate (Invitrogen) and 0.4mM proline (Sigma-Aldrich) and culture expanded. At confluence, the cells were detached using 0.25 wt.% trypsin in sterile PBS, washed with PBS, re-suspended in culture medium, and seeded (passage 2) on the scaffolds. The seeded constructs were incubated with the medium referred above.

For chondrogenic activity assessment studies, freshly isolated chondrocytes (passage 0) from the cartilage tissue were immediately seeded on the scaffolds and the constructs were cultured in chondrocyte differentiation medium composed of high glucose DMEM with 0.1 μM dexamethasone (Sigma), 2mM L-glutamine (Glutamax, Gibco), 100 $\mu\text{g}/\text{mL}$ sodium pyruvate (Sigma), 0.2mM ascorbic acid 2-phosphate (Invitrogen), 0.4mM proline (Sigma-Aldrich), 50mg/mL insulin–transferrin–selenite (ITS + Premix, BD biosciences), 100 $\mu\text{g}/\text{mL}$ penicillin, 100 $\mu\text{g}/\text{mL}$ streptomycin and 10ng/mL transforming growth factor- $\beta 3$ (TGF- $\beta 3$, R&D Systems).

Prior cell seeding in both studies, the scaffolds were sterilized by immersion in a solution of 70 vol.% of ethanol for 4h, washed in PBS for 1h (three times) and left immersed in PBS overnight. Then, the scaffolds were incubated in the following culture media for 2 days: proliferation medium for cell viability studies and differentiation medium (serum-free) for chondrogenic activity studies. Cells in culture flasks and on scaffolds were incubated in a humidified atmosphere of 5% CO_2 at 37°C . The medium was replaced every 2 or 3 days. For both proliferation and differentiation studies, each scaffold was seeded with 5×10^5 cells (in 20 μL of cell suspension).

CELL VIABILITY STUDIES

Cell viability and metabolic activity was studied using a live–dead assay and MTT [3-(4,5-dimethyl-2-thiazolyl)-2,5-diphenyl-2H-tetrazolium bromide] assay. At days 1, 3, 7, 14 and 21, the 3D constructs were rinsed with sterile PBS and stained with calcein/ethidium homodimer using the live–dead assay Kit (Invitrogen). Sections were immediately examined with an inverted fluorescence microscope (Nikon Eclipse E400) using a FITC/Texas Red filter. Calcein AM is capable of permeating the plasma membrane of viable cells, where it is cleaved by intracellular esterases - and produces green fluorescence. Ethidium-bromide homodimer-1 is able to enter cells with damaged membranes and binds to fragmented nucleic acids, thereby producing red fluorescence in dead cells.

MTT staining was performed using 1% (total medium volume) of MTT solution (5mg/mL, Gibco) and an incubation time of 2h. Samples were visualized using a light microscope. Dissolved MTT can be converted to an insoluble purple formazan by dehydrogenase enzymes that catalyze the cleavage of the tetrazolium ring in MTT.

CHONDROGENIC ACTIVITY AND EXTRACELLULAR MATRIX PRODUCTION ASSESSMENT STUDIES

For histological analysis, samples were fixed in 10% formalin for 1h, embedded in paraffin, and processed using standard histological procedures. Sections (5 μ m thick) were obtained with a microtome and used for all stainings. After rehydration with xylene and an ethanol series (from 100 to 70 vol.%) the samples were stained with safranin-O/fast green ^[31] and alcian blue/nuclear fast red ^[32]. Slides were assembled with resinous medium for visualization using a light microscope (Nikon Eclipse E400) and representative images captured using a digital camera (Sony Corporation, Japan) and Matrix Vision Software (Matrix Vision GmbH, Germany).

DNA and GAG quantification assays were performed after 1, 14, and 21 days of culture in differentiation medium. The constructs were taken from the chondrocyte differentiation medium, washed in PBS and frozen at -80°C until further processing. Afterwards, they were digested overnight at 56°C (> 16h) in a Tris-EDTA buffered solution containing 1mg/mL proteinase-K, 18.5 μ g/mL pepstatin A, and 1 μ g/mL iodoacetamide (Sigma–Aldrich).

Quantification of total DNA was performed with Cyquant dye kit according to the manufacturers description (Molecular Probes, Eugene, Oregon, U.S.A.), using a spectrofluorometer (Victor³, Perkin-Elmer, U.S.A.), at an excitation wavelength of 480nm and an emission wavelength of 520nm (n = 3, in triplicate).

GAG amount was determined spectrophotometrically (Monochromator Microplate Reader TECAN Safire2, Austria) after reaction with dimethylmethylene blue dye (DMMB, Sigma-Aldrich) by measuring

absorbance at 520nm. The final amount was calculated using a standard of chondroitin sulphate B (Sigma–Aldrich) (n = 3, in triplicate).

STATISTICAL ANALYSIS

Values on this study are reported as mean and standard deviation. Statistical analysis was performed using the one-way ANOVA test, with $p < 0.05$ considered as being statistically significant.

3. RESULTS AND DISCUSSION

3.1. FIBERS PHYSICAL-CHEMICAL CHARACTERIZATION

100CHT, 75CHT and 50CHT fibers were successfully obtained. The approach reported by Malheiro *et al.* [17] was modified into a simpler system, where the solvent solution is composed of 100 vol.% of formic acid.

Phase morphology and surface properties are important parameters to be considered when a scaffold is being designed. The homogeneity of the CHT/PCL polymeric blends is not only important in terms of their internal structural and mechanical integrity, but also in terms of PCL superficial domains distribution. Therefore, solvent etching was performed and the fiber surfaces were analyzed by SEM (Figure 3.1), before and after etching. In order to remove the PCL phase of the blends, sample fibers were immersed in chloroform for 24h, which dissolves PCL but not CHT.

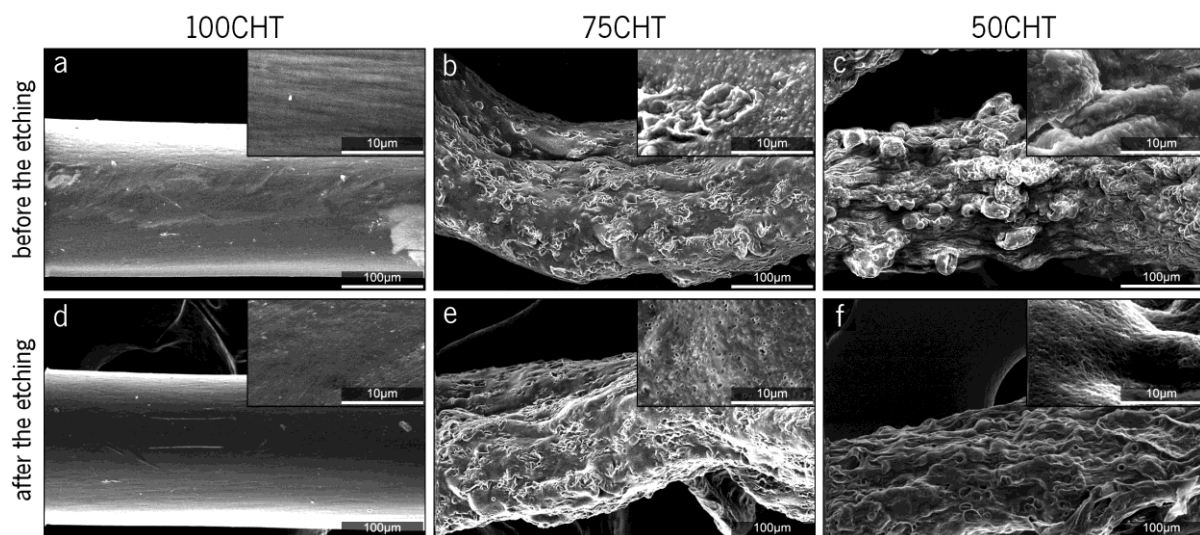


Figure 3.1. SEM microphotographs of the fiber's surfaces, before (a, b, c) and after (d, e, f) the solvent etching procedure.

Before etching, fiber's topography (Figure 3.1 (a – c)) varied between the three formulations with an increase in surface roughness with increasing PCL concentration. After etching (Figure 3.1 (d – f)), the blends kept their dimensional stability, indicating that the CHT is the continuous phase in the blend. This is consistent with Cruz *et al.* [20], who reported the presence of a continuous CHT phase starting at 20 wt.% CHT content. Pore formation was also observed on the fiber surface after etching, thus confirming PCL extracted domains, with sizes in the micron-scale. The distribution of the pores was rather homogeneous in both blends. As expected, lower pore formation was observed in etched 75CHT fibers, when compared to 50CHT fibers. Such distribution of more hydrophobic (PCL) regions dispersed

in a more hydrophilic phase (CHT) may promote protein adsorption and cell attachment under physiological conditions.

The miscibility of the blend components was analyzed by evaluating the changes in the T_m as a function of composition using DSC. The DSC analysis was focused on the thermal properties of the PCL phase in the blends. Thus, the temperature range chosen was from 0°C to 100°C to cover the melting and crystallization processes of the PCL component. The trends obtained (from the first and second heat scans) are presented in Figure 3.2 (a, b). Two heating scans were carried out, being the first one used to infer about any effect of processing on the development of the PCL structure. Analyzing the graphs presented on Figure 3.2 (c, d), both the T_m and χ_c values of PCL in the blends did not vary significantly from the values of pure PCL.

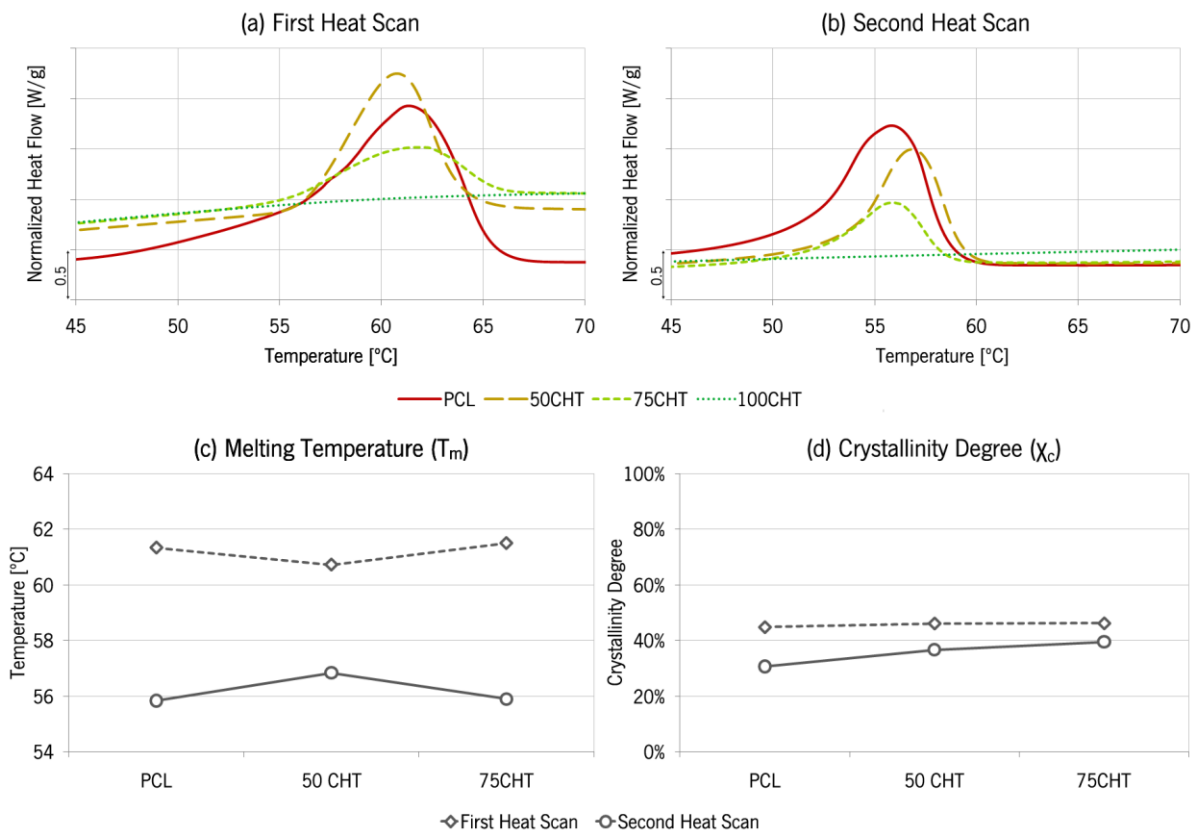


Figure 3.2. DSC (a) first and (b) second heating scans for PCL, CHT and their blend fibers; PCL and blend fibers (c) melting temperature (T_m) and (d) crystallinity degree (χ_c) variations.

The information given by the DSC analysis about polymer mixing homogeneity could offer a preliminary insight about the interaction of both polymer phases in the blends. CHT and PCL are thermodynamically not miscible, and although they may present some compatibility degree, this mainly depends on the preparation method [30]. As already pointed out by Olabarrieta *et al.* [33], a high degree of dispersion occurs between PCL and CHT phases, although mixing is not observed at a molecular level [33]. Some authors pointed out that the melting depression of PCL in CHT/PCL blends (using HFIP [19] and aqueous AcA solution as solvents [8,34]) is an indication of the miscibility of PCL and CHT. Here, we

did not find any linear relationship between the CHT content and the T_m variation, as it did not vary significantly, when compared to pure PCL. This may indicate that phase separation exists between the two polymers. The PCL domains may aggregate and crystallize without significant interference from CHT. Such assumption is supported by the SEM images (Figure 3.1 (d - f)) that show the superficial features of the removed PCL domains. Corroborating this assumption, no significant variations on the χ_c of the blend fibers were observed when compared to pure PCL (Figure 3.2 (d)).

FTIR analysis was performed in 10 μ m thick sections of fibers embedded in epoxy resin to evaluate the distribution of CHT and PCL in the fiber's cross-sections. FTIR spectra and associated chemical maps are presented in Figures 3.3 and 3.4, respectively.

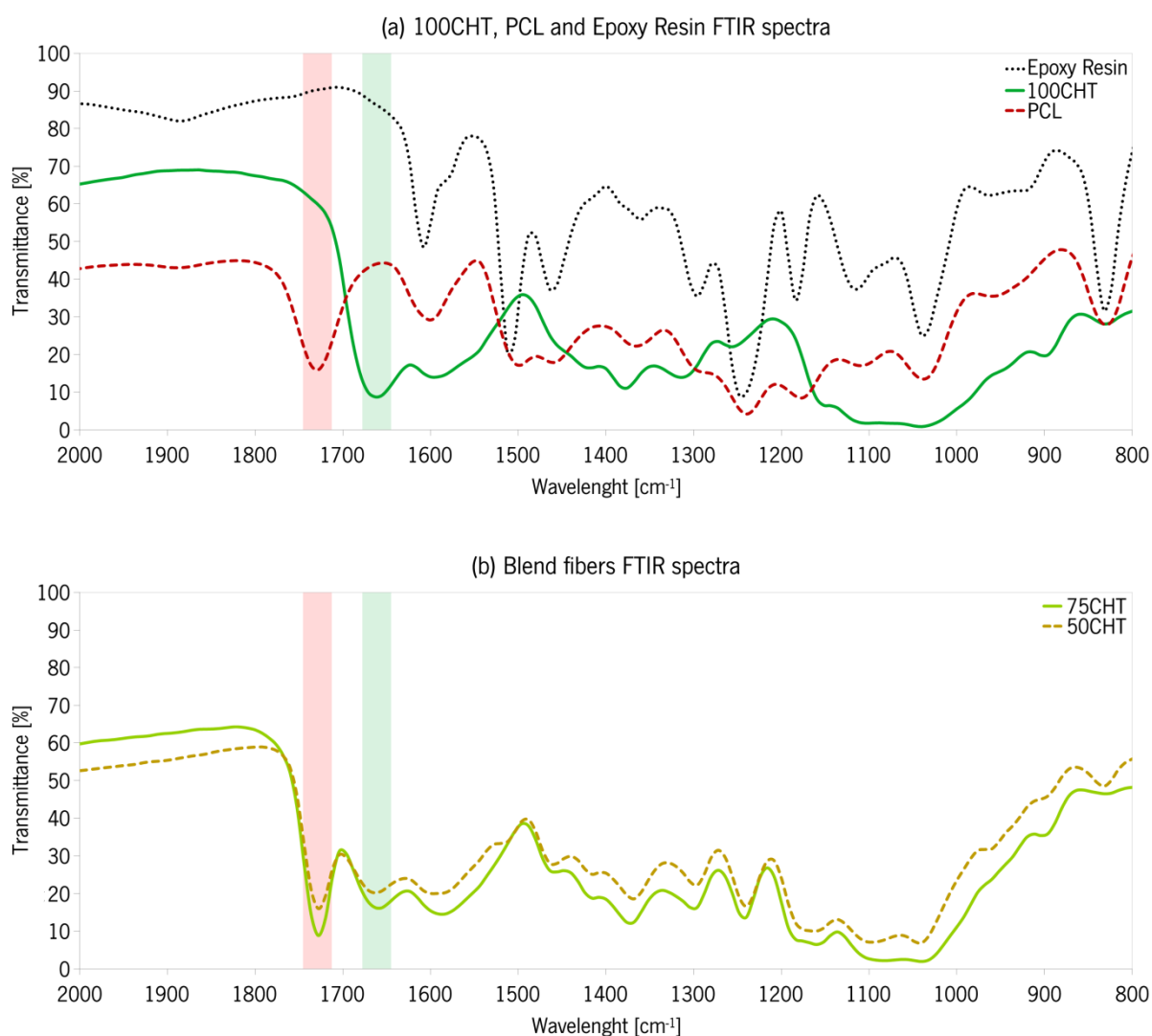


Figure 3.3. Conventional FTIR spectra (only the 2000 to 800cm⁻¹ range is shown) of (a) 100CHT (solid line), PCL (dashed line) and epoxy resin (dotted line) and (b) of the blend fibers (solid line for 75CHT and dashed line for 50CHT). The shadow bands identify the regions that have been selected for the integration procedure used to obtain the images on Figure 3.4.

Figure 3.3 (a) shows the spectra of the individual components, PCL and CHT, and epoxy resin. There is a variety of detectable absorption bands specific for PCL and CHT. The most obvious distinguishing features are a C=O stretching of amide I centered at 1650 cm^{-1} and an amine deformation vibration centered at 1590 cm^{-1} , which is specific for CHT, and a carbonyl stretching absorption at 1730 cm^{-1} for PCL. Figure 3.3 (b) shows the spectra of the blends. These show that no significant frequency shifts of the characteristic functional groups occurred, when compared to pure polymers spectra. This may also indicate that no molecular interactions happened between the referred groups, corroborating previous works conclusions about the interaction between the two polymers in blends [17,35].

The blends chemical mapping (Figure 3.4 (c, d)) showed a predominant yellowish color and the individual polymeric maps similar intensities across the sectioned areas. Thus, although the polymers are not miscible, the PCL domains over CHT seem to be well dispersed at the intrinsic length scale of the technique used, having sizes with dimensions lower than $10\mu\text{m}$.

The used method permitted to disperse PCL domains throughout CHT phase at the micron-level. Thus, homogeneous wet-spun blend fibers were obtained and, as only one common non-aqueous solvent system was used, PCL precipitation during the polymeric solutions preparation was avoided.

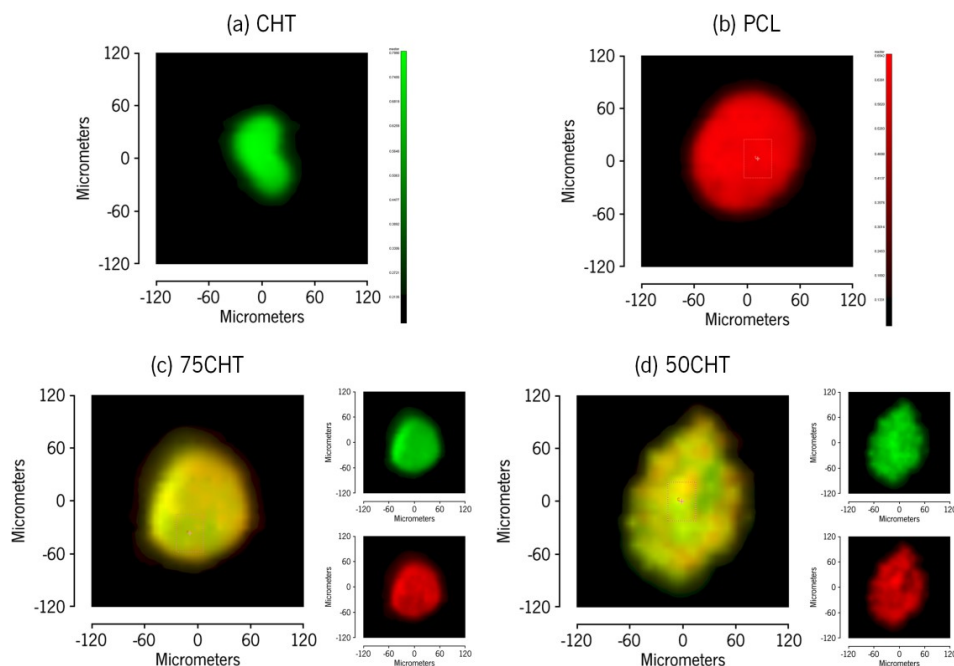


Figure 3.4. Chemical maps of four discrete compositions of the fiber's cross-sections. The different color intensities that can appear in the images may result from the cross-sections different thicknesses. Green indicates the presence of CHT, red the presence of PCL and black corresponds to the epoxy resin. The smaller images present on the right side of the blends chemical maps individualize the presence of the CHT and the PCL in the blends.

3.2. 3D FIBER-MESH SCAFFOLDS CHARACTERIZATION

To increase fiber adhesion after molding, the scaffolds were thermally treated. In this study, the fibers were heated at a temperature (T_a) near the T_m of PCL during different periods of time (t_a). Fibers connectivity of each formulation was analyzed by SEM for each combination of temperature and time (data not shown). The optimal condition was $T_a = 60^\circ\text{C}$ and $t_a = 3\text{h}$. The obtained fiber connectivity can be observed in Figure 3.5 (a – c), with respective magnifications in Figure 3.5 (d – f). In this condition the fibers were connected and maintained the 3D mesh pore network. At $T_a < 60^\circ\text{C}$ fibers could be easily unfolded and no physical connection was observed in SEM analysis. At $T_a > 60^\circ\text{C}$ the superficial PCL melted and was spread over the fiber surface.

Fiber adhesion almost exclusively depended on the pre-melting or melting of superficial PCL, which resulted in satisfactory fiber-mesh stability as the constructs could be easily handled and kept their shape even in a swollen state.

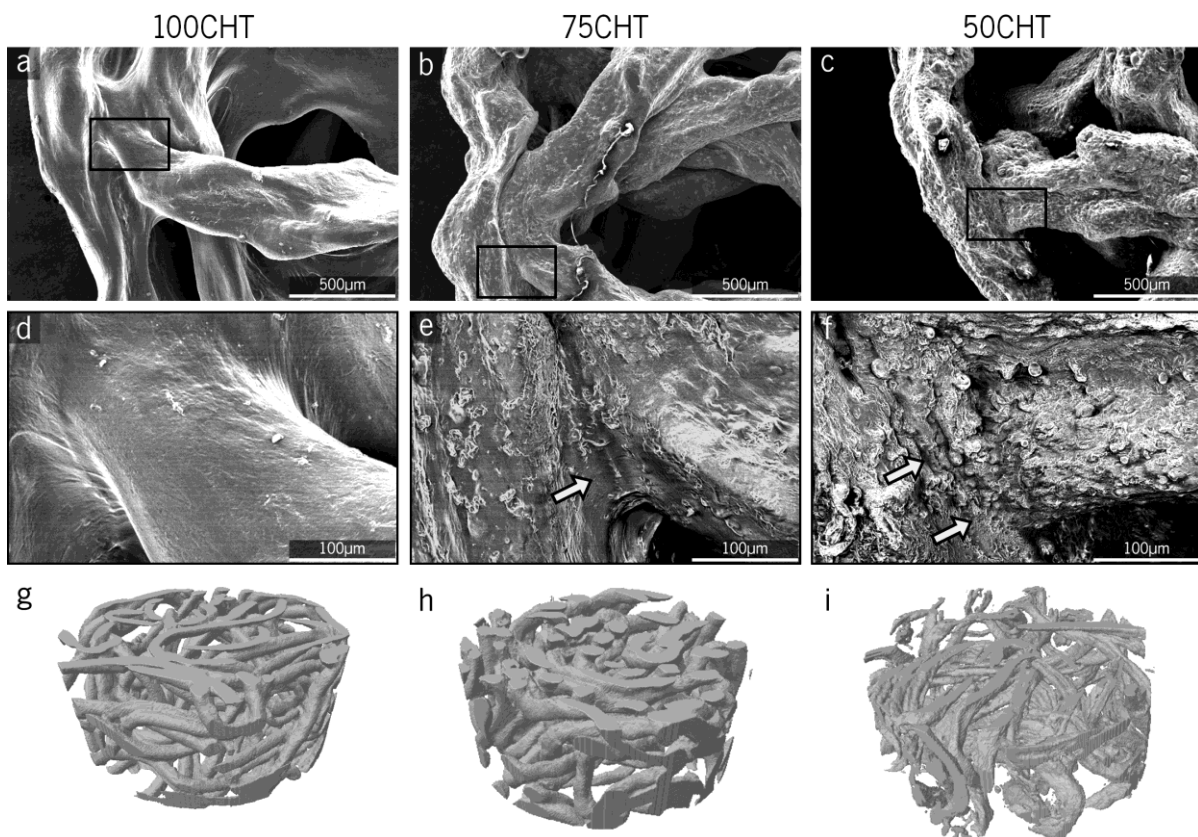


Figure 3.5. SEM microphotographs of the (a, d) 100CHT, (b, e) 75CHT and (c, f) 50CHT fiber-meshes after the thermal treatment at $T_a = 60^\circ\text{C}$ and $t_a = 3\text{h}$. The (d – f) images correspond to the magnification of the area delimited by the rectangular box on the (a – c) images; (g) 100CHT, (h) 75CHT and (i) 50CHT fiber-meshes representative 3D μCT images.

μCT analysis performed resulted in an indicative calculated porosity and pore size (Table 3.2) - from the selected volume of which the reconstructed 3D images are presented on Figure 3.5 (g – i). The analysis also revealed an adequate scaffold porosity range for TE applications and a pore size in the

acceptable range from 250 μ m to 500 μ m, as suggested by Lien *et al.* [36] to support chondrogenic activity and consequent ECM production. The 3D reconstruction showed similar internal structure between scaffold formulations and highly interconnected pores. However, as the μ CT was performed to scaffolds in dry state, it should be mentioned that the scaffold's behavior in a physiological environment would likely result in a different pore size due to swelling and water uptake.

Table 3.2. Mechanical properties of the scaffolds (standard deviation error also presented and (*) stands for statistical significant difference between formulations with $p < 0.05$) and their estimated and exemplificative porosity and pore size, obtained from the μ CT analysis to the representative selected volumes presented on Figure 3.5 (g – i).

SCAFFOLD FORMULATION	YOUNG MODULUS (kPa)	POROSITY (%)	PORE SIZE (μ m)
100CHT	4.43 (\pm 0.29) *	75.6	330.2
75CHT	11.30 (\pm 0.78) *	64.3	265.3
50CHT	23.63 (\pm 3.36) *	83.2	384.7

The swelling behavior of the 3D fiber-meshes (Figure 3.6 (a)) is an important parameter to be evaluated. The physiological conditions imply a hydrated state of the fibers, also providing an insight about the water affinity degree that the scaffolds may have, when comparing formulations. The 100CHT scaffolds showed the highest swelling ratio, followed by the 75CHT and by the 50CHT composition. The increase in PCL (hydrophobic) content in the blends decreased the swelling when compared to 100CHT scaffolds. This reinforces the hypothesis that PCL improves CHT mechanical properties, as the poor mechanical properties of CHT (when compared to the blends) mainly derives from its swollen wet state.

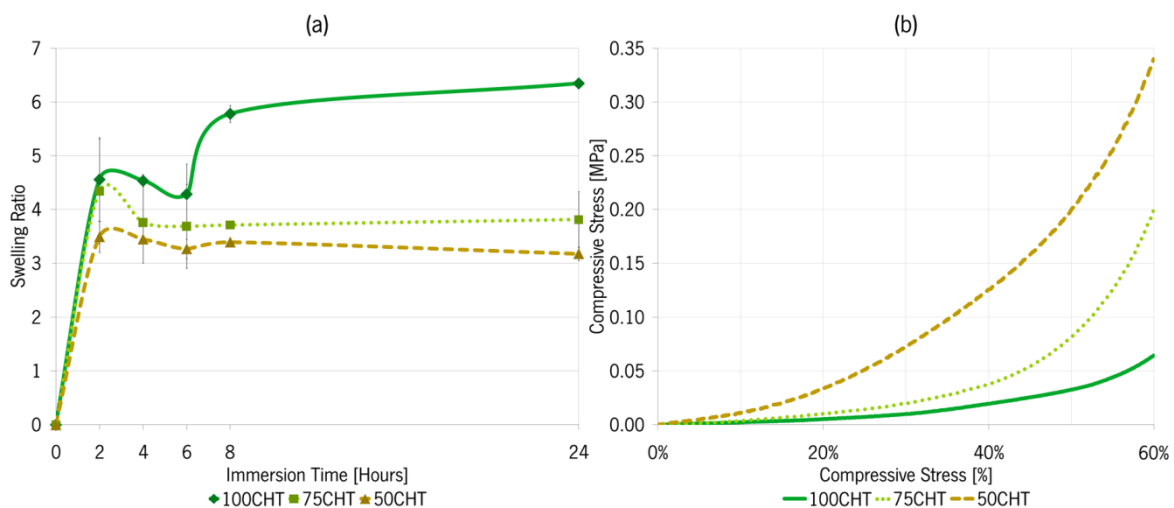


Figure 3.6. (a) Fiber-meshes swelling behavior during 24h immersion in PBS at 37 $^{\circ}$ C and (b) exemplificative stress deformation curves of the three formulations of fiber-meshes.

Compression tests were performed to evaluate the mechanical performance of the 3D fiber-meshes in a wet environment, mimicking the physiological conditions. The results for the Young modulus are presented in Table 3.2 and a representative curve for the deformation behavior of each of the three different fiber-mesh scaffolds is presented on the graph of Figure 3.6 (b). The formulation with lowest

Young modulus value corresponds to 100CHT, followed by 75CHT and 50CHT. Therefore, as the quantity of PCL increases, the scaffolds Young modulus also increases.

3.3. CHONDROCYTES RESPONSE OVER THE FIBER-MESHES

We next examined the interaction of the chondrocytes with the biomaterials. Live-dead assay demonstrated efficient cell attachment and evidence for cell proliferation (Figure 3.7 and SEM analysis – Figure 3.8). The cells were also metabolically active (MTT assay – Figure 3.9). However, cells behaved differently on the scaffolds. On CHT scaffolds, cells tended to aggregate - as indicated, for example, by the green fluorescent spots on Figure 3.7 (a – d). In contrast, cells tended to spread more evenly on scaffolds composed by CHT and PCL (Figure 3.7 (e - h) and Figure 3.8 (e – h)) and 50CHT (Figure 3.7 (i - l) and Figure 3.8 (i – l)). No differences were observed in metabolic activity (Figure 3.9 (e – h) and Figure 3.9 (i - l), respectively).

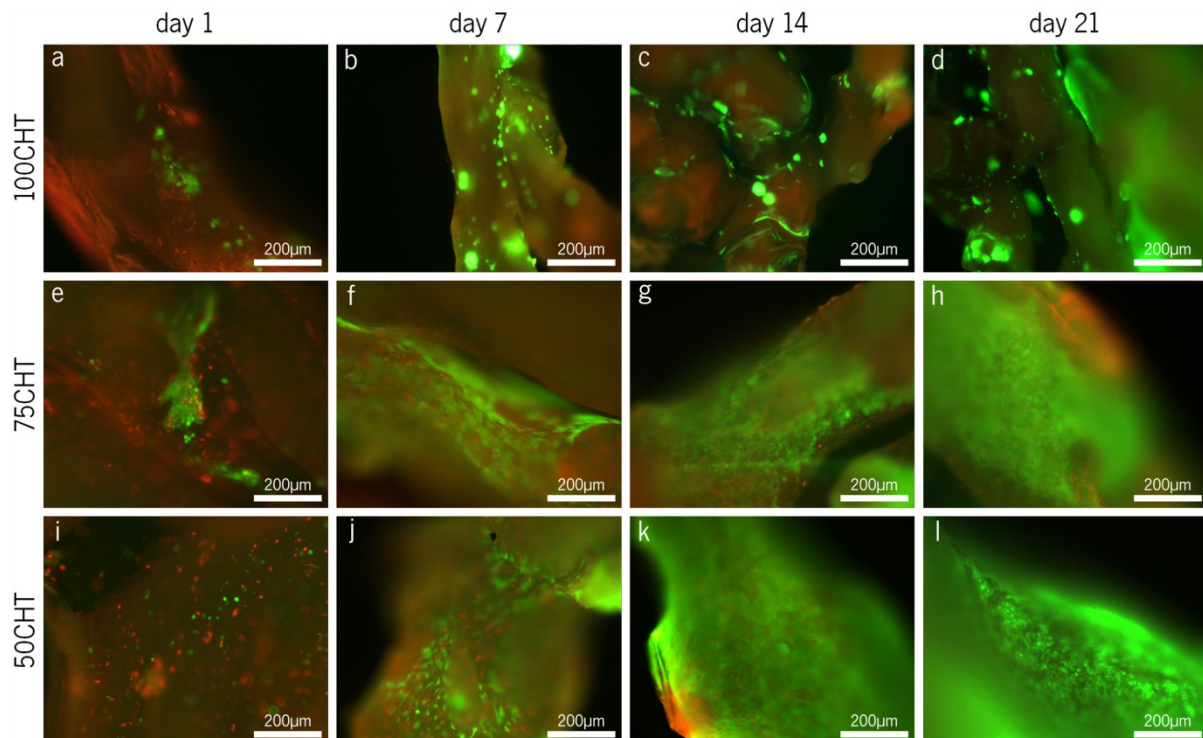


Figure 3.7. Live-dead assay showing chondrocytes at the scaffold fibers at day 1, 7, 14 and 21 of culture, in proliferation medium. Cells were stained with calcein-AM/ethidium homodimer (dead cells stain red and living cells green) and visualized using fluorescence microscopy. Cell density: 5×10^5 cells/ $20 \mu\text{L}$.

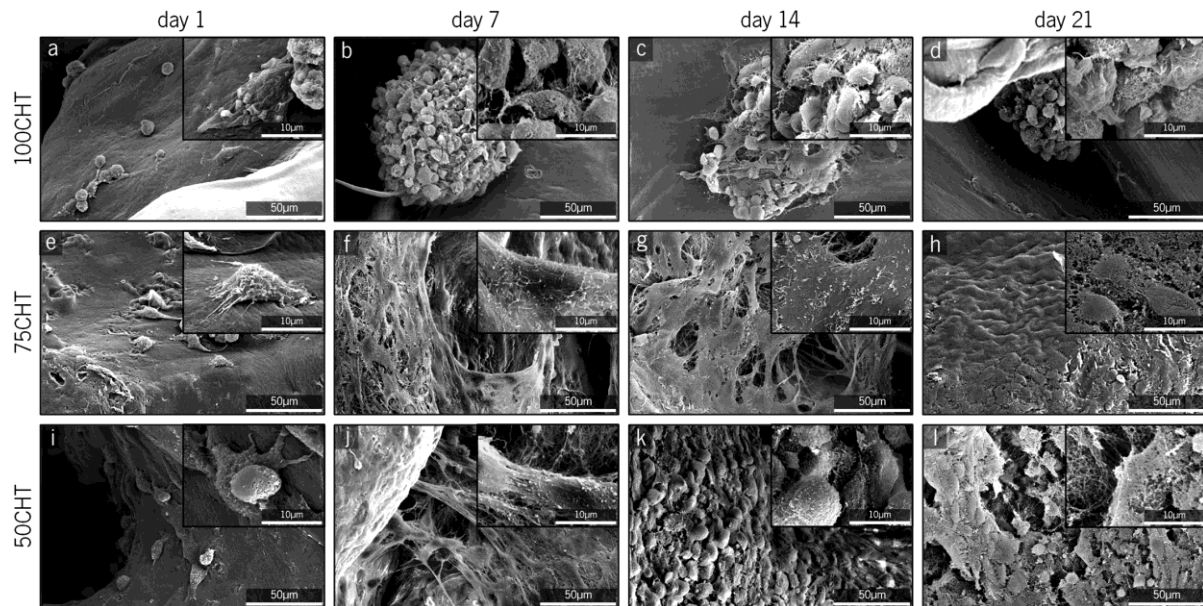


Figure 3.8. SEM images showing chondrocytes distribution and morphology over the scaffolds fibers after 1, 7, 14 and 21 days in culture, with proliferation medium. Cell density: 5×10^5 cells/20 μ L.

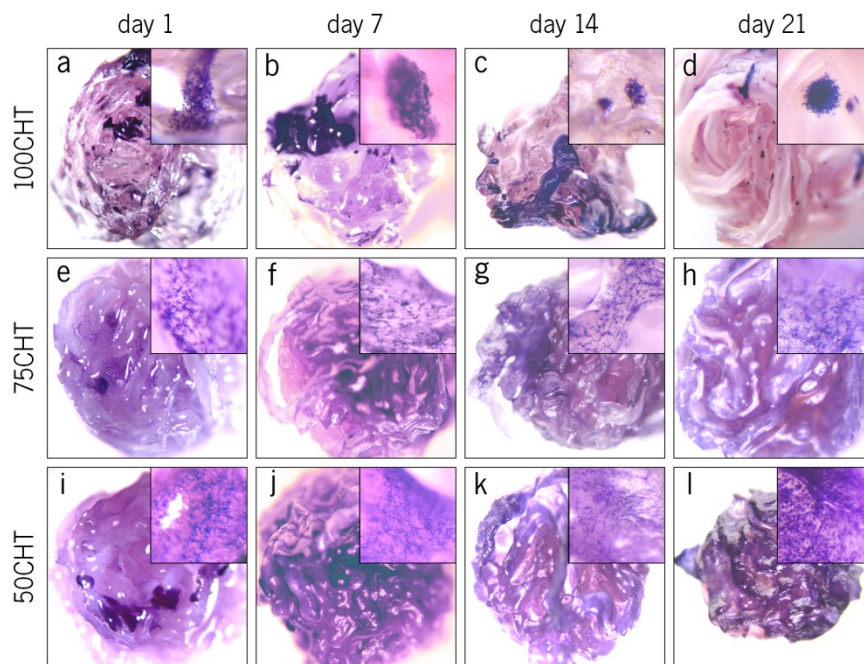


Figure 3.9. MTT assay showing chondrocytes over the scaffolds fibers after 1, 7, 14 and 21 days in culture with proliferation medium. Metabolically active cells stain purple. Constructs were visualized using light microscopy. Cell density: 5×10^5 cells/20 μ L. ((a – l) images: 7.5x magnification; inset images: 50x magnification).

Water uptake ability is intrinsically related to the water affinity of the substrate. Surface tension can be affected by this factor, which is partially responsible and directly related to the degree of cell adhesion [37,38]. Surface energy (tension) of biomaterials may influence which serum proteins adhere to their surface, having a direct impact on their biological response, such as cell adhesion [39,40]. The widely accepted mechanism by which cells adhere to most TE scaffolds involves a two-step process: first, ECM proteins present in serum adsorb onto the scaffold material surface and, second, cells

adhere to these scaffold-adsorbed proteins [41]. Both the composition and structure of this protein layer critically determines cell responses [42]. The homogeneous surface dispersion of PCL and CHT is expected to balance the hydrophobic and hydrophilic features of both polymers.

Surface physical-chemical properties of biomaterials markedly influence cell adhesion as they have an impact on non-receptor mediated and receptor mediated attachment mechanisms [43]. Chondrocyte receptor mediated cell adhesion occurs via their attachment to many ECM proteins, such as fibronectin, vitronectin, various collagen types, perlecan and cartilage oligomeric matrix protein [44].

Chondrocyte-PCL interactions may be considered as non-receptor-mediated cell adhesion, since PCL surfaces are considered inert for peptide conjugation [14,45]. Conversely, CHT presents similarities with some GAGs found on cartilaginous ECM. The combination of PCL and CHT domains in the blends may have been the main reason for the initial spreading of the chondrocytes, besides serum protein adhesion. Alternatively, cell distribution over the blends may also derive from the lack of binding sites over PCL domains and the chondrocytes consequent effort to find other cells or binding sites - like CHT domains. The proliferative behavioral shift observed, when comparing 100CHT with the blend fiber-meshes, is also related to the superficial hydrophilic/hydrophobic character of the fibers surface. Proteins present in proliferative medium may adhere differently to 100CHT and blend fibers due to a difference in surface energy. This may contribute to the difference in cell spreading. However, cell-material interactions are not only governed by the hydrophilic character of material surfaces or surface charge [46], even though moderately hydrophilic surfaces have been found to promote better cell adhesion [42]. Other surface properties such as roughness also influence cell behavior [36]. The differences on surface roughness between 100CHT and 75CHT/50CHT fiber-meshes may have also contributed to the dissimilar chondrocyte behavior observed.

3.4. CHONDROGENIC ACTIVITY EVALUATION OVER THE SCAFFOLDS

The typical differentiated chondrogenic phenotype consists of chondrocytes that possess a rounded-like shape and that secrete ECM proteins, specifically COL2 and aggrecan, with a diffuse actin micro-filament network [47].

Chondrocytes morphology was monitored by analyzing the constructs using SEM during the differentiation studies (Figure 3.10). The typical chondrogenic morphology was observed in all time-points for all fiber-mesh scaffolds formulations. In the differentiation studies, FBS derived protein adhesion onto the scaffolds cannot be responsible for cell adhesion to the fibers surfaces as the differentiation culture medium is serum-free. Therefore, direct cell-biomaterial interactions, in combination with the influence of surface roughness, is likely to play a role in cell attachment.

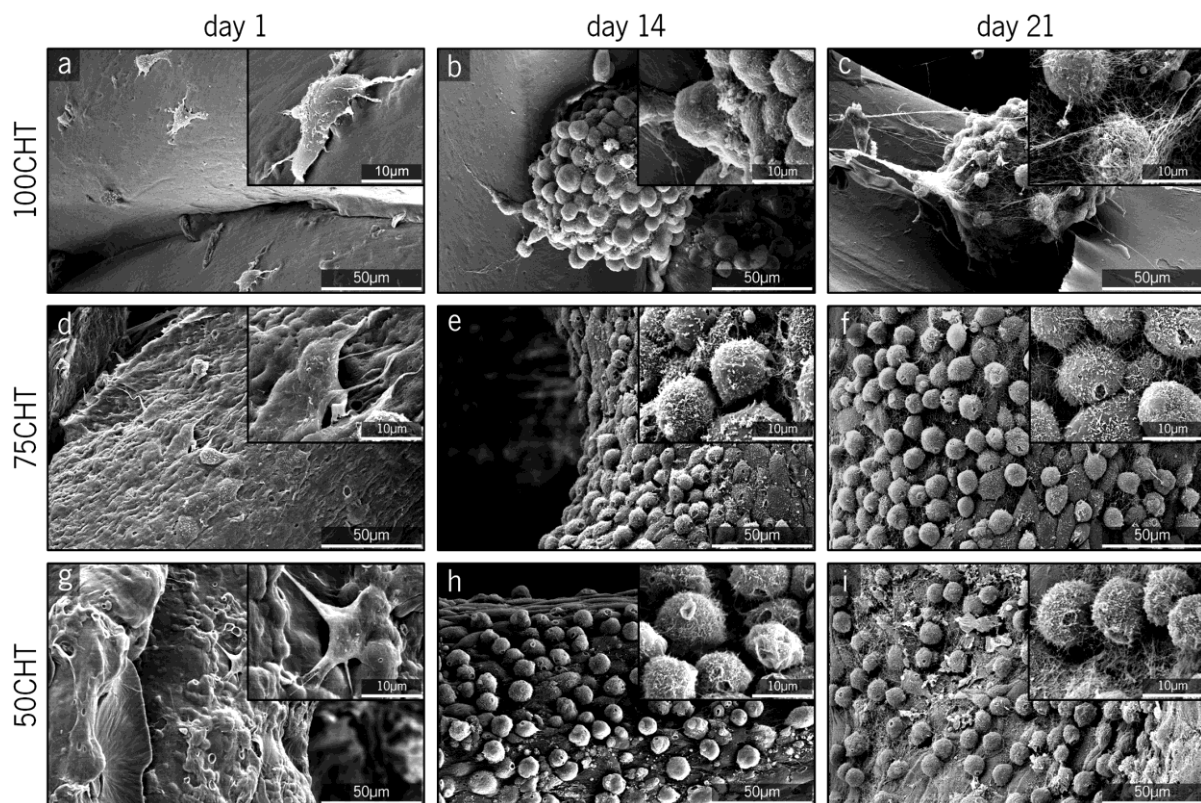


Figure 3.10. SEM micrographs showing chondrocytes distribution and morphology over the scaffolds fibers surface after 1, 14 and 21 days in culture, with differentiation medium. Cell density: 5×10^5 cells/ $20 \mu\text{L}$.

Histological evaluation (Figures 3.11 and 3.12) showed that cartilaginous ECM production was present in all formulations at for both time-points analyzed (14 and 21 days). In all conditions examined, staining intensity increase with culture time is indicative for ECM production. The histological analysis also reveals round-like cell aggregation in the 100CHT fiber-meshes (Figure 3.11 (a – d) and Figure 3.12 (a – d)), in contrast to uniformly distributed round cells covering the scaffolds surface observed in the 75CHT and 50CHT formulations (Figure 3.11 (e – l) and Figure 3.12 (e – l)).

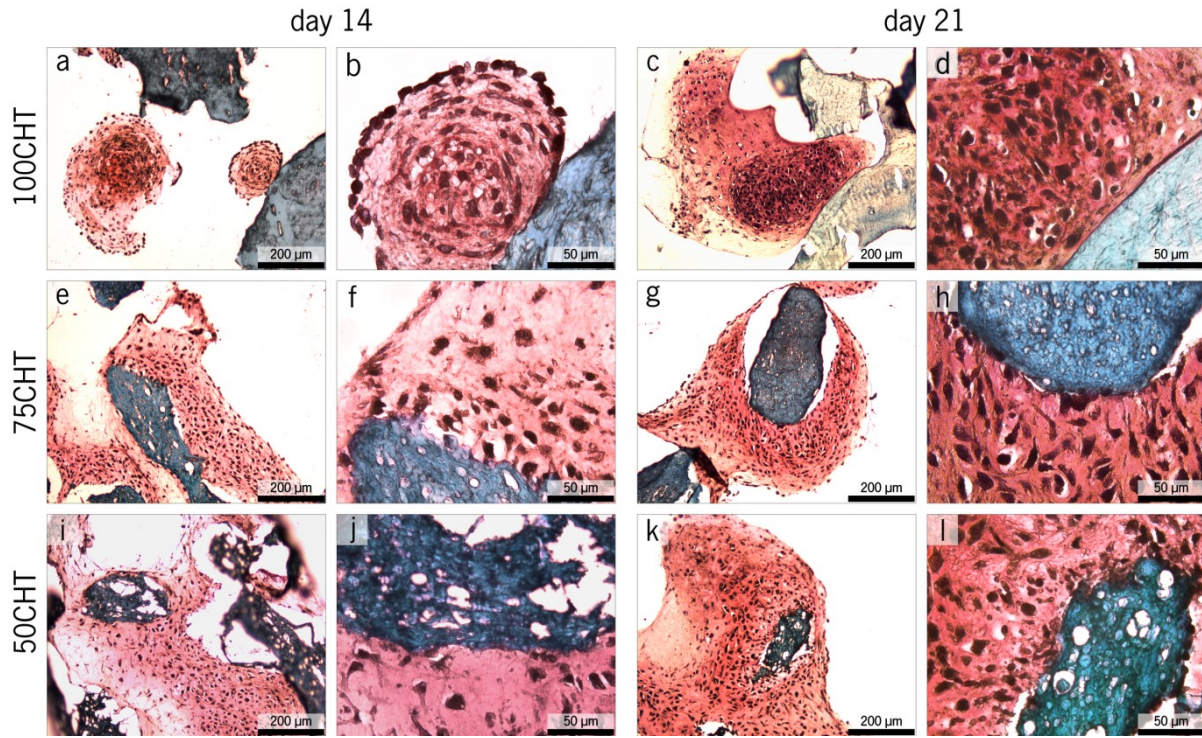


Figure 3.11. Histological cross-sections show GAG production (stained red) on the (a - d) 100CHT, (e - h) 75CHT and (i - l) 50CHT scaffolds, on day 14 (a, b, e, f, i, j) and day 21 (c, d, g, h, k, l) of culture in differentiation medium, by safranin-O staining. Cells are represented by the dark spots and bluish regions correspond to the scaffold material.

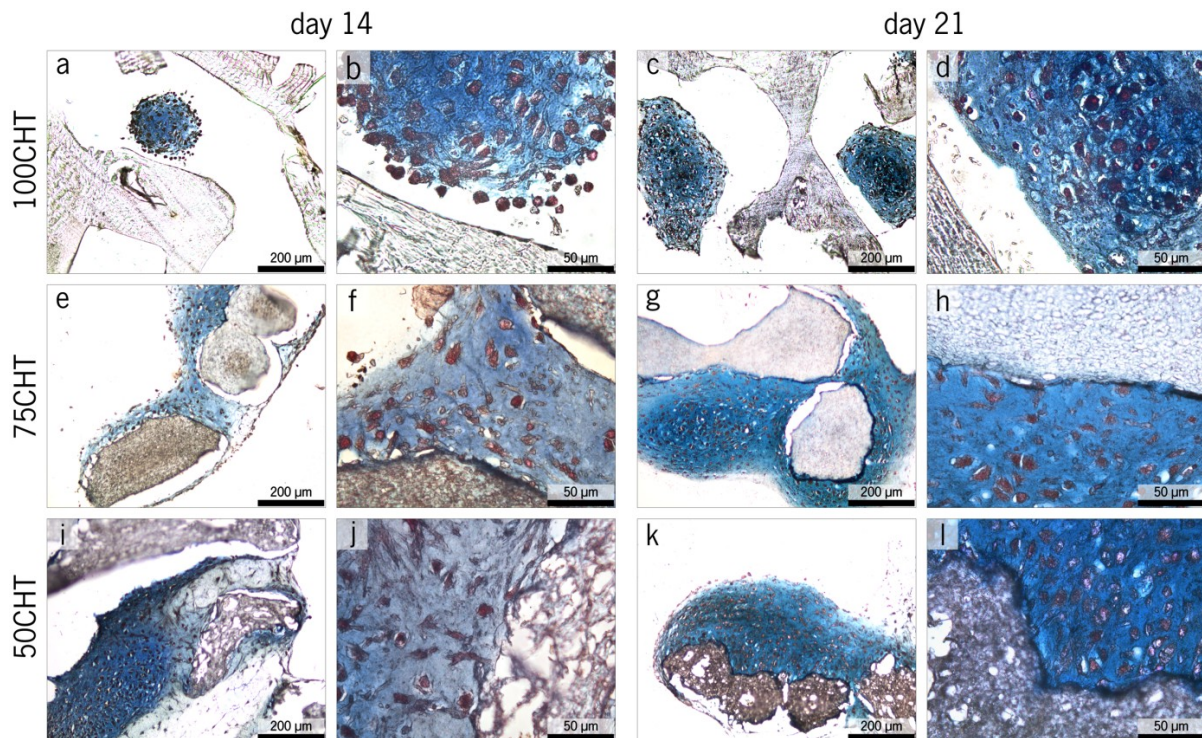


Figure 3.12. Histological cross-sections show GAG production (stained blue) on the (a - d) 100CHT, (e - h) 75CHT and (i - l) 50CHT scaffolds, on day 14 (a, b, e, f, i, j) and day 21 (c, d, g, h, k, l) of culture in differentiation medium, by alcian blue staining. Fast red stained cell nuclei red and pale blue regions correspond to the scaffold material.

When chondrocytes maintain their natural spherical shape they produce more GAGs [48]. This fact is partly corroborated by the GAG/DNA ratio, i.e., GAG produced per cell. The DNA (Figure 3.13 (a)) and GAG (Figure 3.13 (b)) quantification assays, along with GAG/DNA ratio (Figure 3.13 (c)) helped to better understand the chondrocytes activity within the scaffolds during the 21 days of culture.

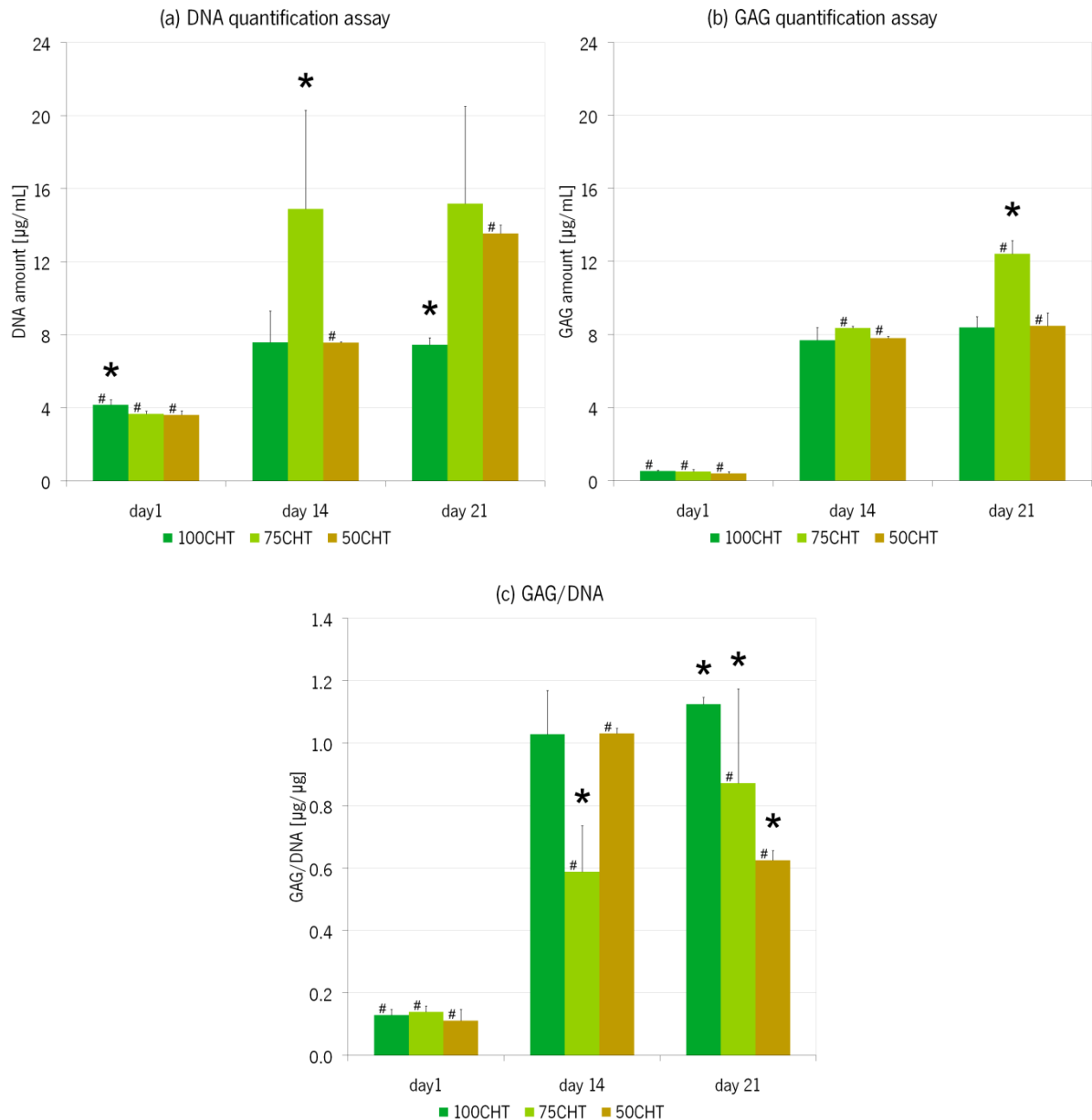


Figure 3.13. DNA, (b) GAG and (c) GAG/DNA ratio quantification assays of the constructs, after 1, 14 and 21 days of culture in differentiation medium. (*) stands for significant differences between different scaffold formulations on the same culture day ($p < 0.05$); (#) represents significant differences between the same scaffold formulation on different culture days ($p < 0.05$).

At day 1, significant differences in cell amount (Figure 3.13 (a)) were only observed between the 100CHT and the blend formulations. From day 1 to day 14, DNA amount increased for each scaffold formulation. On day 14, the DNA content was only significantly different between the 75CHT and the

100CHT and 50CHT formulations. From day 14 to day 21, the DNA amount significantly increased for 50CHT only, while this value remained unchanged for the other combinations.

GAG amount (Figure 3.13 (b)) increased for all scaffold formulations over time. At day 1, GAG amount was not significantly different between formulations. From day 1 to day 14 (Figure 3.13 (b)), there was a significant increase on GAG production by cells on all formulations. The highest production of GAG was observed for the 75CHT. From day 14 to day 21 (Figure 3.13 (b)), all formulations had an increase in GAG amount. The highest production was again observed on 75CHT constructs, followed by the 100CHT and 50CHT constructs presenting a small increase.

The graphical representation of GAG/DNA ratios (Figure 3.13 (c)) shows that, for the first day of culture, the ratios are similar between formulations. As expected, the GAG amount *per* cell amount was increased at the 14th day of culture. The highest ratio values corresponded to the 100CHT fiber and 50CHT constructs. With respect to day 21, 100CHT was the formulation with the highest GAG/DNA ratio, followed by the 75CHT constructs and, at last, the 50CHT.

Figure 3.14 shows the overall distribution of ECM production over the scaffolds structure. On all fiber-meshes formulations, matrix quantity increased during the differentiation culture time period of 21 days. However, the distribution of the ECM throughout scaffolds was different depending on its composition. With respect to the 100CHT constructs, ECM distribution was confined to clusters at days 14 and 21 (Figure 3.14 (b, c)), respectively. On the contrary, a homogeneous distribution of ECM was observed in the 75CHT (Figure 3.14 (e, f)) and 50CHT (Figure 3.14 (h, i)) fiber-meshes.

From the analysis of the SEM images present on Figures 3.10 and 3.14, it can be observed that both 75CHT and 50CHT scaffolds resulted in a better distribution of the cells over the scaffold when compared to the 100CHT formulation. However, it is also known that cell aggregation enhances cell-cell signaling, resulting in a better tissue formation [49]. Cell distribution in the scaffold is an important parameter as it is related to ECM distribution as well. The scaffold design also implies that cells seeded may produce ECM to cover all the scaffold volume homogeneously. Thus, even if the GAG/DNA ratio was higher for the 100CHT constructs, it was observed that the ECM produced by chondrocytes over these constructs resulted into an undesired distribution. The poor spreading of the cells may also be related to the surface roughness, as commented before. Consequently, blend scaffolds would lead to a more homogeneous ECM production over the construct.

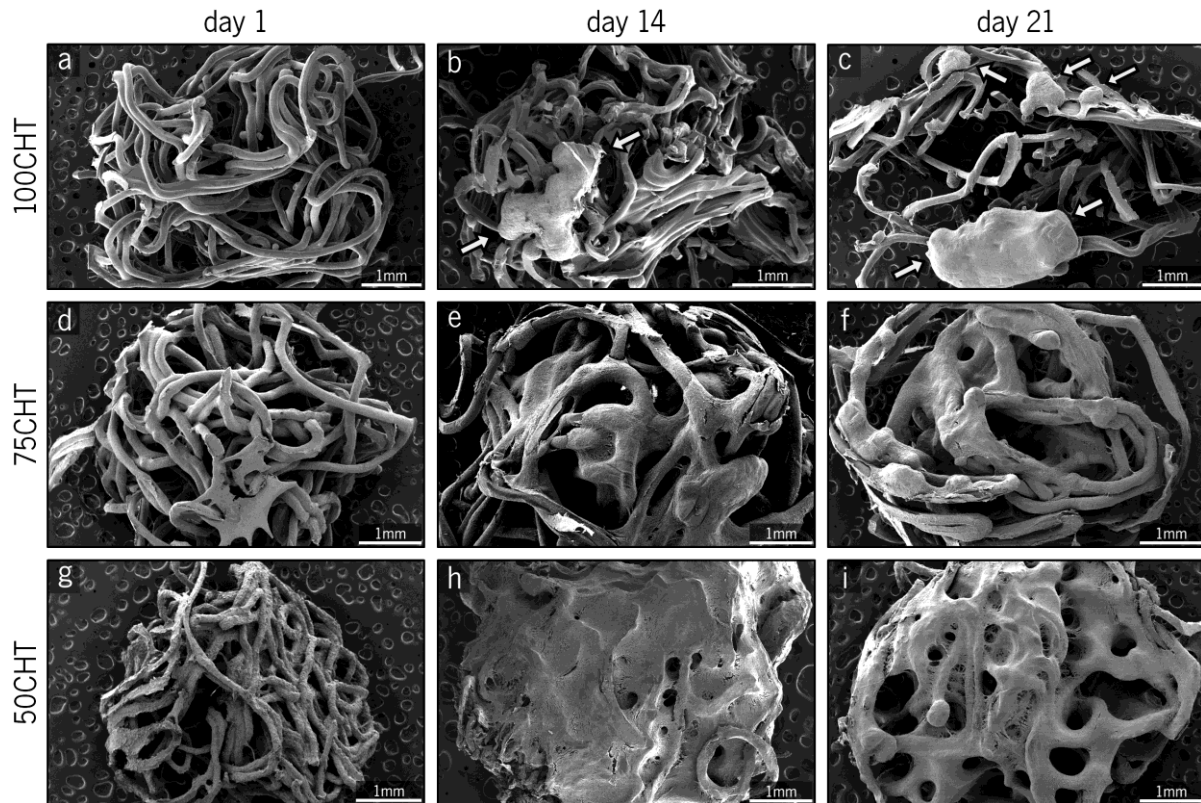


Figure 3.14. SEM micrographs showing the overall ECM distribution over the scaffolds after 1, 14 and 21 days in culture with differentiation medium. Arrows point out ECM aggregates.

When comparing chondrocytes distribution over both blend scaffolds, there are no main differences. This indicates that both would lead to a homogeneous ECM dispersion over the scaffold. This effectively occurs, as proven by the overall observation of the constructs after the 21 days of differentiation culture (Figures 3.14). The main difference was the chondrocytes behavior during the culturing days. On both blends, they proliferated until day 14, with significantly less cell number present on the 50CHT blend scaffolds. However, a major and important behavior shift occurred from day 14 to day 21, when comparing chondrocytes seeded in 75CHT and 50CHT scaffolds. For the 75CHT constructs, cells almost stopped proliferating and GAG production increased. On the contrary, for the 50CHT blend scaffolds, chondrocytes continued to proliferate and GAG production poorly increased. These results may indicate that chondrocytes seeded over the 50CHT tended to present fibroblast-like phenotypic de-differentiation. This leads to a proliferative behavior and a decrease in proteoglycan synthesis (along with a decreased COL2 expression and increased COL1 expression) [48]. The amount of CHT present in the 75CHT blend (i.e., the amount of domains similar to cartilaginous ECM) may also have helped chondrocytes to maintain their typical behavior.

The fiber's adhesion confers structural stability to the 3D constructs. The scaffolds maintained their structure after the compression tests and after cell proliferation and differentiation studies. Blending PCL with CHT improved the mechanical properties of CHT scaffolds, as evidenced by an increase in the

Young modulus, with the highest values observed for the 50CHT scaffolds. However, the scaffolds mechanical properties did not exactly mimic those of AC. Besides the fact that AC has different zones, [2] which are not mimicked in the scaffold design, there are also main differences in the structural organization of cartilage and these fiber-mesh scaffolds. In normal cartilage developmental conditions *in vivo*, chondrocytes produce a very compact tissue and are embedded in a 3D matrix [2]. To facilitate cartilage formation *in vitro*, one needs to provide a 3D environment with ample possibilities for cell-cell contact and supply of nutrients. Our fiber-mesh scaffolds are primarily designed to match these needs. Consequently, the mechanical properties are not as good as those of AC, mainly due to their porosity and CHT content. It is believed, however, that during neo-cartilage formation the mechanical properties will improve. Particularly the homogeneous deposition of ECM in the CHT/PCL blends is likely to improve mechanical properties.

The 50CHT possesses a PCL amount that was proven to be too high (or a CHT quantity too low) that induced a loss of chondrogenic phenotype expression, despite the best mechanical performance. Even though the typical chondrocyte phenotype was maintained in 100CHT scaffolds, this formulation led to cell aggregation and consequently heterogeneous distribution of ECM. Therefore, we believe that the PCL quantity present on 75CHT altered CHT fibers properties in a balanced way, between the 50CHT and 100CHT formulations. Cell distribution over the 75CHT scaffolds was similar to that presented by the 50CHT, but the 75CHT structure was capable of maintaining chondrocytes phenotypical behavior in a similar way as the 100CHT. Despite the fact that 75CHT blend scaffolds showed a lower Young modulus, compared to the 50CHT scaffolds, it is (in long-term) expected that the 75CHT scaffold/neo-cartilage system would surpass the mechanical properties of the 50CHT scaffold/neo-cartilage system based on 75CHT biological performance.

4. CONCLUSIONS

100CHT, 75CHT and 50CHT fibers were successfully obtained by wet-spinning using a common solvent solution of 100 vol.% formic acid. The fibers were folded into cylindrical moulds and underwent a thermal treatment ($T_a = 60^\circ\text{C}$; $t_a = 3\text{h}$) to obtain the scaffolds. PCL domains were homogeneously distributed over the blends, even if phase separation may exist at a micrometric scale. 3D fiber-mesh structures presented good integrity and stability, along with open and interconnected porosity and pore size range suitable for TE applications. PCL incorporation into CHT improved surface roughness of the fibers and diminished the swelling ratio. Blending improved cell spreading and did not affect cell survival nor did it impair metabolic activity. Regarding the differentiation studies, the 75CHT constructs performed the best, with the highest GAG amount and homogenous ECM distribution. As the PCL content increased, the mechanical properties increased accordingly. However, as over 50CHT chondrocytes almost stopped producing GAG, the 75CHT formulation balanced at best the physical-chemical and biological properties of these new CHT/PCL blend 3D fiber-meshes for cartilage regeneration.

5. REFERENCES

- [1] Wakitani S, *et al.* Present status of and future direction for articular cartilage repair. *Journal of Bone Mineral Metabolism*, 2008. 26(2) pp. 115–22.
- [2] Chung C and Burdick JA. Engineering cartilage tissue. *Advanced Drug Delivery Reviews*, 2008. 60(2) pp. 243–262.
- [3] Kosher RA and Church RL. Stimulation of *in vitro* somite chondrogenesis by procollagen and collagen. *Nature*, 1975. 258(5533) pp. 327–330.
- [4] Suh JK and Matthew HW. Application of chitosan-based polysaccharide biomaterials in cartilage tissue engineering: a review. *Biomaterials*, 2000. 21(24) pp. 2589–2598.
- [5] Di Martino A, Sittlinger M and Risbud MV. Chitosan: a versatile biopolymer for orthopaedic tissue-engineering. *Biomaterials*, 2005. 26(30) pp. 5983-5990.
- [6] Kuo YC and Lin CY. Effect of genipin-crosslinked chitin-chitosan scaffolds with hydroxyapatite modifications on the cultivation of bovine knee chondrocytes. *Biotechnology and Bioengineering*, 2006. 95(1) pp.132–144.
- [7] Kim SE *et al.* Porous chitosan scaffold containing microspheres loaded with transforming growth factor- β 1: implications for cartilage tissue engineering. *Journal of Controlled Release* 2003;91:365–374.
- [8] Sarasam A and Madihally SV. Characterization of chitosan–polycaprolactone blends for tissue engineering applications. *Biomaterials*, 2005. 26(27) pp. 5500-5508.
- [9] Woodruff MA and Hutmacher DW. The return of a forgotten polymer - Polycaprolactone in the 21st century. *Progress in Polymer Science*. In Press, Corrected Proof, Available online 7 April 2010. doi: 10.1016/j.progpolymsci.2010.04.002.
- [10] Ishaug-Riley SL, *et al.* Human articular chondrocyte adhesion and proliferation on synthetic biodegradable polymer films. *Biomaterials*, 1999. 20(23-24) pp. 2245-2256.
- [11] Hoque ME, *et al.* Processing of polycaprolactone and polycaprolactone-based copolymers into 3D scaffolds, and their cellular responses. *Tissue Engineering A*, 2009. 15(10) pp. 3013-3024.
- [12] Garcia-Giralt N, *et al.* A porous PCL scaffold promotes the human chondrocytes redifferentiation and hyaline-specific extracellular matrix protein synthesis. *Journal of Biomedical Materials Research Part A*, 2008. 85(4) pp. 1082-1089.
- [13] van Dijkhuizen-Radersma R, *et al.* Chapter 7: Degradable Polymers for Tissue Engineering. In: van Blitterswijk C (editors). *Tissue Engineering*. Academic Press Series in Biomedical Engineering, 2008. P. 202.
- [14] Zhu Y, *et al.* Surface modification of polycaprolactone membrane via aminolysis and biomacromolecule immobilization for promoting cytocompatibility of human endothelial cells. *Biomacromolecules*, 2002. 3(6) pp. 1312–1319.
- [15] Cruz DMG, *et al.* Blending polysaccharides with biodegradable polymers. II. Structure and biological response of chitosan/polycaprolactone blends. *Journal of Biomedical Materials Research. Part B, Applied Biomaterials*, 2008. 87(2) pp. 544-554.
- [16] Eyrich D, *et al.* *In vitro* and *in vivo* cartilage engineering using a combination of chondrocyte-seeded long-term stable fibrin gels and polycaprolactone-based polyurethane scaffolds. *Tissue Engineering*, 2007. 13(9) pp. 2207–2218.
- [17] Malheiro VN, *et al.* New poly(ϵ -caprolactone)/chitosan blend fibers for tissue engineering applications. *Acta Biomaterialia*, 2010. 6(2) pp. 418-428.
- [18] Honma T, Senda T and Inoue Y. Thermal properties and crystallization behaviour of blends of poly(epsilon-caprolactone) with chitin and chitosan. *Polymer International*, 2003. 52(12) pp. 1839-1846.
- [19] Senda T, He Y and Inoue Y. Biodegradable blends of poly(epsilon-caprolactone) with alpha-chitin and chitosan: specific interactions, thermal properties and crystallization behavior. *Polymer International*, 2002. 51(1) pp. 33-39.
- [20] Cruz DMG, Ribelles JLG and Sanchez MS. Blending polysaccharides with biodegradable polymers. I. Properties of chitosan/polycaprolactone blends. *Journal of Biomedical Materials Research. Part B, Applied Biomaterials*, 2008. 85(2) pp. 303-313.
- [21] Nielsen GD, *et al.* Sensory irritation mechanisms investigated from model compounds: Trifluoroethanol, hexafluoroisopropanol and methyl hexafluoroisopropyl ether. *Archives of Toxicology*, 1996. 70(6) pp. 319-328.
- [22] Sarasam AR, *et al.* Blending chitosan with polycaprolactone: porous scaffolds and toxicity. *Macromolecular Bioscience*, 2007. 7(9-10) pp. 1160-1167.
- [23] Wan Y, *et al.* Compressive mechanical properties and biodegradability of porous poly(caprolactone)/chitosan scaffolds. *Polymer Degradation and Stability*, 2008. 93(10) pp. 1736-1741.

- [24] Wan Y, *et al.* Development of polycaprolactone/chitosan blend porous scaffolds. *Journal of Materials Science: Materials in Medicine*, 2009. 20(3) pp. 719-724.
- [25] Wan Y, *et al.* Fibrous poly(chitosan-g-DL-lactic acid) scaffolds prepared via electro-wet-spinning. *Acta Biomaterialia*, 2008. 4(4) pp. 876-886.
- [26] Tuzlakoglu K, *et al.* Production and characterization of chitosan fibers and 3-D fiber mesh scaffolds for tissue engineering applications. *Macromolecular Bioscience*, 2004. 4(8) pp. 811-819.
- [27] Prabhakaran MP, *et al.* Electrospun biocomposite nanofibrous scaffolds for neural tissue engineering. *Tissue Engineering Part A*, 2008. 14(11) pp. 1787-1797.
- [28] Yang X, Chen X and Wang H. Acceleration of osteogenic differentiation of preosteoblastic cells by chitosan containing nanofibrous scaffolds. *Biomacromolecules*, 2009. 10(10) pp. 2772-2778.
- [29] Shalumon KT, *et al.* Single step electrospinning of chitosan/poly(caprolactone) nanofibers using formic acid/acetone solvent mixture. *Carbohydrate Polymers*, 2010. 80(2) pp. 413-419.
- [30] Chiono V, *et al.* Characterisation of blends between poly(ϵ -caprolactone) and polysaccharides for tissue engineering applications. *Materials Science and Engineering C*, 2009. 29(2) pp. 2174-2187.
- [31] Lien SM, Ko LY and Huang TJ. Effect of pore size on ECM secretion and cell growth in gelatin scaffold for articular cartilage tissue engineering. *Acta Biomaterialia*, 2009. 5(2) pp. 670-679.
- [32] Alves da Silva ML, *et al.* Chitosan/polyester-based scaffolds for cartilage tissue engineering: Assessment of extracellular matrix formation. *Acta Biomaterialia*, 2010. 6(3) pp. 1149-1157.
- [33] Olabarrieta I, *et al.* Transport properties of chitosan and whey blended with poly(ϵ -caprolactone) assessed by standard permeability measurements and microcalorimetry. *Polymer*, 2001. 42(9) pp. 4401-4408.
- [34] She H, Xiao X and Liu R. Preparation and characterization of polycaprolactone-chitosan composites for tissue engineering applications. *Journal of Materials Science*, 2007. 42(19) pp. 8113-8119.
- [35] Wan Y, *et al.* Thermophysical properties of polycaprolactone/chitosan blend membranes. *Thermochimica Acta*, 2009. 487(1-2) pp. 33-38.
- [36] Lien SM, Ko LY and Huang TJ. Effect of pore size on ECM secretion and cell growth in gelatin scaffold for articular cartilage tissue engineering. *Acta Biomaterialia*, 2009. 5(2) pp. 670-679.
- [37] Lampin M, *et al.* Correlation between substratum roughness and wettability, cell adhesion, and cell migration. *Journal of Biomedical Materials Research*, 1998. 36(1) pp. 99-108.
- [38] Chang G, *et al.* Physical and hydrodynamic factors affecting chondrocyte adhesion to polymer surfaces. *Journal of Biomedical Materials Research*, 1988. 22(1) pp. 13-29.
- [39] Boyan BD, *et al.* Role of material surfaces in regulating bone and cartilage cell response. *Biomaterials*, 1996. 17(2) pp. 137-146.
- [40] Olivieri MP, *et al.* Comparative biophysical study of adsorbed calf serum, fetal bovine serum and mussel adhesive protein. *Biomaterials*, 1992. 13(4) pp. 201-208.
- [41] Liu H and Webster TJ. Nanomedicine for implants: A review of studies and necessary experimental tools. *Biomaterials*, 2007. 28(2) pp. 354-369.
- [42] Elbert DL and Hubbell JA. Surface treatments of polymers for biocompatibility. *Annual Review of Materials Science*, 1996. 26 pp. 365-394.
- [43] Tsai WB and Wang MC. Effects of an avidin-biotin binding system on chondrocyte adhesion and growth on biodegradable polymers. *Macromolecular Bioscience*, 2005. 5(3) pp. 214-221.
- [44] Wyre RM and Downes S. The role of protein adsorption on chondrocyte adhesion to a heterocyclic methacrylate polymer system. *Biomaterials*, 2002. 23(2) pp. 357-364.
- [45] Santiago LY, *et al.* Peptide-surface modification of poly(caprolactone) with laminin-derived sequences for adipose-derived stem cell applications. *Biomaterials*, 2006. 27(15) pp. 2962-2969.
- [46] Lee JH, *et al.* Platelet adhesion onto chargeable functional group gradient surfaces. *Journal of Biomedical Materials Research*, 1998. 40(15) pp. 180-186.
- [47] Wang L *et al.* Flow cytometric analysis of the human articular chondrocyte phenotype *in vitro*. *Osteoarthritis and Cartilage*, 2001. 9(1) pp. 73-84.
- [48] Moroni L, *et al.* 3D fiber-deposited electrospun integrated scaffolds enhance cartilage tissue formation. *Advanced Functional Materials*, 2008. 18(1) pp. 53-60.
- [49] Wong M, *et al.* Cyr61, product of a growth factor-inducible immediate-early gene, regulates chondrogenesis in mouse limb bud mesenchymal cells. *Developmental Biology*, 1997. 192(2) pp. 492-508.

CHAPTER IV

GENERAL CONCLUSION AND FUTURE RESEARCH

GENERAL CONCLUSION AND FUTURE RESEARCH

The potential of CHT/PCL blend 3D fiber-mesh scaffolds to support chondrogenic activity was evaluated, for the first time, in this work.

A simpler common solvent solution of 100 vol.% of formic acid was successfully used to blend CHT and PCL and fibers of three different formulations (100:0, 75:25 and 50:50 wt.% CHT/PCL) were prepared by wet-spinning, using methanol as coagulant. The combined analysis of the fibers by SEM, FTIR and DSC showed that, although both polymers are not miscible, the blends presented a good homogeneity and that PCL domains were well dispersed within the CHT phase at a very fine scale (< 10 μ m).

The processed fibers were randomly folded into cylindrical moulds and thermally treated in order to obtain 3D fiber-mesh scaffolds. By μ CT and SEM analysis, fibers were well attached and scaffolds presented an adequate interconnectivity, porosity and pore-size range for TE applications. Furthermore, as PCL quantity increased in the blends, the fibers surface became rougher, scaffolds mechanical properties were enhanced and the structures swelling and water uptake ability diminished. From a structural point of view, blending CHT and PCL surpassed pure CHT mechanical properties as the blends possess a lower water uptake capacity.

The biological performance of these blends was also assessed for the first time. Chondrocytes were viable, metabolically active and proliferated during the 21 days of *in vitro* studies, as the live-dead/MTT assays and SEM analysis showed. However, chondrocytes behaved differently over the 100CHT scaffolds, as they aggregated, in contrast to a better distribution observed for the blend structures. This results from the different fibers surface properties, as the blend fibers are rough and their surface energy is balanced by the two polymers properties.

The chondrogenic potential was also assessed by SEM, histology and DNA and GAG quantification studies. Chondrocytes maintained their round-like shape and cartilaginous ECM production was observed for all formulations, in chondrogenic culture medium, for 21 days of culture. However, a heterogeneous distribution of ECM was observed over the 100CHT scaffolds as a consequence of cell aggregation. When comparing the blend scaffolds, DNA and GAG quantification assays showed that chondrocytes tended to de-differentiated over the 50CHT scaffolds. Thus, even the 50CHT scaffolds mechanically performed the best, the 75CHT proved to be the formulation that balances the highest ECM production, a homogeneous dispersion of cartilaginous tissue and CHT enhanced mechanical properties.

Some studies could be performed as future developments. Thus, it would be interesting to:

- quantify the surface energy of these blends, in order to validate the theory that the hydrophilic and hydrophobic nature of CHT and PCL (respectively) are balanced in the blends;
- perform degradation studies, trying to predict the degradation kinetics of these newly developed scaffolds in a mimicked physiological environment. CHT is degraded enzymatically by lysozyme and PCL hydrolytically. This may also be an interesting parameter to study as their interaction in the blends may vary their individual degradation kinetics;
- quantify the fibers surface roughness and correlate it with the cell behavior;
- improve and enhance cartilaginous tissue formation, creating a hybrid system. These fiber-mesh scaffolds could be immersed into a hydrogel that would have chondrocytes entrapped on. This would promote cell contact and avoid cell loss during culture. On the other hand, the fiber-meshes would function as “backbone” for this system, providing the mechanical stability that the hydrogel lacks. Another kind of hybrid system could be obtained processing nano-fibers by electrospinning or freeze-drying within these fiber-mesh 3D structures.